



Dossier de prolongation pour une durée illimitée de l'autorisation du 03 février 1997 relative au stockage souterrain de produits dangereux non radioactifs

Tierce-expertise

NOTE TECHNIQUE RELATIVE AUX PHENOMENES GEOMECHANQUES DANS LE CHAMP PROCHE



ARTELIA Eau et environnement

6 rue de Lorraine
38130 – Echirolles
France
Tel. : +33 (0) 4 76 33 43 32
Fax : +33 (0) 4 76 33 43 74



K-UTEC AG Salt Technologies

Am Petersenschacht 7
99706 Sonderhausen
Germany
Tel. : +49 3632 610 100
Fax : +49 3632 610 105



Institut für Gebirgsmechanik GmbH (IfG)

Friederikenstr. 60
04279 Leipzig
Germany
Tel.: 0049-341-33600-220
Fax: 0049-341-33600-308

SOMMAIRE

1. INTRODUCTION	1	
2. GEOMECHANICAL ASSESSMENT OF CONVERGENCE AND FLOODING PROCESS	2	
2.1. OBJECTIVES	2	
2.2. MECHANICAL BEHAVIOR OF THE SALT MASS	2	
2.2.1. Long-term deformation mechanisms - Fundamentals		2
2.2.2. Geomechanical studies on the StocaMine storage facility		4
2.2.3. INERIS-approach		5
2.2.3.1. CREEP		6
2.2.3.2. DAMAGE		8
2.2.4. Closure of underground openings in the storage area		9
2.3. ASSESMENT OF THE ASSUMED CONVERGENCE SCENARIO	11	
2.3.1. The INERIS reference scenario / IfG approach		11
2.3.2. Initial convergence (open) and subsidence rate with and without self-backfilling		12
2.3.3. Convergence of flooded cavities		14
2.4. CONCLUSIONS	17	
3. GEOTECHNICAL MULTI-BARRIERS CONCEPT	19	
3.1. INTRODUCTION	19	
3.2. GEOLOGICAL BARRIER – THE SALT	21	
3.2.1. Investigation approach		21
3.2.2. Hydro-mechanical behavior of salt - synopsis		22
3.2.3. The geological barrier at the StocaMine		24
3.2.4. Minimum salt barrier thickness – analogues		26
3.2.5. In situ-permeability in the undisturbed and disturbed state		28
3.2.6. Evaluation of the transient state – numerical modelling		32
3.2.7. Consequences of damage caused by fire in block 15		34
3.2.8. Assessment of the long term stability of the pillar system		36
3.2.9. Summary		38
3.3. SEALING CONCEPT	40	
3.3.1. Investigation approach		40
3.3.2. The ERCOSPLAN concept		40
3.3.3. Assessment in terms of the present international experiences		44
3.3.4. Proof of function of sealing dams in a disposal facility		48
3.3.5. Back-filling measures in the storage area		50
3.3.6. Summary		52
3.4. RECOVERY OF HYDRAULIC INTEGRITY WITHIN THE STORAGE REPOSITORY	53	
3.4.1. Lab results		53
3.4.2. Field observations		56
3.4.3. Evaluation of the site conditions - Numerical simulations		58
3.4.4. Conclusions		61
3.5. GROUNDWATER INFLOW AND OUTFLOW SCENARIO INSIDE THE WASTE REPOSITORY	62	
LITERATURE	63	

TABLEAUX

TABL. 1 -	RELATION BETWEEN CREEP CLASS K AND PRE-COEFFICIENT V	7
TABL. 2 -	PARAMETERS OF THE APPLIED NORTON MODEL FOR THE ROCK SALT	7
TABL. 3 -	TIME-DEPENDENT CONVERGENCE BEHAVIOR (PRE-REQUISITE: DRY; INITIAL CONVERGENCE AT T_0 $VV = 0.1\%/A$) – GREEN: SCHREINER-APPROACH (3) (WITH BACKFILL); ORANGE: APPROACH (1).	13
TABL. 4 -	TIME-DEPENDENT CONVERGENCE BEHAVIOR (PREREQUISITE: FLOODED).	16
TABL. 5 -	DAM CONSTRUCTIONS OF THE STOCAMINE – GEOMETRY, MEAN DIAMETER INCL. DILATED ZONES (EDZ) AS WELL AS NEW ALZ AFTER REMOVAL OF EDZ (DRIFT SURFACE CUTTING).	43
TABL. 6 -	CALIBRATED PARAMETERS OF STORMONT'S LAW FOR THE WITTELSHEIM ROCK SALT.	59

FIGURES

FIG. 1.	SCHEMATIC DRAWINGS OF A) PHENOMENOLOGICAL CREEP PHASES, AND B) MICROSTRUCTURAL PROCESSES THAT CAN OPERATE DURING DEFORMATION OF ROCK SALT AT TEMPERATURES IN THE RANGE 20 – 200°C. DIFFERENT SHADES OF GREEN REPRESENT CRYSTALS WITH DIFFERENT ORIENTATIONS (URAI & SPIERS, 2007)	3
FIG. 2.	CREEP OF ROCK SALT FROM THE STOCAMINE IN COMPARISON TO ROCK SALT FROM DIFFERENT SITES AND STRATIGRAPHY (REFERENCE TEMPERATURE: 22°C).	6
FIG. 3.	FAILURE AND DAMAGE CRITERIA IN COMPRESSION AND EXTENSION FOR MDPA SALT (THOREL & GHOREYCHI, 1996)	9
FIG. 4.	QUASI-LINEAR DEFORMATION CHANGES (ROOM CLOSURE) OVER TIME, MEASURED AT THE STOCAMINE. THE RED LINE INDICATES THE AVERAGE OF 0,9%/YEAR.	10
FIG. 5.	MINING FIELD GEOMETRY - SYSTEM-SURFACE.	12
FIG. 6.	GEOMECHANICAL PROGRESS OF CONVERGENCE UNDER CONSIDERATION OF VARIOUS CALCULATION APPROACHES.	13
FIG. 7.	GEOMECHANICAL PROGRESS OF CONVERGENCE UNDER CONSIDERATION OF VARIOUS CALCULATION APPROACHES AND CONSIDERING A BRINE INFLOW AFTER CA. 240 YEARS.	15
FIG. 8.	MEASUREMENTS OF THE SURFACE SUBSIDENCE ABOVE MINING AREAS IN SALINIFEROUS DEPOSITS BEFORE AND AFTER FLOODING. LEFT (A): SUBSIDENCE-DIAGRAM OF FLOODING OF THE FRIEDENSHALL MINE (GER) (PELZEL ET AL., 1972); AND RIGHT (B): SUBSIDENCE-DIAGRAM OF FLOODING OF THE PLÖMNITZ MINE (GER) (TINCELIN & WILKE (1991).	15
FIG. 9.	SCHEMATIC OVERVIEW OF THE SAFETY CONCEPT "MULTI-BARRIER SYSTEM" FOR THE UNDERGROUND WASTE DISPOSAL OF STOCAMINE (TAKEN FROM ERCOSPLAN, 2013). THE GREEN CIRCLE INDICATES THE "ISOLATING ROCK ZONE" (IRD), I.E. THE NEAR-FIELD BARRIER COMPLEX.	20
FIG. 10.	THE "DILATANCY CONCEPT" – CURRENT UNDERSTANDING OF THE BEHAVIOUR OF THE EDZ IN ROCK SALT AS A FUNCTION OF STRESS STATE (MODIFIED AFTER HUNSCHKE & SCHULZE, 2002).	23
FIG. 11.	GEOLOGICAL SITUATION. A) GENERAL STRATIGRAPHY BASIN OF MULHOUSE. B) DETAILED GEOLOGICAL PROFILE STOCAMINE.	25
FIG. 12.	INTEGRITY OF THE GEOLOGICAL BARRIER AFTER THE ROCK BURST. IN ADDITION, TYPICAL GAS FRAC PATTERNS ARE SHOWN (THE CORE SAMPLES WERE RECOVERED BY A 250M LONG BOREHOLE DRILLED INTO THE FORMER GAS FRAC ZONE. (LEFT) PERMEABILITY IN THE LOWER WERRA ROCK SALT NA1 α A FEW SECONDS AFTER THE ROCK BURST. (RIGHT) TIME DEPENDENT RECOVERY OF INTEGRITY AS CHARACTERIZED BY THE MINIMUM PRINCIPAL STRESS σ_{MIN} .	27
FIG. 13.	BOREHOLE SET-UP A) USED BY COSENZA ET AL. (1999); B) POSITION AND ORIENTATION OF REFERENCE HOLES AT THE SITES INVESTIGATED BY IBEWA (2013A, B).	29
FIG. 14.	SITES FOR THE PERMEABILITY MEASUREMENTS [EXPLANATION: BLUE MARK AREA – MASSIVE PILLAR OF POTASH MINING FIELD IN THE HANGING WALL]. T1-X AND T2-X INDICATE DIFFERENT MEASURING CAMPAIGNS (TAKEN FROM IBEW, 2013A).	30
FIG. 15.	PROFILES OF PERMEABILITY WITH THE DISTANCE TO THE EXCAVATION FOR BOREHOLES DRILLED AT VARIOUS ORIENTATIONS TO THE DRIFT, THROUGH THE PILLAR ZONE - CASE OF DOUBLE TUNNELS (MODIFIED AFTER IBEWA, 2013A).	30
FIG. 16.	PLASTIC VOLUMETRIC DEFORMATION IN % IN THE DRIFT CONTOUR AFTER 28 YEARS FREE CREEP BEFORE CONTOUR CUTTING (LEFT HAND SIDE) AND AFTER CONTOUR CUTTING (RIGHT HAND SIDE) (TAKEN FROM KAMLOT ET AL., 2012).	33
FIG. 17.	LOCATION OF THE DAMAGED AREA AROUND THE STORAGE AREA (TAKEN FROM ITASCA, 2012)	33
FIG. 18.	LOAD BEARING STRENGTH OF QUADRATIC SALT PILLARS. A) PILLAR STRENGTH (σ_{PF}) OF VARIOUS SERIES OF LOADING TESTS ON DIFFERENT SALT SPECIES VS. PILLAR HEIGHT-WIDTHS RATIO ($H : W =$ SLENDERNESS RATIO) (TAKEN FROM UHLENBECKER, 1974); B) PILLAR STRENGTH (σ_{PF}) VS. ASPECT RATIO $W : H$, AFTER FORMULA 4.2.	36
FIG. 19.	CONCEPTUAL DESIGN OF THE DRIFT SEALING DAM (TAKEN FROM ERCOSPLAN, 2013)	42
FIG. 20.	OBSERVATIONS AFTER DISMANTLING THE SONDRSHAUSEN DAM. A) MEASURED FLUID DISTRIBUTION IN THE SEALING ELEMENT I (VERTICAL CROSS SECTION) B) OUTFLOW OF BRINE FROM THE WET ROCK CONTOUR THROUGH A BOREHOLE IN THE ROOF (AFTER SITZ, 2003)	42
FIG. 21.	THE DAM-BUILDING LEOPOLDSHALL (DIMENSION IN M) (AFTER FLIß, 2003).	44
FIG. 22.	CONCEPT OF THE DRIFT SEAL IMMENRODE (AFTER ALAND ET AL., 1999).	45

FIG. 23.	REALIZED MOCK-UP TESTS OF MGO-BASED DRIFT SEALS IN R&D-PROJECT CARLA AT THE TEUTSCHENTHAL MINE. A) SITE CONCRETE DAM GV1. B) SHOTCRETE DAM GV2 (AFTER GTS, 2010).	46
FIG. 24.	FLOW RATES (LEFT) VS. LENGTH OF THE DAM (SEALING ELEMENT) AND (RIGHT) VS. FLUID PRESSURE.	50
FIG. 25.	EVOLUTION OF PERMEABILITY IN DEPENDENCE ON TIME DURING STEPPED ISOSTATIC LOADING WITH A TIME DEPENDENT TRANSIENT COMPACTION AND DECREASE OF THE PERMEABILITY. EXPERIMENTAL RESULTS OF TWO EXPERIMENTS (ARROWS AND CIRCLES) ARE DEPICTED, WHICH REPRESENTS SIMILAR PRE-DAMAGE CONDITIONS (POPP ET AL., 2012).	54
FIG. 26.	FIG. PRESSURE INDUCED PERMEABILITY DECREASE WITH TIME. A) EVALUATION OF ISOSTATIC LONG-TERM COMPACTION TESTS WITH CONTINUOUS PERMEABILITY MONITORING (COMPARE FIGURE 8) USING A SIMPLE EXPONENTIAL APPROACH. B) DEVELOPMENT OF THE NORMALIZED PERMEABILITY WITH TIME AT VARIOUS PRESSURE STAGES ACCORDING TO THE RESPECTIVE COMPACTION COEFFICIENTS A AS DETERMINED BEFORE (POPP ET AL., 2012).	55
FIG. 27.	PERMEABILITY-POROSITY RELATIONSHIP FOR DILATED ROCK SALT AT $\sigma_{MIN} = 2$ AND 10 MPA (TAKEN FROM POPP, 2002) AND THE REVERSE CASE CASE DURING COMPACTION OF PRE-DILATED SALT (ASSE-ROCK SALT: PROBEN 208 / K1 UND K4) (AFTER POPP ET AL. 2007).	55
FIG. 28.	DEVELOPMENT OF NEW FRACTURE PLANES DURING DIRECT TENSIONAL STRENGTH TESTS AFTER HEALING OF ALREADY FRACTURIZED SALT SAMPLES (AFTER MINKLEY ET AL., 2005).	56
FIG. 29.	CLOSURE OF UNDERGROUND OPENINGS; OBSERVATIONS AT THE ASSE SALT MINE FROM PARTLY BACK-FILLED DRIFT (RESIDUALS OF POTASH HOT-LEACHING) – SCALE BAR CA. 30 CM.	56
FIG. 30.	PROFILES OF PERMEABILITY AROUND THE BULHEAD (LEFT) AND THE NEIGHBORED OPEN DRIFT (RIGHT) (AFTER WIECZOREK & SCHWARZIANEK, 2004).	57
FIG. 31.	CROSS SECTIONS OF CORE MATERIAL ($\varnothing = 100$ MM) FROM THE CONTACT ZONE BETWEEN SALT CONCRETE AND SALT. (RIGHT) THE ARROW INDICATES SEALED SALT CONTOUR FRACTURES.	57
FIG. 32.	PERMEABILITY VS. MEAN STRESS VARIATION LAW FOR THE ROCK SALT (ITASCA, 2013B).	59
FIG. 33.	PERMEABILITY EVOLUTION OVER 5,000 YEARS ALONG A VERTICAL PROFILE IN THE ROOF OF A SEALED DRIFT (TAKEN FROM ITASCA, 2013B).	60

1. INTRODUCTION

Cette note présente les certains aspects techniques répondant au premier point de la demande de tierce expertise formulée par le préfet du Haut Rhin (en date du 17 février 2015).

L'étude de sureté du confinement des déchets à long terme dans le milieu récepteur, en partie présentée ici, porte sur:

- les phénomènes géomécaniques de convergence du sel,
- le concept de confinement multi-barrière (barrière géologique, barrages, récupération des caractéristiques hydrauliques du stockage, ...)

Cette note est rédigée par les experts géomécaniciens du sel de l'*Institut für Gebirgsmechanik* (IfG).

2. GEOMECHANICAL ASSESSMENT OF CONVERGENCE AND FLOODING PROCESS

2.1. OBJECTIVES

Assessment of the fundamentals and the reliability of all conclusions regarding the closure of the underground openings is the main impact factor to assess the risks associated with the unlimited storage of industrial waste in the StocaMine.

There are two reasons for detailed analyses of the convergence rates of the various underground openings (storage area, access drifts, caved terrain), together with the following problems:

- Impact of creep convergence on the movement of pollutants towards the outside.
- Time dependent closure or healing of localized damage in the dilated rock contour around underground workings. This topic will be also discussed in more detail in section 3.4.

Despite significant progress in the knowledge of salt mechanical behavior over 30 last years, long-term risk assessment of the underground structures in salt formations remains a challenge. This is because the coupling between creep and damage of salt is not simple. However, storage of hazardous waste in the StocaMine is not paradoxical if reliable conclusions about the long-term safety can be drawn based on well documented and proven safety assessment which is mainly based on the work of INERIS (2010).

The approach adopted in the following is based on a critical analysis of the existing knowledge and assumptions, in particular the studies conducted by INERIS and by Ecole des Mines Paris. The analysis will focus on the following points:

- Geomechanical studies at the StocaMine Site – reliability of INERIS approaches
- Initial convergence of open cavities and subsidence under or without consideration of the process of self-backfill – Are the results in the frame of general experiences?
- Impact of flooding on creep – convergence of flooded cavities

Because an understanding of the mechanical and rheological behaviour of salt is essential for predicting deformations and stresses around underground openings of repository in an evaporite formation that may occur in the long term, first a short introduction in the general deformation characteristics of salt is given.

2.2. MECHANICAL BEHAVIOR OF THE SALT MASS

2.2.1. Long-term deformation mechanisms - Fundamentals

In recent decades, several research groups have compiled a large experimental and theoretical database on the geomechanical behavior of rock salt. The progress of understanding on the deformation behavior of salt, related to its various aspects (e.g. mining, experimental, modelling), is documented, besides an enormous amount of literature, published elsewhere, in the proceedings of the so-called conferences on "The Mechanical Behavior of Salt" which have been taking place since the beginning of the 1980's:

- 1st Conference: Pennsylvania State University, USA. 9-11 November 1981;
- 2nd Conference: Hannover, Germany. 24-28 September 1984;
- 3rd Conference: Palaiseau, France. 14-16 September 1993;
- 4th Conference: Montreal, Canada. 17-18 June 1996;
- 5th Conference: Bucharest, Romania. 9-11 August 1999;
- 6th Conference: Hannover, Germany. 22-25 May 2007;
- 7th Conference: Paris, France. 16-19 April 2012; and
- 8th Conference: Rapid City, Germany. 26-28 May 2015.

It is well known that the deformation of salt rock has components of elastic and visco-plastic strain. The time-dependent stress-strain behaviour is denoted as creep. Creep may be classified into the following three phases according to the typical behaviour observed in a creep test (see Fig. 1a):

- Primary creep, also denoted as transient or non-stationary creep;
- Secondary or stationary creep; and
- Tertiary creep or creep failure.

These three phases of creep are closely related, and they change into each other as a result of intra-crystalline deformation processes, corresponding to the range of load and temperature conditions. The deformation mechanisms known to operate at temperatures relevant for engineering and natural halokinetic conditions (20 – 200°C) are summarized in Fig. 1a.

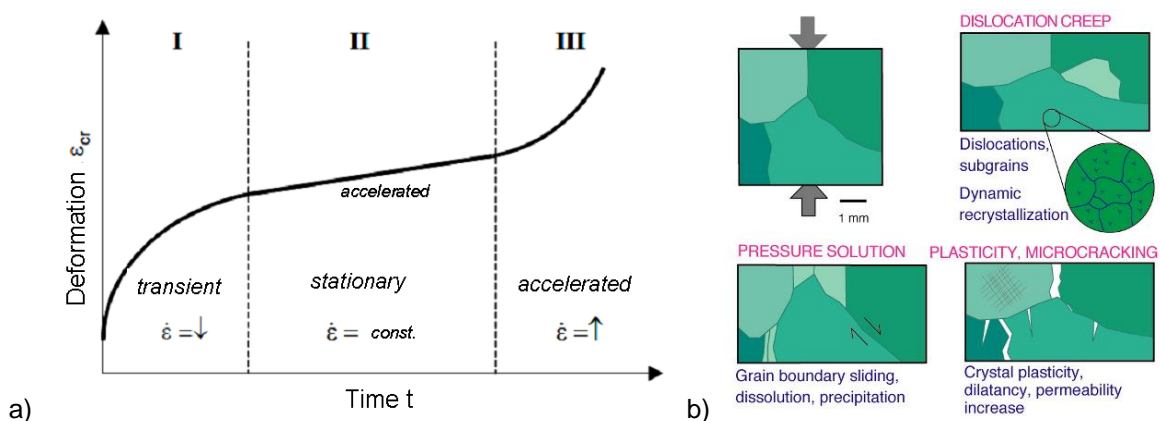


Fig. 1. Schematic drawings of a) phenomenological creep phases, and b) microstructural processes that can operate during deformation of rock salt at temperatures in the range 20 – 200°C. Different shades of green represent crystals with different orientations (Urai & Spiers, 2007)

Primary creep is characterized by high deformation rates which decrease continuously until a stationary creep rate is reached, i.e. secondary creep. The process for primary creep and the creep rate controlling mechanism results from the movement of dislocations (i.e. imperfections in the [salt] crystal lattice) through the crystal, dominated by cross-slip and/or climb controlled dislocation creep mechanisms. The dislocations start to move when stress increases. The dislocations raise the energy of the crystal lattice, and the process of dislocation movement is driven by the stress field and by the crystal lattice trying to achieve a lower energy level. It leads to lattice preferred orientations, dislocation substructures, subgrain formation and dynamic re-crystallization.

With increasing deformation, the capacity of the existing dislocations to move diminishes. If the deformation continues, new dislocations will be produced within the crystal lattice. Thus, the dislocation density rises, and this process causes an increasing resistance to deformation. The deformation rate will decrease even when the load is kept constant; to maintain a constant deformation rate an increasing force is necessary. This material hardening, which increases with increasing deformation, is counteracted by the annihilation of dislocations. This process results in stationary creep if the formation rate becomes equal to the annihilation rate of the dislocations. In this phase, the dislocation density (microscopic scale), the deformation resistance, and consequently the creep rate (macroscopic), evolve to constant values. At the same time, subgrains are formed in the halite, and the diameter of the subgrains is correlated with the deviatoric stress (e.g. Urai & Spiers, 2012).

Tertiary creep is caused by intra-crystalline fissures, i.e. damage. Damage occurs only if the applied stress exceeds the dilatancy boundary (see 3.2.2). Closely associated with the development of damage is volume dilatancy. If either the damage or the strain reaches a critical value, creep will change into the tertiary phase and creep-failure will occur.

Both in the field and also in laboratory experiments, the type of deformation (i.e. brittle or ductile) depends strongly on the load conditions, temperature and the humidity content, e.g. Urai & Spiers, 2007; Hunsche & Schulze, 1996, 2002. At very low effective confining pressures (i.e. less than 3 – 5 MPa) and high deviatoric stresses, inter- and intra-granular micro-cracking, grain rotation and inter-granular slip are important strain accumulating processes alongside crystal plasticity, and the mechanical properties and dilatational behavior are dependent on the effective mean stress or effective confining pressure (for illustration of the different deformation mechanisms see Fig. 1b). At high enough deviatoric stresses, the material fails in a (semi-) brittle manner, with failure described by a pressure (effective mean stress) dependent failure envelope. With increasing effective mean stress, micro-cracking and dilatancy are suppressed, and crystal plasticity dominates.

However, if the polycrystal contains small but significant amounts of water in the form of saturated brine inclusions or grain boundary films, as is generally the case for both natural and synthetic samples, fluid assisted grain boundary migration is an efficient process of reducing dislocation density, and hence removing the stored energy of dislocations, even at room temperature (e.g. Urai & Spiers, 2012).

While dislocation creep processes take place in the crystal lattice of the halite grains, solution-precipitation creep, or “pressure solution”, is a process that occurs in the grain boundaries. This process is accompanied by inter-granular sliding and rotation (grain rearrangement), and can lead to compaction of porous salt or to deviatoric strain of non-porous aggregates.

2.2.2. Geomechanical studies on the StocaMine storage facility

In addition to the more general (site-independent) understanding of the deformation behavior of salt reported before the specific knowledge adopted for the geomechanical assessment of the StocaMine is based on comprehensive knowledge obtained from the following sources:

- An analysis of previous studies ordered by StocaMine: in particular, the studies conducted by Ecole des Mines de Paris (under the authorisation file, 2006 and 2009 studies) – Laouafa (2010).
- Analysis of the in situ measurements and data available to StocaMine:
 - Relative horizontal and vertical strain measurements in the storage drifts;

- Surface subsidence measurements, made by MDPA, resulting from the closure of underground cavities and compaction of self-backfill of caved terrain (MDPA, 2008).
- Consideration of general knowledge due to research in France and abroad:
- in particular, research done by Ecole Polytechnique during the 1990s, as part of European and ANDRA programmes (5th R&D framework programme). This concerns three important in situ experiments, conducted in the MDPA Amélie mine (close to the StocaMine site):
 - two thermo-mechanical experiments (Ghoreychi, 1991 and Kazan and Ghoreychi, 1996) ⇒ PhD: Y.N. Kazan (1996)
 - one experiment on the permeability of salt and "mechanical-transport" couplings (Cosenza, 1996) ⇒ PhD: P. Cosenza (1996)
 - In addition, numerous laboratory tests were carried out on salt samples taken from in situ test sites. They led to the development of rheological models characterising
 - creep (Pouya, 1991) and ⇒ PhD: Pouya, A. (1991)
 - damage to salt in the Amélie mine ⇒ PhD: Thorel, L. (1994)
- Numerical 3D and 2D modelling-studies of storage and neighbored structures, done by INERIS, 2010 (see below).

Most of the results are summarized in ETUDE GEOMECANIQUE DU STOCKAGE DE STOCAMINE (INERIS 2010). The study was driven by three objectives:

- The evaluation / assessment of the mechanical stability of the storage site and the corresponding access infrastructures, with detailed studies of accessibility to the site in a medium term, and possibilities of destocking at short or long-term.
- The assessment of creep rate / creep velocity of the different structures (storage areas, drifts, caved stope areas), linked to the problem of impact of the creep rate on the migration of contaminants, and the possibility of access to the underground site during time.
- Assessment of damages on the storage roof induced by the Block 15 fire which underlined the question of a possible hydraulic connection through the damaged salt formations (for discussion of this topic, see section 3.2.7).

2.2.3. INERIS-approach

The INERIS approach bases on a comprehensive description of the mechanical salt behavior. As mentioned in section 2.2.1 deformation of salt is attributed to have components of elastic and visco-plastic strain, whereby its rheological behavior is characterized by:

- irreversible deformations (visco-plasticity) occur under any deviatoric stress independently of the mean stress, i.e. no creep boundary exists. As a consequence, the following results:
 - any stress deviator in the salt relaxes completely over time, i.e. during the long-term (geologic times) an isostatic stress state is usually reached.
 - any cavity excavated in the salt will be close with time (over a period depending on the depth), but the convergence will be delayed to the impact of self-backfill, i.e. brittle deformation in the rock contour will produce crushed salt components which will impede the room closure. However, humidity will accelerate this process and results in weakening (see below).

- the resulting creep rate increases non linearly with the deviatoric stress, the humidity and the temperature (see below).

In addition, it has to be taken in mind, that at a given threshold for damage, that depends on the mean (or minimal) stress and the deviatoric stress, i.e. the so-called dilatancy boundary (see section 3.2.2 respectively Fig. 10) cracks are initiated and the creep rate accelerates (tertiary creep).

2.2.3.1. CREEP

To represent the long-term creep behavior usually the secondary creep rates are experimentally determined in creep tests (not shown here), whereby the resulting secondary creep rate ϵ_{cs} is majorly dominated by the 2nd invariant of the stress deviator resulting from the differential stress:

$$\sigma_{\text{eff}} = \sqrt{\frac{1}{2} \cdot [(\sigma_1 - \sigma_2)^2 + (\sigma_2 - \sigma_3)^2 + (\sigma_3 - \sigma_1)^2]} \tag{2-1}$$

For comparison the creep test results are presented in a double-logarithmic diagram of creep rate vs. differential stress, representing a significant data scatter (Fig. 2).

For the StocaMine the interrelation of creep rate vs. differential stress is represented by two principal rheological models, proposed by the different authors (mentioned above): (1) the Lemaitre model (e.g. Pouya, 1991) and (2) the NORTON model (used by INERIS). The difference between these two models is the evolution of creep with time for a constant state of stress.

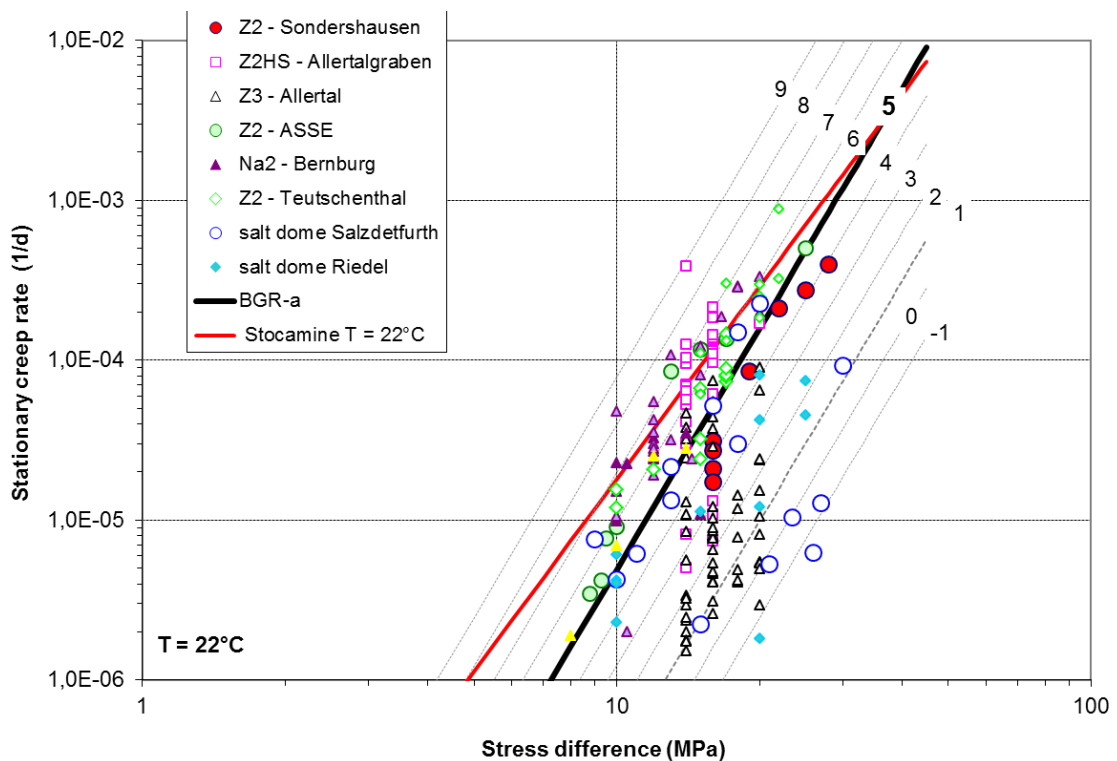


Fig. 2. Creep of rock salt from the StocaMine in comparison to rock salt from different sites and stratigraphy (reference temperature: 22°C).

According to Lemaitre model, the creep rate reduces with time, i.e., both, steady-state and transient behavior, are described by the same power law. On the contrary, Norton model considers that, after a short transition phase, the creep reaches a stationary regime (linear evolution), where only a change of the stress state – for example the modification of the excavation geometry due to creep – can affect the rate of creep.

In the Wittelsheim disposal site, in situ measurements have showed that convergences vary quasi-linearly with time over a period of around ten years. Consequently, studies by INERIS and others have adopted the NORTON model, which is the classical description for dislocation creep.

In the NORTON-approach (non-dilatant deformation), $\dot{\varepsilon}_{CS}$ results from:

$$\dot{\varepsilon}_{CS} = V \cdot A_s \cdot \exp\left(\frac{-Q_{DC}}{RT}\right) (\sigma_1 - \sigma_3)^n \quad (2-2)$$

with A_s is a material parameter, Q_{DC} represent the (apparent) activation energy for dislocation creep, R is the gas constant, T is the absolute temperature, σ_1 and σ_3 are the maximum and minimum principal compressive stresses, and n is the exponent of stress.

Because the creep behavior of salt rocks shows a significant variation by a few factors (e.g. due to variations in size and distribution of secondary constituents or grain size of the rock salt matrix) the BGR¹ developed so-called creep classes to describe these variations and to categorize the creep behavior. Therefore, a pre-coefficient V is prefixed to the creep law BGR-a (for details see Plischke, 2007; Hunsche et al, 2003):

$$V = \frac{2^K}{32} \quad \text{with } K = \text{creep class} \quad (2-3)$$

Tabl. 1 - depicts the relation between creep classes K and pre-coefficient V . Creep class 5 equates to the reference creep law BGR-a.

Tabl. 1 - Relation between creep class K and pre-coefficient V

Creep Class K	0	1	2	3	4	5	6	7	8	9
Pre-Coefficient V	1/32	1/16	1/8	1/4	1/2	1	2	4	6	8

INERIS (respectively ITASCA) used a more comprehended form:

$$\dot{\varepsilon}_{CS} = V \cdot A \cdot \sigma_{eff}^n \quad (2-4)$$

$$\text{with } A = A_s \cdot \exp\left(-\frac{K_s}{T}\right) \quad (2-5)$$

The respective parameters of the Norton model are given in Tabl. 2 - .

Tabl. 2 - Parameters of the applied Norton model for the rock salt

Parameter	Description	Value
A_s (1/day)	Reference rate	0.015
n_s	Stress exponent	4
K_s (K)	Constant of Arrhenius law	4700

¹ Federal Institute for Geosciences and Natural Resources, Hannover, Germany.

T (K)	Temperature	308
---------	-------------	-----

The stationary creep as described by the INERIS-approach is depicted in Fig. 2 in comparison with rocksalt samples from other respectively with the standard creep-law BGRa. Regarding the relevancy of the various parameters the following points have to be noted:

- The slope of the stress/strain rate curve with $n = 4$ is lower than the reference BGRa, but n is usually between 3 and 5, depending on the variety of salt. that the deformation rate increases in a non-linear way with deviatoric stress. From this, we can see that the speed of convergence is multiplied by a factor of around 16, if the depth of the structure is doubled, e.g. from 500 m to 1000 m;
- The relationship for the StocaMine salt lies at the upper distribution fields of experiences from different sites. It is well known, that the so-called older rock salt (z2) creeps usually faster than the younger rock salt (z3), which is referred to the role of impurities (e.g. Hunsche et al., 2003). Nevertheless, the creep capability of the StocaMine salt is higher, which is usually observed for bedded salt, and which may be referred to higher interstitial water content.
- The diagram is valid for 22°C. Note that the deformation rate also increases exponentially with temperature. This dependency is expressed by Arrhenius' equation (frequently used in thermodynamics). For illustration purposes, a temperature increase of 10 K (in a temperature range of 20°C to 50°C) leads to an increase of the stationary creep rate to a factor 2 – 5 at differential stresses of 10 MPa. This factor is smaller at high temperatures and larger at little stresses.
- In addition, also wetting of salt results in creep acceleration (humidity-creep, see Hunsche et al., 2003) which is mainly referred to hydro-chemical weakening, due to various processes, e.g. grain boundary diffusional pressure solution and plasticity-coupled pressure solution (see e.g. Urai et al., 1986; Urai & Spiers, 2007). As consequence, the stress exponent n will become 1. In addition, increasing fluid pressures may change the deformation style (from ductile to brittle) due to the reduction of the effective stress (see below). – **These processes are not considered here.**

2.2.3.2. DAMAGE

Initiation of damage, i.e. opening of micro-cracks, means a loss of hydro-mechanical integrity due to development of permeability (see section 3.2.2). Usually, crack initiation or damage accumulation is referred to the following stress boundaries:

- Determination of the failure criterion by measuring rock strength using triaxial laboratory tests. As for other rocks, rock salt compressive strength depends on strain rate (Wallner, 1981).
- Determination of dilatancy criterion, i.e. using different indicators of crack initiation, e.g. volume change, ultrasonic velocities or permeability.

To assess the amplitude and extension of the damaged areas around the storage facility and access tunnels, the model developed by Thorel (1994).

It defines initiation of damage as the onset of irreversible volumetric strains, which is measured during laboratory experiments. Axisymmetric triaxial tests following compression and extension stress paths have been performed, with an overall volumetric strain measurement. The experimental results are used to set up a non-standard elastoplastic model dealing with instantaneous mechanical behavior of rocksalt. The derived model corresponds qualitatively to other approaches, e.g. Cristescu & Hunsche (1991) and Hunsche (1993).

The experimentally derived failure and the dilatancy boundary are depicted in Fig. 3. It can be seen, that all dilatant creep data are found systematically above the failure criterion whereas non-dilatant creep data are gathered below this criterion (compare also Fig. 10).

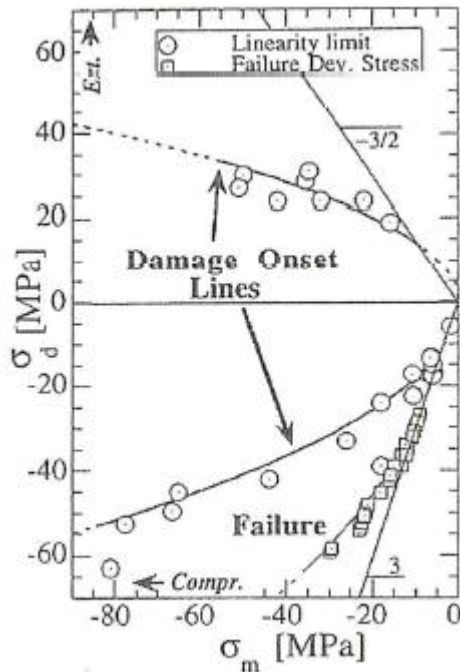


Fig. 3. Failure and damage criteria in compression and extension for MDPA salt (Thorel & Ghoreychi, 1996)

In summary, it can be stated that the rock-mechanical approaches used by INERIS represent a sufficient base for assessment of time- and damage dependent processes taking place during underground-openings in salt.

2.2.4. Closure of underground openings in the storage area

Convergence measurements (relative distance between two reference points) started at the StocaMine between 1998 and 2002 in the various storage blocks and are still being taken in two or three places in each block in two sections at the east and west ends of the different blocks. Readings are taken every two or three months. They consist of measuring the distances between three pairs of reference points:

- between the roof and the wall, providing a reading for the vertical convergence, denoted H2;
- between the roof and the mid-height of the rooms, a measurement also intended to measure vertical convergence, denoted H1;
- between the mid-heights in the rooms (LAR), in order to measure horizontal convergence.

For each measurement, the relationship is given between the movement measured and the initial distance (height or width), expressed as a percentage, which facilitates the comparison of

measurements taken over distances varying to a greater or lesser extent, from one measurement base to another.

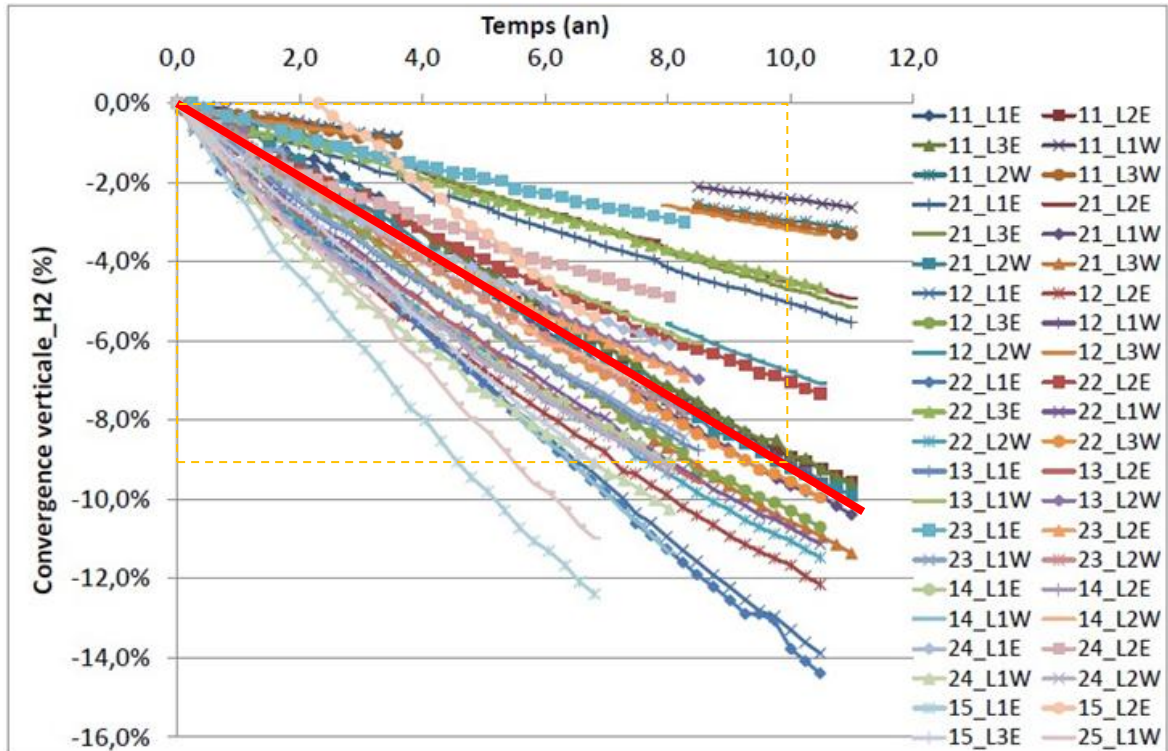


Fig. 4. Quasi-linear deformation changes (room closure) over time, measured at the StocaMine. The red line indicates the average of 0,9%/year.

As noted by INERIS (2010), the measurements are consistent and quite precise, in spite of the missing values. The measuring time covers actually more than 10 years and are continued, where access to the underground openings exist. The following points are worth to be noted:

- The changes in convergence are practically linear wherever they are measured (Fig. 4). This observation is attributed by INERIS to the specific mechanical behavior of rock salt, marked by steady state creep, i.e. no transient behavior is measured because the measurements started only some time after excavation of the underground openings.
- The average value for the blocks, estimated by INERIS is 0.92% per year, despite some systematical differences depending on the position of measuring position (random or center of the Storage area). The range varies between 0,5 and 1,4%/year.
- The "horizontal speed / vertical speed" ratio is 0.57, and shows that, for a given time, the horizontal convergence is less than the vertical (on average, the horizontal convergence speed is 0.53% a year as against 0.92% a year in the vertical direction).

Remark: As mentioned by INERIS, the reasons for the increased horizontal deformation are not well known. Probably, because the bedding acts a weakness plane shear displacement along the marl layers may result in higher deformation.

- Higher creep rates measured temporary in block 15 in 2003 (after the fire) are referred to the temperature impact, i.e. increasing temperatures accelerated the creep capability.

2.3. ASSESMENT OF THE ASSUMED CONVERGENCE SCENARIO

2.3.1. The INERIS reference scenario / IfG approach

A consequence of closure of underground openings is that the water or air contained in voids left by mine workings is forced to go elsewhere; in this particular case, creep is causing the flood waters to rise to the surface and, as they do so, towards the Alsace aquifer situated just above the mine. The creep effect diminishes over time, as the caved ground is compacted (effect of opposing forces), and finally stops when all the voids are closed.

With respect to the closure of the underground openings and the resulting long-term safety scenarios the following INERIS geomechanical conclusions are of crucial relevance, which therefore need to be proven regarding their correctness:

- The convergence rate roof / wall is expected to reach **0.9% per year (initial value)** for the storage area and double drifts at 550 m².
- The storage area (including drifts) is expected to be completely closed after about 200 years but INERIS mentioned that room closure usually does not result in waterproof "encapsulation", from a hydraulic point of view (i.e. the permeability in the drifts will be significant). The hypothesis of 5% to 10% residual opening after flooding with 90% of closure could be justified at depths of 1,000 m, but might probably be overestimated for the StocaMine scale.
- A compaction rate of **0.1% per year is expected before flooding**.
- Flooding will probably take place after several centuries (**in the reference scenario after 240 years**)³. Because the developing hydrostatic pressure of flooding, linked to brine and fresh water, will significantly decrease the stress deviator in the voids, the overall convergence rate will be reduced to 0.01% per year.

Due to the fact, that own numerical calculations regarding the large-scale subsidence behavior are not part of the task, an appraisal of the long-term convergence behavior of the disposal site of the mining area bases exclusively on analytic investigations. Two different approaches were used:

- In a first approach very simply only convergence of the open cavities is considered without the influence of self-backfill, whereby the actual residual volume can be estimated as follows:

$$V(t) = V_0 \cdot \exp\left(-\frac{\dot{V}}{V} \cdot t\right) \quad \text{with } V_0 = 300 \text{ Tm}^3 \quad \text{and } \frac{\dot{V}}{V} = 1\%/a \quad (\text{approach 1}) \quad (2-6)$$

Secondly, as worst case scenario the convergence rate was halved to 0,5%/a. (approach 2).

- A more sophisticated approach (SCHREINER approach: approach 3) bases on the empiric formulations of Schreiner & Kamlot (1991a, b). These were extended to consider possible effects of self-backfilling in cavities and openings due to contour failure (e.g. wall

² INERIS mentioned that the convergence rate is strongly influenced by the depth under the combined effect of (1) the stress deviator which is twice as strong at 1000m as at 500m resulting in 16x higher convergence rate (due to the power law creep law with a factor n = 4) and (2) the increased temperature of the solid rock which is close to 35°C at 550 m and 50°C at 1000 m. The temperature affects the creep rate exponentially (Arrhenius's equation) and leads to double the convergence rate between these two depths.

³The general brine level is expected to reach the storage area after 240 years, taking into consideration that about 7% (2.06 million m³) of the Western Sector is probably already flooded. The complete mine would be flooded after 305 years (StocaMine and upper levels from Amelie mine).

loosening, floor heave, roof failure). A detailed description is given as a technical IfG-report in the attachments. This should be used as reference for the INERIS assumptions.

It has to be mentioned, because only a rough testing of the above stated general assumptions should be performed, simplified mining action parameters (drift width 6 m, drift height 3 m) were assumed.

2.3.2. Initial convergence (open) and subsidence rate with and without self-backfilling

The investigated mining area is situated in shallow bedding, where short-pillar entry workings were realized. The abandoned pillars are of squared shape (Fig. 5). The main as well as the subordinated workings are identical and are of b_k whereby the heights in the mining area are constant with k .

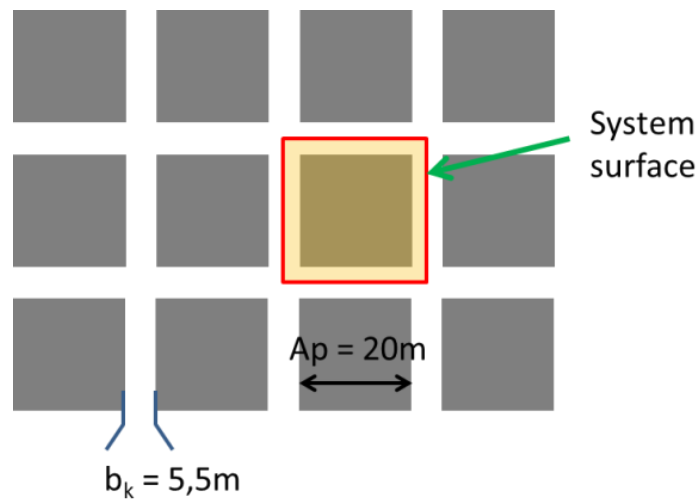


Fig. 5. Mining field geometry - system-surface.

Using the numerical evaluation as developed by SCHREINER, as well with the following parameters $a_p = 20$ m, $b_k = 6$ m, $h = 3$ m, and a relative volume creep rate of the intact rock of $n_k = 1\%/a$, results in a correlation between volume $V_{(\epsilon)}$ and volume convergence rate \dot{V}

$$1/\dot{V} = \frac{t_0}{V_{(\epsilon)}} - a \quad \text{with } t_0 = 265 a \text{ and } a = 0.2 a/m^3. \quad (2-7)$$

As final step the decrease of convergence rate resulting from the progressing reduction of cavity volume (under consideration backfill) can be predicted by integration of the linear differential equation in dependence of the durability t :

$$1/\dot{V} = \frac{dt}{dV} = \frac{t_0}{V} - a \Rightarrow dt = t_0 \cdot \frac{dV}{V(t)} - a \cdot dV \quad (2-8)$$

$$\Rightarrow t = \int_{V_0}^{V(t)} t_0 \cdot \frac{dV}{V} - a \cdot \Delta V(t) = t_0 \cdot \ln\left(\frac{V_0}{V(t)}\right) - a \cdot \Delta V(t) \quad (2-9)$$

Therefrom, the following volume convergence dependent on the durability can be calculated (see examples in Tabl. 3 -).

The resulting volume convergence respectively the convergence rate (under consideration of self-backfilling) and its progress are given in Fig. 6, in comparison with the so-called “simple” approaches with initial convergence rates of 1 resp. 0,5%/year..

Concerning the convergence-dependent development of the dilated respectively damaged zone it can be stated that these zone will strongly extend within a few decades. Assuming a convergence of $\frac{\Delta V}{V_0} = 40\%$ its maximum volume will be in the order of 1.2 of the initially mined volume or the double of the still open cavity volume.

Tabl. 3 - Time-dependent convergence behavior (pre-requisite: dry; initial convergence at $t_0 \frac{\dot{V}}{V} = 0.1\%/a$) – green: Schreiner-approach (3) (with backfill); orange: approach (1).

t	(3) $\frac{\Delta V}{V_0}$	(3) $\frac{\dot{V}}{V}$	(3) $V_{residual}$	(3) \dot{s}_{max}	(1) $\frac{\Delta V}{V_0}$	(1) $V_{residual}$
[a]	[-]	[%/a]	[Tm ³]	[mm/a]	[-]	[Tm ³]
0	0	1	300	12	1,00	300
11	0.1	0.78	270	10	0,90	271
26	0.2	0.60	240	7	0,78	233
45	0.3	0.47	210	6	0,64	193
69	0.4	0.36	180	4	0,50	151
101	0.5	0.27	150	3	0,37	110
143	0.6	0.20	120	2	0,24	72
203	0.7	0.14	90	2	0,13	39
295	0.8	0.09	60	1	0,05	16

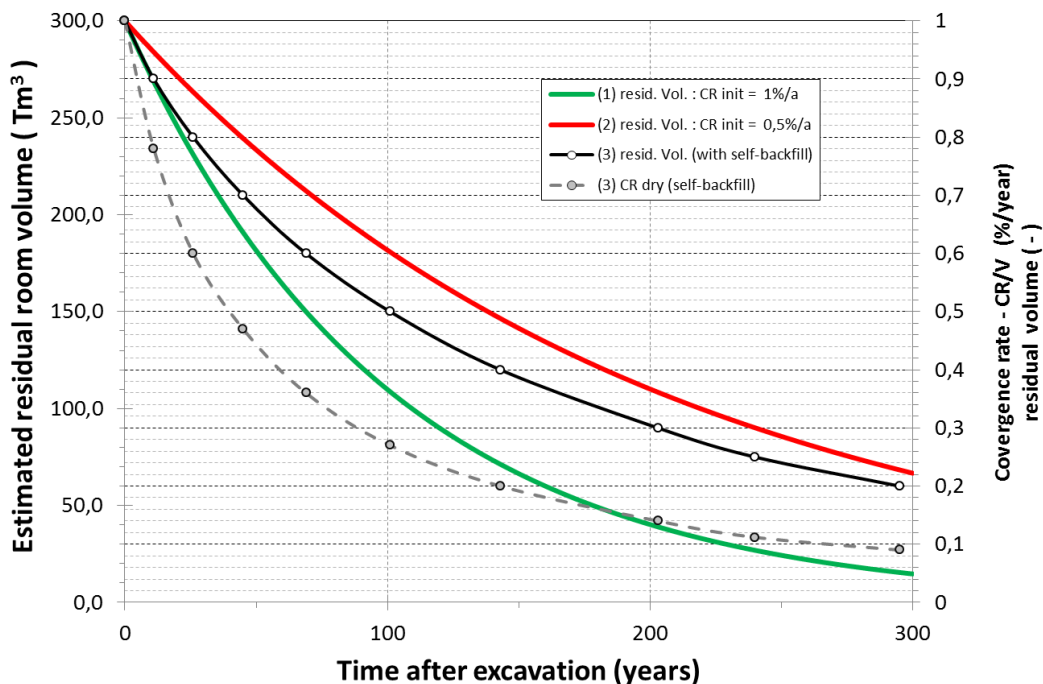


Fig. 6. Geomechanical progress of convergence under consideration of various calculation approaches.

The volume of the dilated and damaged zone will be reduced in the further convergence progress. After duration of 101 years the convergence is $\frac{\Delta V}{V_0} = 50\%$ and the maximum of the dilated and damaged zone is already reduced to 95%; after 250 years the convergence will be $\frac{\Delta V}{V_0} = 75\%$ and the volume of these zones will be reduced down to 58%. But, the volume of the EDZ will be the 2.76 of the open cavity volume. With ongoing convergence this ratio will increase (e.g. $\frac{\Delta V}{V_0} = 0.9$ in the order of 3) where the volume of the dilated and damaged zone will be reduced to 25% of the maximum value.

However, despite of self-backfill the resulting convergence rate is after 300 years in the order of around 0,1%/year (remaining cavity volume = ca. 60 Tm³ (20%)).

Comparison with the so-called simple exponential approach (reference scenario with convergence rate: 1%/year) demonstrates that the convergence rate is already in the order of 0,05% per year, which mainly results from a volume closure of about 95% (ca. 16 Tm³), which is unrealistic due to the effects of self-backfill.

However, if only an initial convergence rate of 0,5%/year is considered, after 300 years the remaining volume is 67 Tm³ (ca. 23%), i.e. slightly higher than the reference case Schreiner-approach (with backfill).

It can be stated, that after 300 years for all investigated cases a final convergence in the order of ca. 0,1%/year or lower is plausible.

In addition, also the effects of cavity closure on the resulting subsidence were estimated for the SCHREINER-approach. Under consideration of the geometry of the underground openings the maximum subsidence follows from:

$$\dot{s}_{max} = \frac{V}{(a_p + b_k)^2} \cdot \frac{\dot{V}}{V} \quad \text{with } V = 828 \text{ m}^3 \text{ (701 m}^3 \text{ for } b_k = 5.5 \text{ m} \\ \text{and } h = 2.8 \text{ m) and } a_p + b_k = 26 \text{ m (25.5 m)} \quad (2-10)$$

The resulting values are given in Tabl. 3 - . It can be stated that for t = 300 years, the subsidence rate = 1 mm/a which is nearly negligible.

2.3.3. Convergence of flooded cavities

Analyses of the inflow of surface water through the shafts led to the assessment, that the observed mining area will be flooded in ca. 240 years in the case that no additional flow barriers (dams) will be installed. At this time the open cavity volume would be reduced to 25% due to convergence. Assuming an open volume of 300 Tm³ at t = 0, then 75 Tm³ would be open and could be flooded.

The initial convergence rate for this mining area would be 1.12 0/00/a resp. 336 m³/a at dry conditions. Remarkably, flooding would result, as far as known from experiences with other potash deposits in a strong increase (3 times) of this rate, i.e. 3.5 0/00/a resp. 1050 m³ per year (see Fig. 7).

This assumption of a temporarily increase of the convergence rate in the given order is proven by documented convergence leap while flooding of the Friedenshall Mine (GER) as shown in Fig. 8. The therefore majorly responsible effect is the so-called humidity-induced creep (increase of the creep rate by increasing humidity due to the humidity-supported reduction of relocation status within the NaCl crystal lattice) was intensely investigated and quantifies by BGR Hannover in the 90's of the last century. It has to be noted that this effect mainly occurs in loosened or dilated rock salt (e.g. contour zones of pillars or galleries) and decreases with increasing load-bearing (i.e. in Hunsche & Schulze, 1996, 2003).

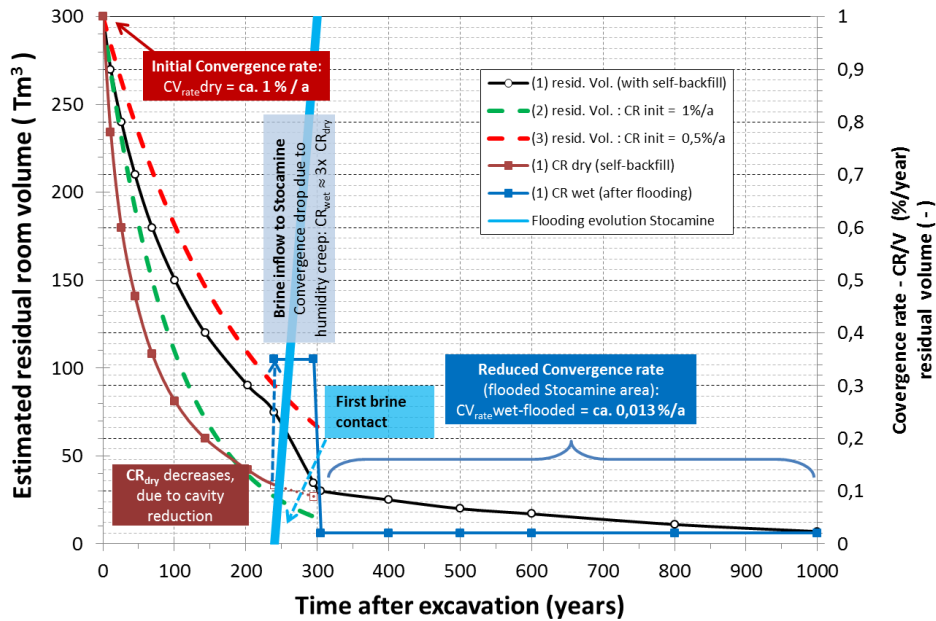


Fig. 7. Geomechanical progress of convergence under consideration of various calculation approaches and considering a brine inflow after ca. 240 years.

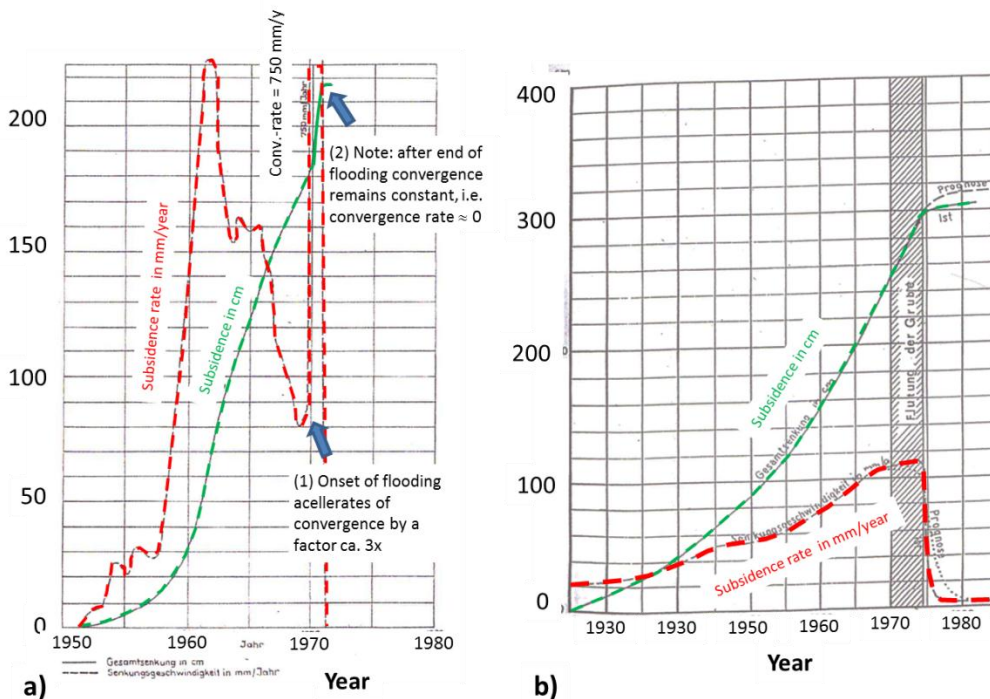


Fig. 8. Measurements of the surface subsidence above mining areas in saliniferous deposits before and after flooding. Left (a): subsidence-diagram of flooding of the Friedenshall Mine (GER) (Pelzel et al., 1972); and Right (b): subsidence-diagram of flooding of the Plömnitz Mine (GER) (Tincelin & Wilke (1991).

The humidity-induced increase of the volume convergence while flooding of the StocaMine area is given Fig. 7, whereby a strong leap in the cavity evolution occurs. This results in an approximation of the estimated residual volumes which were given by various assumptions. Finally, this supports the reliability of the simplified method of approach.

Furthermore it is given that the mine will be completely flooded within the successive 65 years. The convergence behavior for that period can be estimated as follows:

$$V(t) = V_0 \cdot \exp\left(-\frac{\dot{V}}{V} \cdot t\right) \quad \text{with } V_0 = 75 \text{ Tm}^3, t = 65 \text{ a und } \frac{\dot{V}}{V} = 0.014/\text{a} \quad (2-11)$$

Thereby, the open volume decreases in that final stage of flooding from ca. 75 Tm³ to 30 Tm³ and is only 10% of the recent volume (300 Tm³).

Tabl. 4 - . Time-dependent convergence behavior (prerequisite: flooded).

V _{residual} [Tm ³]	T [a]	\dot{V} [m ³ /a]
30	305	60
25	400	50
20	500	41
17	600	33
11	800	22
7	1000	15

The given convergence-dependent volume difference of 45 Tm³ equates the brine volume that is squeezed out within a period of 65 years (start of flooding until complete flooding of the mine) whereby the initial rate of ca. 1000 m³/a will reduce to ca. 400 m³/a, that means $\frac{\Delta V}{V} = 1.3 \text{ }^0/_{00}/\text{a}$.

Due to the rise of the brine level up to the upmost horizons of the overburden a hydraulic pressure within the mining area will develop after complete flooding of the mine.

Assuming a depth of 550 m and considering the before given mining parameters as well as a lithostatic pressure of $\gamma \cdot H = 12.65 \text{ MPa}$ (specific density), the pillar load bearing capacity reduces in the given working of $\frac{(a_p + b_k)^2}{a_p^2} = 1.69$ (1.625 for $b_k = 5.5 \text{ m}$) from $\sigma_p = 21.3 \text{ MPa}$ (20.55 MPa) to $\sigma_p = 16.8 \text{ MPa}$ (16.2 MPa). This results in a reduction of the acting stress deviator (vertical stress minus the horizontal stress) to the half and the convergence rate to 1/6, i.e. $\frac{\Delta V}{V_0} = 0.2 \text{ }^0/_{00}/\text{a}$ resp. 60 m³/a, as well. The convergence progress could be estimated (as described; see Tabl. 4 -):

$$V(t) = V_0 \cdot \exp\left(-\frac{\dot{V}}{V} \Delta t\right) \quad \text{with } V_0 = 30 \text{ Tm}^3, \Delta t = 305 \text{ a and } \frac{\dot{V}}{V} = 0.002/\text{a}. \quad (2-12)$$

In this final flooding phase the convergence behavior within the flooded area is characterized by a mixture of broken material (mined rock) and saturated brine in a nearly constant ratio of $\frac{V}{V_{AZ} + V} = 0.25$. V is the brine quantity and V_{AZ} is the volume of broken material. This conglomerate is characterized of 6.7 t saliferous rocks and 1 m³ brine. Its density is ca 1950 kg/m³ and the water content is ca 11%. The convergence-dependent squeezing rate with an accordant conglomerate

volume of $\frac{V}{V+V_{AZ}}$ is ca. $0.5 \text{ }^0/_{00}/\text{a}$ (after complete flooding; $V = 30 \text{ Tm}^3$, $t = 305 \text{ a}$) and will be nearly constant (with $0.4 - 0.5 \text{ }^0/_{00}/\text{a}$) with further lifetime.

2.4. CONCLUSIONS

The geomechanical studies carried out by INERIS deliver the fundamental base for discussing the different scenarios for the future of the StocaMine industrial waste storage focusing on the following aspects:

- Impact of creep convergence on the movement of pollutants towards the outside.
- Time dependent closure or healing of localized damage in the dilated rock contour around underground workings.

The geoscientific knowledge and used rheological approaches benefitted significantly from research done by Ecole Polytechnique during the 1990s, where some pioneering work was done in the framework EUROPEAN and ANDRA research dedicated to storage of hazardous waste in salt formations. This research had led to the development of two rheological models: that of NORTON on the creep of salt and a damage model. Described in the laboratory and in situ, these models were used for further mechanical and thermomechanical studies.

Regarding the general knowledge and approaches for assessment of the long-term behavior of underground cavities it can be stated that a detailed experimental and theoretical knowledge of the geomechanical behavior of rock salt has been acquired, sufficiently to support the general scenarios and conclusions:

- Comparison of the creep properties of StocaMine salt demonstrates that it is a fast creeping salt, slightly more than the so-called older rocksalt (z2), preferred for repository purposes in Germany, due to its favorable creep properties. The used numerical parameters are in the range of international experiences, although $n = 4$ is slightly lower than often used BGRa with $n = 5$.

As a minor deficit, humidity creep, which is characterized by a significant higher creep rate, due to the action of hydro-chemical weakening processes, is not considered by the used creep laws. This is of importance during the transient flooding phase (see below).

- The material law of Thorel (1990) is a justified approach to describe the stress dependent onset of damage, whereby the necessary criterions are site-specific determined.

With regard to the general convergence of the underground openings at around 500 m depths NORTON's creep law was calibrated for numerical analysis of the time-dependent closure of underground openings.

The average convergence rate is 0.9% per year (ranging between 0.5 and 1.4), which is, related e.g. to sealing of dams or recovery of damaged salt portions, fortunately high.

However, demonstration of the reliability of the assumptions of time-dependent convergence is essential for assessment of flooding-scenarios. Because own numerical calculations were not part of the work, only estimates of time-dependent volume closure based on analytical expressions were performed: (1) simple exponential approach without backfill with a general convergence rate of only 1.0% / year, (2) for a general convergence rate of only 0.5% / year, and (3) a more sophisticated approach for the case of delayed convergence due to self-backfill.

Generally, the hereby given analytic examinations supply the validity of previous prognoses, namely

- the decrease of the initial convergence rate of $1\%/a$ to $0.1\%/a$ (after 300 years) due to cavity reduction, i.e. the INERIS reference case.

Remark: Under consideration of self-backfill the convergence process is slightly delayed due to the support of the crushed salt mass. However, water flooding results in a significant convergence acceleration which is followed by a convergence drop. Thus, no significant differences are obvious between the case (1) and (2).

- With flooding and the evolution of a hydraulic pressure the convergence rate will be evidently reduced as well (to 0.01%/a).

Remark: It has to be mentioned, that the influence of the internal pressure to the convergence rate in the flooded mining area is well-proven by numerous in situ subsidence-measurements at the surface, especially at the so-called Stassfurt-area in Germany (see Fig. 8).

3. GEOTECHNICAL MULTI-BARRIERS CONCEPT

3.1. INTRODUCTION

A geotechnical multi-barrier concept has been developed by MDPA due to the fact that the underground openings left by the salt mine workings (mainly potash and minor rock salt) are flooded with water for the more or less long term (several centuries) once mining stops (supposed as pumping operations are stopped, prior to the backfilling of the first shafts in 1956). If some amount of hazardous waste will remain in the StocaMine the flood waters represent a potential vector for transferring the pollutants contained in the waste in the storage facility.

Thus, safe isolation of the deposited waste in StocaMine, acting as a repository⁴, has to be ensured from the biosphere which can only be attained through the as completely as possible inclusion of the waste in the host rock (in this case rock salt) taking into account a multi-barrier⁵ system.

The geotechnical safety concept of “safe isolation” developed for the StocaMine origins from

- geomechanical studies carried out by INERIS in particular, and former work on technical sealing measures in salt mines by other organizations, particularly ERCOSPLAN;
- research and practical experiences on salt in France and internationally, in particular, for conventional salt mining or repository projects for storage of radioactive and other hazardous waste in salt mines , as part of European and national programs in Germany and the US. This research led to a comprehensive understanding of hydro-mechanical properties of salt, defined in the laboratory and in situ.

The evaluation of the safety concept of “safe isolation” has to be done in consideration of different scales, as depicted in Fig. 9, i.e.

- Far field: geological barrier + shaft seals
- Near field: surrounding host rock, and technical seals, e.g. drifts and backfill.

In more detail the outer barrier complex (far field) consists of:

- The geological barriers around the Amelie and Marie-Louise mines, which comprise below a depth of 300 m the Upper Salt Zone of about 550 m thickness and the Middle Salt Zone of about 300 m thickness. They are attributed to be impermeable, free of water and contain the marls of the Middle Stampien above the Upper Salt Zone which have a very low permeability.

In addition, also the overlaying cap rocks may act as an additional geological barrier, because they consist of impermeable geological formations such as anhydrite, gypsum and marls. The latter's (e.g. as part of the Stampien) fortunately have the capability to absorb eluted material. These formations are themselves covered, directly above the storage zone, by about 35 m of Quaternary ground, which contain the Alsatian aquifer (about 30 m thick).

⁴ The repository system is comprised of the repository mine, the isolating rock zone, and the geological strata surrounding or overlying this rock zone up to surface level, insofar as these need to be taken into account for the safety case.

⁵ A barrier is a natural or technical component of the repository system, performing an important safety function, i.e. preventing or inhibiting the intrusion of liquids to the waste.

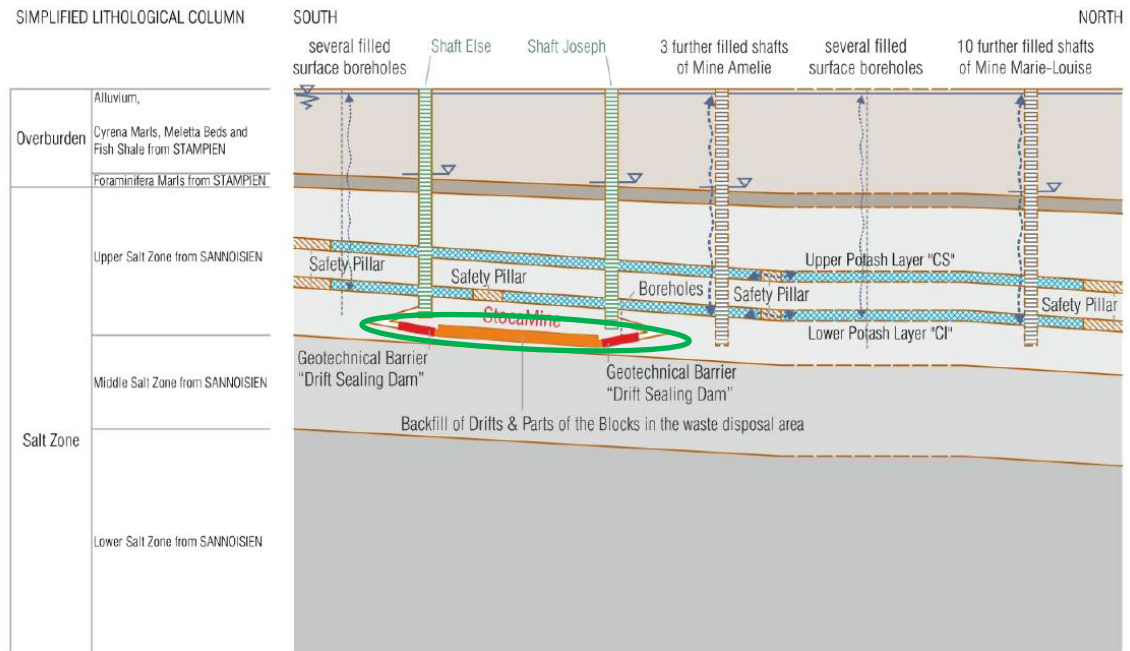


Fig. 9. Schematic Overview of the Safety Concept “Multi-Barrier System” for the Underground Waste Disposal of StocaMine (taken from ERCOSPLAN, 2013). The green circle indicates the “isolating rock zone” (IRD), i.e. the near-field barrier complex.

However, this outer barrier complex is violated by the access shafts, which may not be tightly sealed, because the Amelie and Marie-Louise mines are subject to a flooding process. Thus the efficient long-term inclusion of the waste has to be ensured by an inner barrier complex.

An isolation of the waste results mainly from the “inner barrier complex” (near field), or, in more detail, the “isolating rock zone” (IRD) is part of the repository system which, in conjunction with the technical seals (chamber sealing structures, dam structures, backfill, ...) ensures containment of the waste (see Fig. 9).

It comprises the following:

- The geological barriers around the waste disposal site, which is situated in a depth at around 550 m,
 - which comprise the 23 m - 25 m thick roof beam of rock salt between the waste disposal site and the Lower Potash Layer "CI", to the flanks the safety pillar around the shafts Joseph and Else and the adjacent Upper and Middle Salt Zone (upper and lower salt barrier).
- The geotechnical barriers,
 - which consist of all technical sealing measures, i.e. installing of plugs, for sealing of access drifts and borehole, which cut across the geological barriers of the inner barrier complex

As a preliminary note, for the general concept, final disposal of hazardous waste in salt formations differs in an essential point from the other host rock options, e.g. clay, because rock salt in the undisturbed state is attributed as impermeable, which justifies the concept of safe inclusion of the waste by the storage in the salt. However, the required barrier thickness or the dimensioning of the isolating rock zone (IRZ) has to be defined.

This can only be done on basis of existing experiences, whereby the following three main processes may lead to a potential loss of salt barrier integrity:

- Mechanical damage due to transgression of the dilatancy boundary. This process acts mainly in the EDZ and its extension is limited
- Convergence accompanied with (thermo-)mechanical induced stress re-distribution. These processes depend on the size and depth of the underground excavations, which may reach from some meters to several ten meters.
- Fluid pressure driven creation of hydraulical pathways along discontinuities in the micro- and macro-scale in the rock salt (grain boundaries, bedding planes) at fluid pressures > minimal principal stress, i.e. σ_{min} . The reach depends mainly on the rock permeability, as a function of over-pressurization.

Therefore, the assessment of the integrity of a salt repository has to focus on:

- the adequate definition of the required thickness of the natural geological saliferous barrier, the IRZ, to ensure the complete containment under all forthcoming developments and events
- effectiveness of geotechnical barriers for the sealing of shafts and drifts penetrating into the IRZ in interaction with the EDZ

Both key aspects will be discussed separately in the following.

3.2. GEOLOGICAL BARRIER – THE SALT

3.2.1. Investigation approach

For the sealing of the disposal site, the geological barriers (apart from the geotechnical barriers) are the decisive safety elements in the long-term and their integrity⁶ must remain intact during the entire period covered by the safety assessment.

- Salt in its undisturbed state is attributed to be “tight”.
 - what are the reasons for that unique rock property and is this assumption satisfied in a general case and more specific for the situation at the StocaMine?
 - **section 3.2.2:** Hydro-mechanical behavior – synopsis
 - **section 3.2.3:** The Geological barrier at the StocaMine
 - **section 3.2.4:** Minimum salt barrier thickness – natural analogues
- It is well known that during installing underground openings in salt and during operation a facility local damage in the surrounding rock portions are unavoidable but it has to be guaranteed that no damage occurs which could initiate pervasive pathways through the neighbored salt barriers., i.e. the integrity of the “isolating rock zone” (IRD) has to be demonstrated under all load conditions (short- and long-term period):

⁶ The term “integrity” refers to retention of the isolating rock zone’s containment capabilities in a repository site.

- Short-term-period during operation of the repository.

Because the thickness of the overlying salt barrier at the StocaMine is limited to around 30 m assessment of damage in the roof of the storage facility is of critical importance with respect of the possibility of water passing through the damaged salt. This includes the assessment of the possible consequences of additional damage caused by the fire in block 15 in 2002.

- **section 3.2.5:** In situ-permeability in the undisturbed and disturbed state

- **section 3.2.6:** Evaluation of the transient stage

- **section 3.2.7:** Consequences of damage caused by fire in block 15

It has to be pointed out that assessment of the roof stability, which is essential during operation of the facility, e.g. for (partial or complete) recovery of waste is not in the focus of the analysis.

- Long-term period under consideration, e.g. of the long-lasting effects of exploitation in the overlaying two potash seams and the overall stability of the load bearing room-and-pillar system of the storage area.

- **section 3.2.8:** Assessment of the long-term stability of the pillar system

- see also - **section 3.2.4:** Minimum salt barrier thickness

3.2.2. Hydro-mechanical behavior of salt - synopsis

Understanding the transport properties of rock salt, and their relationship to its mechanical behaviour under consideration of its individual lithological characteristics, is important, both, for the design and for the safety analysis of underground cavities (in particular with respect to the long-term storage of hazardous waste) in salt formations. The integrity of the geological barrier may require a sufficiently watertight and gastight behaviour, which has to hold during construction, operation and after closure of a repository. Therefore, damage and subsequent self-healing are competing processes which have to be understood if one wants to model near-field behaviour and long-term effects (e.g. the recovery of hydraulic integrity).

The integrity of a rock salt formation depends on the applied stress field, as illustrated in Fig. 10. The axes of the graph represent the normal (σ) and the deviatoric (τ) stresses. Stress states that lie below the failure boundary (i.e. the short-term failure strength boundary) are separated into two domains (i.e. compaction and dilatancy) by the dilatancy boundary. As long as the stress state is in the (non-dilatant) compaction domain, the ductile rock salt deforms without cracks forming or propagating. The dilatancy boundary corresponds to the transition from ductile deformations (i.e. no volume increase, $\Delta V = 0$) to dilatant deformations ($\Delta V > 0$), which are associated with increases in permeability.

The figure also indicates the important property changes associated with dilatancy. The dilatant domain is characterized by micro-cracking, causing accumulation of damage. Accordingly permeability and the probability of creep failure increase. Air-humidity in the mine, or fluids from inherent brine inclusions, can permeate through the dilating salt, causing a humidity-assisted increase in ductility (Urai & Spiers, 2007). In the non-dilatant domain, rock salt is "compressible": micro-cracks are compacted, closed or even healed, and further micro-cracking is suppressed. Consequently, permeability decreases, and there is no failure even during long-term deformation.

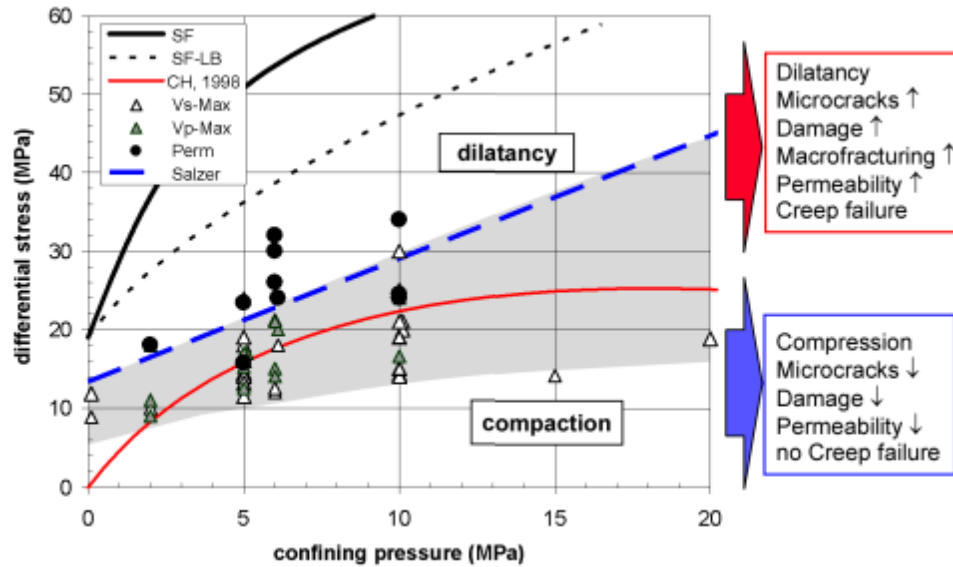


Fig. 10. The “dilatancy concept” – current understanding of the behaviour of the EDZ in rock salt as a function of stress state (modified after Hunsche & Schulze, 2002).

Taking this stress dependent behavior in mind, the processes and properties of salt, relevant for its hydro-mechanical integrity, have to be discussed in relation to the following states (after Popp et al., 2012):

- (1) **Initial state:** Rock salt in the undisturbed state has low porosity and permeability, and is almost impermeable to fluids, as pointed out by several authors.

What are the reasons for this special characteristic of rock salt?

- a. *It is a polycrystalline, chemical sediment that creeps in response to slowly-acting stresses (i.e. visco-plastic behaviour) without developing a joint system, as occurs in crystalline hard rocks. Thus the undisturbed rock mass is characterized by a nearly isotropic stress state. Referring to MOHR's concept it follows that the shear stresses are nearly zero even at the weaker grain boundaries and that the normal stresses are equal to the minimum stresses. At such conditions no inter-connected pore space exists in the rock mass.*
- b. *It has minimal water content. Transport of mass arises only from solid-state diffusion along grain boundaries, and not from advection. Therefore, transport of mass in rock salt is orders of magnitude slower than, for example, diffusion through fluid-filled pores in clay (e.g. GRS, 2008)*

Due to diagenesis of the primary salt (Warren, 2006), the final porosity is extremely low and, in addition, fluid transport may be inhibited by capillary effects. Experimental results demonstrate that low-permeability rocks require very high gas-injection pressures, which may exceed the minimal stress (Davies, 1991). Thus, undisturbed rock salt is watertight and gastight, as discussed above. In addition, many permeability measurements indicate that pore fluid pressures inside the salt mass are in the order of the lithostatic pressure (e.g. Beauheim & Roberts, 2002).

However, the observation that fluids remain fixed within the salt for at least 250 Mio. years may serve as natural analogue of tightness (e.g. Siemann, 2007).

(2) **Transient phase, i.e. during the operational phase or post-closure phase: Loss of integrity:**

What are the reasons for a loss of integrity? On basis of existing experience (e.g. the following three main processes may lead to a potential loss of salt barrier integrity:

- *Mechanical damage due to transgression of the dilatancy boundary. This process acts mainly in the EDZ and its extension is limited – Near field (dm up to several metres)*
- *Convergence induced stress re-distribution. These processes depend on the size of the underground excavation*
⇒ **assessed by the dilatancy criterion**
- *fluid pressure driven creation of hydraulic pathways along discontinuities in the micro- and macro-scale in the rock salt (grain boundaries, bedding planes) at fluid pressures > minimal principal stress, i.e. σ_{min} ⇒ **assessed by the minimum stress criterion***

(3) **Site specific situation - dilatant state:** During construction of underground openings in a rock salt formation, the change of stress state in the vicinity of the openings will affect the mechanical and hydraulic integrity of the surrounding rock salt by initiating local damage.

The creation of a disturbed zone and the development of potential hydraulic pathways is related to changes in stress dependent properties (i.e. the onset of dilatancy). This process is often referred to in literature with the acronyms EDZ (“Excavated Disturbed Zone”) or DRZ (“Disturbed Rock Zone”), where the properties of the rock become different than those of the intact rock. This has been demonstrated through permeability measurements both in field tests and in the laboratory. Depending on the size of the permeability increase, the EDZ could have a high capacity for transporting fluids around a drift seal.

(4) **Recovery of hydraulically integrity in the long-term:** It has to be pointed out that the host rock salt is fortunately characterized by its capacity for self-sealing or probably even healing. After closure of the repository, when the stress state changes so that dilatancy stops, the EDZ will self-heal (probably due to fluid-assisted compaction creep), restoring the initial fluid-tight performance of the salt.

In more detail, under conditions of very slow deformation, as might occur during stress recovery, the micro-structural deformation mechanisms are of major importance. In addition to dislocation creep in the crystal lattice of salt grains pressure solution and dynamic re-crystallization at grain boundaries play a dominant role – if small amounts of brine are present (e.g. Urai & Spiers, 2007). For these mechanisms, surface energy driven grain boundary migration and joint healing processes occur. During halokinesis, this leads to entrapment of fluids on grain boundaries or enrichment in intra crystalline pores.

The different aspects of hydro-mechanical behaviour are also of relevancy for discussing the various states of the StocaMine, i.e. construction, operation and after closure. In the following, they will be discussed in the framework of general knowledge and the local situation.

3.2.3. The geological barrier at the StocaMine

The geological sections in Fig. 11a, show that the Mulhouse basin comprises three salt-bearing zones, dating from the tertiary (Sannoisian) period. Each zone contains one or two stratified salt-bearing series, formed by beds of salt and insoluble marl-anhydrite (Fig. 11b). The two potash-containing layers (sylvite, KCl), worked by MDPA are found in the Salt IV series, in the upper salt-bearing layer (Fig. 11a):

- the Lower Layer (LL), 4 m thick, and
- the Upper Layer (UL), 1,5 m thick.

They were worked for around a hundred years (1910-2002) using the longwall method with caving. The depth of the workings varies, depending on the area, between 500 m and more than 1000 m.

Regarding the general tectonical situation, i.e. related to geological accidents (catastrophic water inflow during mining) encountered elsewhere, it was stated by INERIS (2010a) that there are no faults affecting the sector where the storage facility is located.

In addition, it's worth to note, that in Alsace the caving technique has caused subsidence at ground level of up to 6 m. In spite of this subsidence, no hydraulic communication has been observed with the Alsatian aquifer outside of the shafts: the ground covering the mine is sealed off by a number of impermeable marly geological layers. The main hydraulic communication pathways between the aquifers and the storage zone are the access shafts, whose total tightness cannot be guaranteed long term.

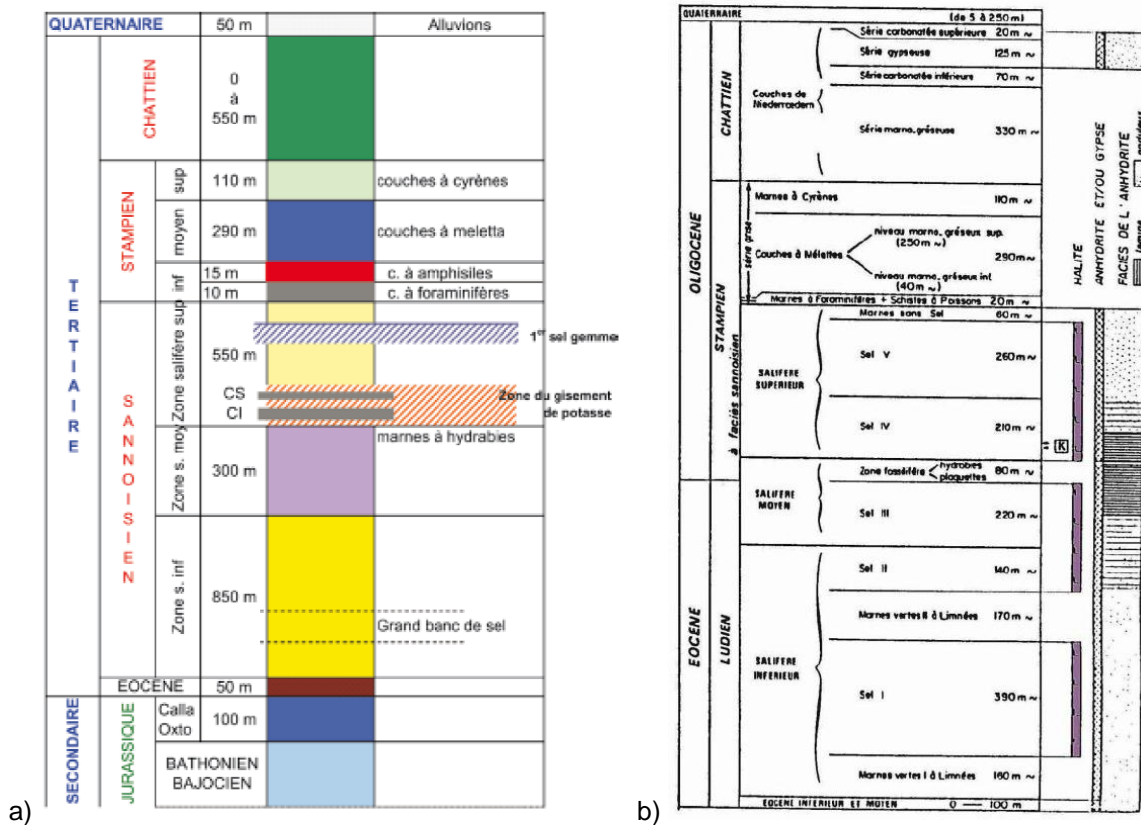


Fig. 11. Geological situation. a) General stratigraphy basin of Mulhouse. b) Detailed geological profile StocaMine.

The StocaMine storage area is located at a depth of approximately 550 m, 23-25 m above the level of the workings. It can be accessed from the Joseph and Else shafts, the only ones still not backfilled.

The salt ceiling at the StocaMine is at a depth of 300 m. The dip angle is 6 to 8° N-NW. The overlying cap-rocks comprise Stampian and Chattian formations: marls, anhydrites, gypsum and sandstone, formations surmounted by approximately 35 m of quaternary materials in the middle of which is located the Alsace aquifer (some 30 m thick). Ground level is at an elevation of 270 m NGF (French standard height).

As shown in Fig. 11b, the geological barriers around the waste disposal site comprise the roof beam between the waste disposal site and the Lower Potash Layer "CI", the safety pillar around the Joseph and Else shafts and the adjacent Upper and Middle Salt Zone.

The roof beam between the waste disposal site and the Lower Potash Layer "CI" is made up of massive Halite interbedded with laminated Marno-Anhydritic or marl layers from the lower part of the Upper Saliferous Zone. It has been shown that this geological formation particularity has an importance in the creep rate process.

The most relevant thickness of the roof beam, above the storage area, is about 25 m and it separates the Lower Potash Layer "CI" exploited in Amelie mine from the storage blocks and drifts.

3.2.4. Minimum salt barrier thickness – analogues

For the saliferous rock mass (undisturbed by miner's activities) numerous examples, e.g. natural and technical analogues, demonstrate tightness and inclusion of gases for geologic periods (see section 3.2.2). The principal challenge for realising a final disposal of hazardous waste in salt is to preserve this fundamental property also under all circumstances of a final repository with consideration of convergence followed by stress redistribution and local damage.

It is well known that in the past in several cases the existing barrier thickness was not sufficient to resist against the hydro-mechanical loadings acting on the remaining salt barriers, which leads to flooding of the underground openings (an overview is given by Herbert & Schwandt, 2007). However, the reasons, e.g. inflow of water due to geological inhomogeneity in the overburden or due to technical mistakes (e.g. under-dimensioning of the load-bearing pillar system), have to be analysed individually⁷. In addition, flooding of salt mines is in Lower Saxony the preferred option for stabilization (§7 ABVO, 1996).

To avoid such accidental events the actual mining standards in Lower Saxony (Germany) demand a security pillar to the salt surface, the salt dome base and the salt dome flanks of at least 150 m in domal salt formations, according to §224 ABVO (1996). According to paragraph (e) the safety distance to 200 m is to be increased when the position of the boundaries cannot be determined exactly.

With respect to repository sites for radioactive waste in domal salt formations the BGR Hannover defined minimum requirements for the necessary salt barrier thickness (BGR, 1977, 1995 and 2006). According to BGR (1995) the necessary salt barrier above the repository area should be ≥ 300 m, to the footwall 100 meters with a minimum thickness of rock salt of 500 m. To the salt flanks area a thickness of at least 200 m is to be set. **However, it can be stated that these requirements are very conservative**, especially because the additional loading effects of thermo-mechanical interactions of heat-generating radioactive waste were considered.

Focusing on a scientifically based definition of necessary salt barrier thickness IfG (2010) précised the recommendations for preliminary assessment of underground dimensioning in the framework of VSG⁸, based on observations made in the former potash mine "Merkers"⁹.

⁷ In this context the loss of integrity of the salt barrier of the Asse salt mine is often discussed as a typical example of a miserable failure contradicting the use of salt mines as waste deposits. However, it has to be mentioned that the Asse mine was initially constructed and designed as an exploitation facility for salt and potash mining. As a consequence of the former mining activities the remaining salt thickness of only some few meters between the most upper floors and the associated water bearing strata was obviously not sufficient to avoid water inflow.

⁸ VSG = Acronym for the „Vorläufige Sicherheitsanalyse Gorleben“ (preliminary safety analysis Gorleben).

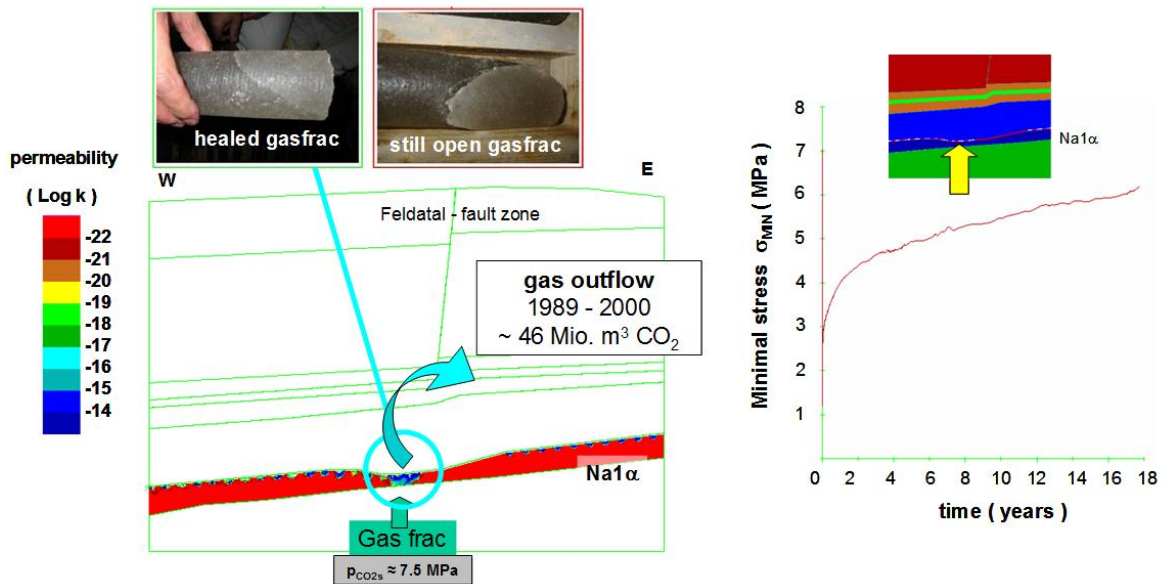


Fig. 12. Integrity of the geological barrier after the rock burst. In addition, typical gas frac patterns are shown (the core samples were recovered by a 250m long borehole drilled into the former gas frac zone. (Left) permeability in the Lower Werra rock salt Na1 α a few seconds after the rock burst. (Right) time dependent recovery of integrity as characterized by the minimum principal stress σ_{min} .

At the site of the Merkers salt mine a unique geomechanical constellation exists that allows evaluating the following processes:

- (1) **The long-term impact of a high fluid pressure** ($p_{CO_2} = 7$ to 7,5 MPa) on a salt barrier which is characterized by a comparatively low salt thickness (about 30 m) and influenced by effects of large-scale room-and-pillar mining. Numerical modeling (Minkley, 2004) - under consideration of (1) the dilatancy and (2) the minimum stress criterion - demonstrated that despite the acting high pressure no failure of the salt barrier occurred, i.e. that the barrier remains intact under the acting fluid pressure.
- (2) **The recovery of hydraulic integrity** of this only 30 m thick barrier could be studied because in connection with the rock burst Völkershausen (13.03.1989) a fluid-pressure induced frac (CO_2 -gasfrac) occurred i.e. loss of integrity.

During the rock burst a complete mining field was destroyed, which was accompanied with a significant unloading of the underlying salt barrier, the Lower Werra rock salt (Fig. 12). Because of the reduction in the minimum principal stress to a few MPa, the minimum stress criterion was violated resulting in a gas breakthrough (gas frac with a significant CO_2 discharge) representing clearly a loss of integrity (Minkley, 2004). However, immediately after re-stabilization of the system a time-depending recovery of the minimum stress was observed resulting in a healing phase in the salt barrier (note the healed gas frac in Fig. 12, left part). The time-dependent recovery of minimal stress, depicted in Fig. 12, right part, restored the integrity of the salt barrier, at least only partially, over a period of a few years. The validity of the numerical simulations was demonstrated by

⁹ These large-scale events (so-called technical analogues) represent, equivalent to natural analogues, an important tool for evaluating the future behavior of geological structures and formations because in contrast to classical field tests only with them large-scale and long-term temporary phenomena can be evaluated (e.g. Wolf & Noseck, 2015).

observations of re-establishment of salt tightness (no CO₂-outflow after 1 year) respectively by measuring increased stress values in the formerly unloaded salt barriers (for details s. Popp et al., 2007).

In summary, the technical analogue Merkers demonstrates quantitatively

- (1) that there even with a rock salt thickness of just 30 m no gas-breakthrough occurred to the mine cavities despite an acting CO₂ gas pressures of about 7 MPa (in the order of the hydrostatic pressure). **Thus, this value of 30 m corresponds to a previously detected minimum salt thickness that must be maintained as minimum value.**

The salt thickness of the overlaying salt barrier above the StocaMine is in the same order. Thus, in a first approach, the hydro-mechanical efficiency of the salt barrier can be assumed.

- (2) Rock salt is able to restore its tightness, even after a fluid breakthrough, because recovery of the minimal stress state will occur ⇒ **proof of large scale healing.**

3.2.5. In situ-permeability in the undisturbed and disturbed state

Although it is a fact that undisturbed rock salt is usually tight against fluids, as already mentioned before. This unique salt property has to be demonstrated by site specific in-situ measurements. In the framework of a PhD-study (Cosenza, 1996) a field test was carried out in the Amelie Mine (MDPA) at conditions which are comparable for the StocaMine site. The investigations were completed by laboratory triaxial tests with fluid injection tests carried out on samples taken from the same site.

The experimental set-up is shown Fig. 13a, which facilitates both gas and brine injection tests (MDPA, France) for the purpose of measuring rock salt permeability away from underground facilities. The selected salt bed is about 1 m thick and located 16 m away from the gallery floor. The permeability was measured by means of nitrogen and saturated brine injection.

The results published by Cosenza et al. (1999) showed that fluid flow in salt is in reality a multiphase flow of immiscible fluids (brine and gases) consisting of capillary which effectively inhibit fluid flow, in addition to the existing low porosity and resulting low permeability, as already mentioned before. However, the measurements performed with brine were interpreted in a satisfactory way by a model based on Darcy's law. As results an intrinsic permeability value of $2 \cdot 10^{-21} \text{ m}^2$ and an initial pore pressure value of 1 MPa were determined. Interpretation of the measured gas flow rate shows that: (a) after brine percolation, the capillary pressure effect is significant and (b) gas migration in salt is not controlled by Darcy's law; the Knudsen effect and partial saturation may play an important role.

The site-specific results of a general tight salt with overlapping 2-phase flow effects correspond fairly well to observations made by other authors at bedded salt deposits, e.g. for the WIPP site in the US (Beauheim & Roberts, 2002); Bernburg site (Popp et al., 2007) and Merkers salt mine (Popp et al., 2015).

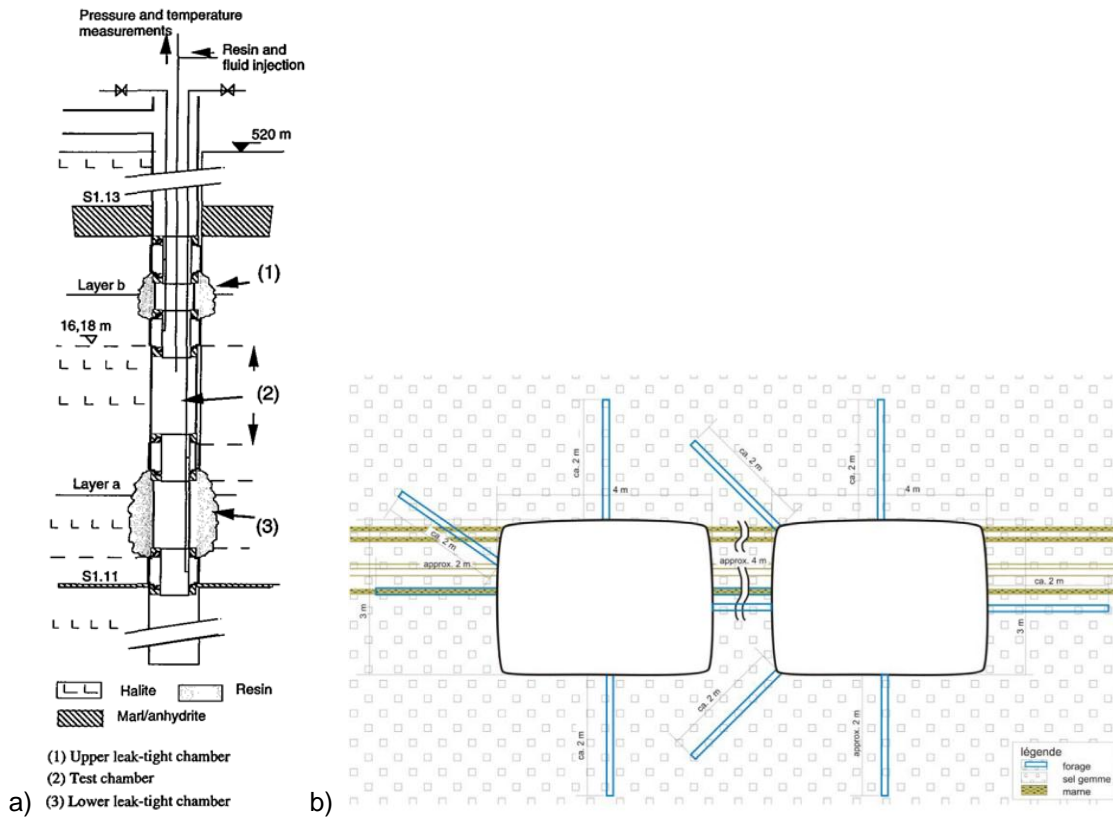


Fig. 13. Borehole set-up a) used by Cosenza et al. (1999); b) Position and orientation of reference holes at the sites investigated by IBEWA (2013a, b).

But it is well known that potential hydraulic pathways may be generated due to the occurrence of the EDZ, which is related to stress-dependent property changes. This has been demonstrated through permeability measurements in field tests at various sites since the 1980s (for a comprehensive review, see e.g. Rothfuchs et al., 2005). It has been confirmed that the extent of the EDZ is typically in the order of a few decimeters up to 1 m or even 2 m but depends significantly on the geometry of the opening and the stress state. Permeability measurements at the 800m level of the Asse salt mine show that the usual cross section of a drift (i.e. with a flat floor and a domed roof) leads to a larger extent of the EDZ below the floor as compared to the walls and roof – corresponding to the stress state around the drift (Wieczorek & Schwarziarek, 2004).

To quantify the possible extent of the zone influenced by the hydraulic flow, local in-situ permeability measurements for the rock salt surrounding the repository zones were performed by IBeWa Consulting (Germany). They consist of injection tests of gas (dry air) inside boreholes excavated starting from the surface of the drifts (IBEWA, 2013a, b).

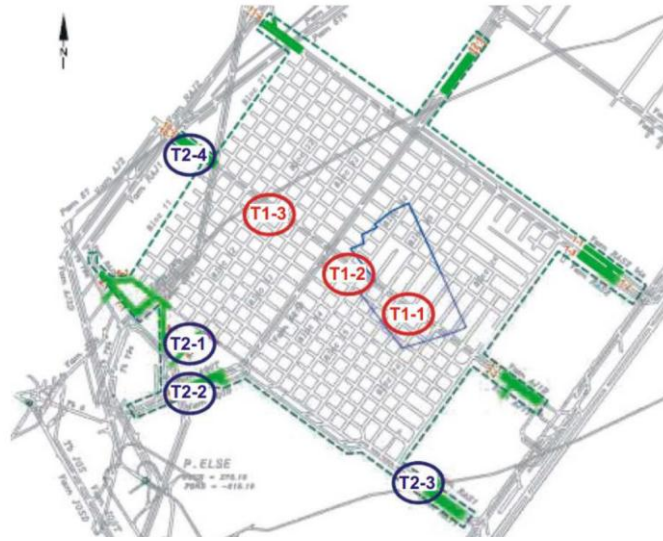


Fig. 14. Sites for the permeability measurements [Explanation: blue mark area – massive pillar of potash mining field in the hanging wall]. T1-x and T2-x indicate different measuring campaigns (taken from IBEW, 2013a).

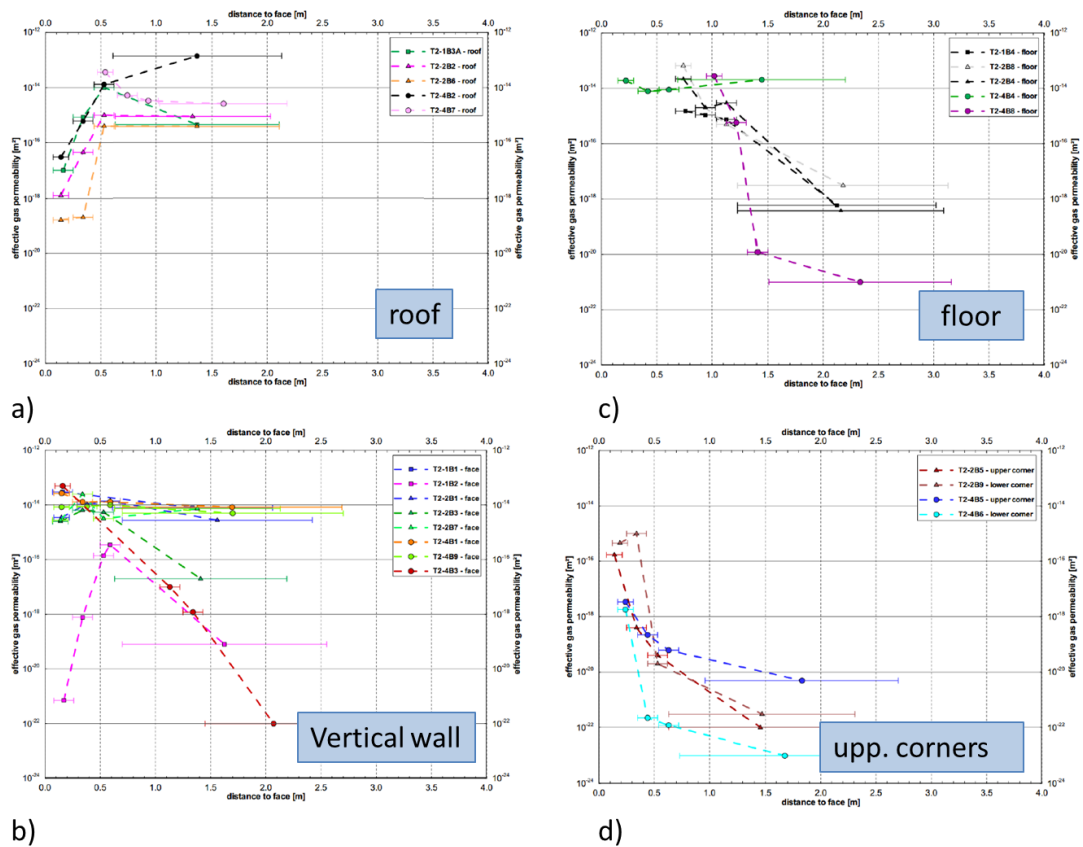


Fig. 15. Profiles of permeability with the distance to the excavation for boreholes drilled at various orientations to the drift, through the pillar zone - case of double tunnels (modified after IBEWA, 2013a).

Fig. 14 shows the sites chosen by IBeWa for the measurements campaign. These are located along the access tunnels, where bentonite sealing dams are planned to be constructed, and thus where the evolution of the rock salt permeability is crucial to insure the efficiency of the adopted system of containment. Moreover, special packer configurations were used inside the boreholes to get the variation of permeability along the borehole axis, with smaller test intervals in the vicinity of the tunnel (damaged zone). For determination of the spatial distribution of the permeability field around the specified drift sites, boreholes were drilled into the floor, roof and the rock wall related to the geology (Fig. 13b).

Two test-types using only gas as injection medium are performed, which were evaluated with a numerical model simulating the fluid spreading into the porous rock wall:

- Pulse test – instationary test
- Constant pressure/ rate test – stationary test

The variation of permeability with the distance to the tunnel wall is given in the graphs of Fig. 15. These graphs show the totality of available permeability measurements for the boreholes located in the roof, floor, face and corners of the access drifts.

Despite the observed scattering of the data the following conclusions can be derived as outcome of the in situ permeability tests:

- The tested rocks (rock salt and marl/clay) have generally low permeabilities compared to other non-saliferous rocks, but close to the contour the permeability may increase, depending on
 - the mining site condition, resulting in contour disturbances generated by the change in stress due to the excavation,
 - the geologic situation according to the rock heterogeneity due to the presence of marl inclusions, and
 - the measurement conditions itself (e.g. test type, e.g. pulse or stationary test, test fluid – gas or water - length of the measuring intervals along the borehole axis, humidity)
- Generally, the level of permeability depends on the distance to contour caused by unloading and some mechanical disturbance (dilatancy) effects, usually described as EDZ:
 - Within the first meter from the contour the permeability is usually $> 10^{-16} \text{ m}^2$ for the most performed tests. Some measurement points however yielded permeabilities $\leq 10^{-16} \text{ m}^2$, which may represent more or less intact salt portions.
 - In distances $> \text{ca. } 1 \text{ m}$ the bulk of permeabilities show values $\leq 10^{-16} \text{ m}^2$
 - In distances $> \text{ca. } 3.5 \text{ m}$ the bulk permeability is generally $\leq 10^{-18} \text{ m}^2$.

The findings are in the well-known range, observed for dilated salt in lab and field tests. However, the measurements confirm the usual trend of decreasing permeabilities with greater contour distances. Thus, it can be concluded, that the assumption of initial tightness for the salt barrier surrounding the StocaMine has been convincingly demonstrated.

- It has to be mentioned that due to contrasts in mechanical competence of rocks within a sedimentary layering and the resulting differences in deformation behavior of rock salt and intercalated marl/clay the dilatancy effects in the contour zones may be amplified by relative movement along such weakness planes in the sense of shear strain (simple shear).
- The marl layers itself were tested as well in small rock intervals (where the inclined borehole intersects a layer) or over a longer interval if the borehole is drilled along the bedding. The measured values show a significant data scattering from $>10^{-15} \text{ m}^2$ to 10^{-20} m^2 .

Remark: Although the properties of the marl were not systematically evaluated it has to be taken in mind, that in contrast to the nearly dry rocksalt (humidity content, in the order of $<0.1 \text{ wt } \%$) marl samples contain usually humidity contents in the order of about $10 \pm 5 \text{ wt. } \%$

% (IBEWA, 2013). Thus, the permeability measurements itself may not be overlapped by stress-induced damage, but also some de-saturation, resulting in a significant gas flow which implies that the performed gas injection tests are not representative for the undisturbed marl rock state¹⁰.

In summary, a comprehensive data base is available for assessment of the overall rock integrity and a purposeful planning of optimization measures in the near-field of sealing elements (e.g. removal of the main part of the EDZ) (see section 3.4.3).

Regarding the general reliability of the permeability tests of IBEWA and for further investigations the following comments are given:

- IBEWA uses a well proven measuring approach, which has been designed for quantifying the permeability state in the dilated rock contour. Due to the packer arrangement (4 packer with one central measuring and two control chambers) gas flow effects along the dilated rock contour around the packers may be identified;
- If the salt is dilated, due to the confirmed low water content, 2-phase flow phenomena can be neglected (in contrast to the undisturbed in situ-state as investigated by Cosenza, 1996). However, because depending on the durability of the borehole seal the existence of moisture in the vicinity of the measuring point cannot completely excluded, all in situ gas permeabilities have to be considered as effective gas permeability in dependence of the saturation with brine;
- The problems regarding humidity effects regarding the marl are obvious (e.g. drying, disturbances). Because the marls are an important constituent of the salt barrier, more reliable data sets are required for final assessment of tightness, but an improved approach should be developed for future measurements. The test should be executed under realization of mostly undisturbed conditions (outside of the EDZ) , using brine as test fluid and ensuring re-saturation of the material due to the local disturbance induced by the test hole, which requires a long-lasting injection test.
- Permeability is a consequence of stress and deformation induced damage which develops with time, but only limited information about the stress state in the rock contour is available. From IfG experience, stress probing using e.g. the hydro-frac method are recommended.

3.2.6. Evaluation of the transient state – numerical modelling

The transient state of an underground drift is that due excavating the underground opening and due to the stress relaxation during salt creep a significant EDZ has been created. As the removal of the EDZ before erection of the seal is of highest importance, model calculations have to be performed accompanied by in-situ investigations (e.g. permeability and hydrofrac-measurements to determine the depth of the damaged contour zone.

Exemplarily Fig. 16 shows the extent of the EDZ for a drift in the Asse mine at the 775-m-level in rock salt Na3 (with a width of 5 m, a height of 3 m and a length of about 55 m) (for details see Kamlot et al., 2012). Under consideration of the real stress state, influenced by neighbored underground openings and the overall acting deformation field the drift is unsymmetrically deformed, representing the initial state after 28 years of free convergence. It can be seen that the damage as described by the parameter plastic volumetric deformation (\approx porosity) is significantly increased in the middle part of floor, walls and roof, but not symmetrically. Corresponding to the stress state, nearly no damage occurs at the edges. However, it is important to note, that despite

¹⁰ It has to be stated that from knowledge of IfG, clay bearing intercalations, which are part of the sedimentary lithology of salt deposits, are part of the general salt barrier, i.e. they are tight, as it has been demonstrated for the so-called Red Clay (T4) investigated at various sites, both in the lab and field scale (Minkley et al., 2013)..

the high depth the hydraulically relevant EDZ has an extent only up to 1 m, as verified by permeability measurements.

Because of the damaged contour zone a removal of the broken plates and of the EDZ was necessary. The depth of machine cutting (0.5 m at floor and roof, 0.2 m at vertical edges, extended area after cross cut about 20 m²) was proposed on basis of the calculation results.

After removal, permeability measurements were performed and the determined amounts are sketched in Fig. 16 at the right hand side. They fit very well the magnitudes which are to expect on basis of the calculated dilatancy (lower than 1 ‰) and the dilatancy-permeability relation after Popp (2002).

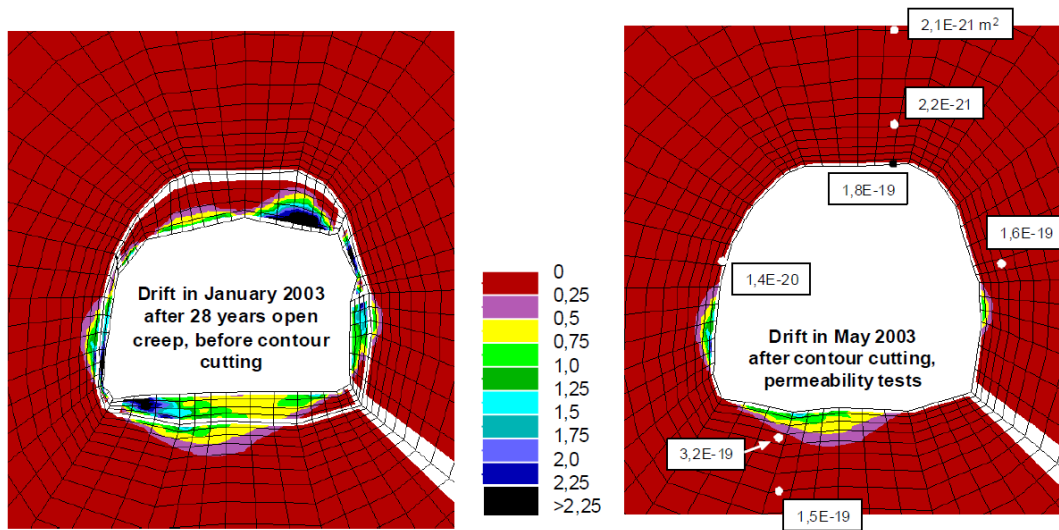


Fig. 16. Plastic volumetric deformation in ‰ in the drift contour after 28 years free creep before contour cutting (left hand side) and after contour cutting (right hand side) (taken from Kamlot et al., 2012).

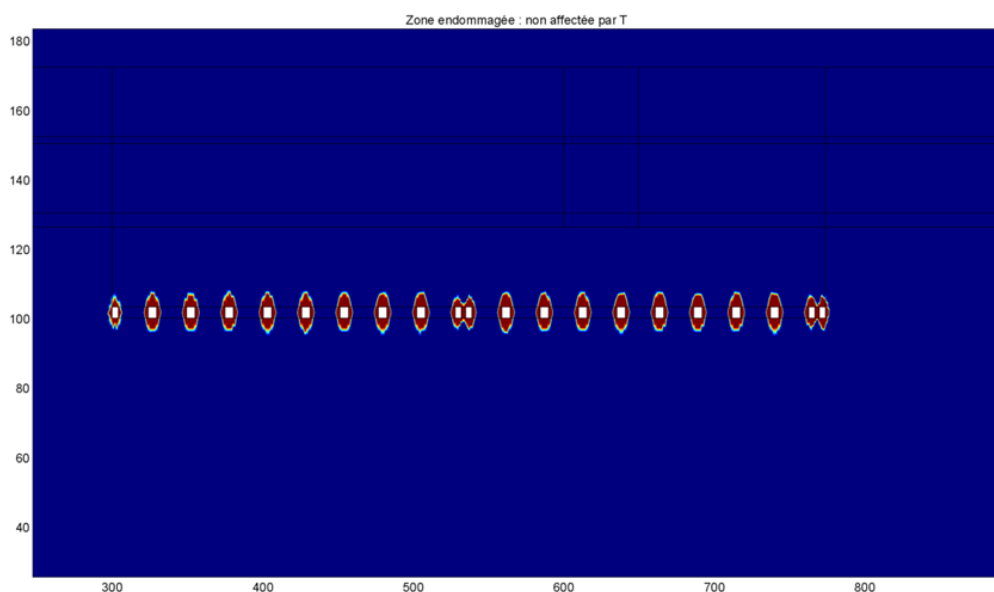


Fig. 17. Location of the damaged area around the storage area (taken from ITASCA, 2012)

The state of underground damage has been also assessed by INERIS based on numerical modelling using the THOREL model. Figure 34 shows the location of the damage (outline of the area where the damage criteria are reached), in a cross-section of the storage. Note that the damaged area extends further into the roof and the wall than into the pillars.

According to the model, the damaged area extends to 3 m into the roof of the storage area, i.e. about the height of galleries. This phenomenon is caused by tensile stresses related to the bending of the beds which are considered by the model not to have traction resistance (a realistic hypothesis in the medium term).

Remark made by Itasca: *It has to be taken in mind that the extent of the damage to the roof may be greater than the 3m provided by the model, because the latter fails to take realistically account of the detachment of the beds, a phenomenon observed in situ.*

However, it can be concluded that the here presented results from the different numerical in-situ studies correspond very well to the findings shown in section 3.2.5 for the StocaMine. Thus, it is assumed that the damage in the contour zone is limited to, at least, some few meters (depending on the spatial stress field and geology), which may be of importance as permeable zone for installing drift seals.

Nevertheless, it has to be mentioned that the analysis did not refer explicitly to the well-known dilatancy and minimal-stress criterion which offer a simple documentation of damaged or non-damaged rock portions (see section 3.2.2).

3.2.7. Consequences of damage caused by fire in block 15

On September, the 10th 2002, a fire occurred in one of the blocks of the StocaMine storage, where mainly wooden pallets and big packs burned. Because the mechanical behavior of salt is sensitive to temperature and significant stresses may be generated in the overlying roof above block 15, this provokes the question of a possible hydraulic connection through the damaged salt formation.

The additional effects of increased temperature on the roof stability have to be evaluated based on impact of temperature, which results mainly from two factors:

- Maximum temperature, respectively temperature gradient inside the salt: According to INERIS (2010) temperature values, measured by infrared thermography, ranged from 100 to 370°C.
- Duration: The fire lasted approximately for 10 days (COPIL, 2011).

INERIS (2010) performed a systematic analysis of the amount of damage on the storage roof induced by the Block 15 fire, assuming a worst case scenario, i.e. considering fire duration of 3 months with Peak temperatures of more than 300°C.

The calculation was performed in two steps: (1) the temperature field was calculated by the thermal model; (2) the outcome (reach of temperature field and gradients) was introduced into the thermo-mechanical model taking into account damage, facilitating estimate of the thermal-induced extension of the damaged area. The results indicate,

- that the salt is already damaged due to the excavation of the storage galleries
- that the area affected by the damage is greater the higher the temperature in the walls of the galleries.
- that the area affected by the damage is greater, as higher the temperature in the walls of the galleries are. However, it only reaches the caving level (Figure 41), at the ends of block

15, only under the at-first-sight unrealistic assumption of a rise in temperature to about 300°C, covering the whole wall of block 15.

However, as argued by INERIS it has to be considered “...that thermal stresses (resulting from the thermoelastic behaviour of the ground) relax over time due to the viscoplastic behaviour of salt. This relaxation goes hand in hand with the creep of the salt which increases with temperature. Relaxation is greater as the temperature rises. This phenomenon is therefore unrelated to the gradual cooling of the solid rock after the fire was stopped.”

Based on these results INERIS concluded that the additional effects of fire on the general roof integrity are of minor relevancy, because an additional contribution to the existing rock permeability can be assessed to be small, i.e. the permeability of the damaged salt remains moderate (in the order of 10^{-15} m^2).

Regarding the general plausibility of INERIS main conclusion, that the consequences of the salt are small compared to the dilatancy-induced salt disturbances, experiences from natural and technical analogues may be considered:

- Final storage of heat generating radioactive waste in salt, e.g. outcome of investigations for the Gorleben site (e.g. Kock et al., 2012):

Emplacement of heat-generating waste in the repository results in the early post-closure in a sharp rise in temperature in the near field (T_{max} on the container surface 200°C). The spread of the temperature field and the resulting expansion of the host rock were investigated with thermo-mechanical simulations. The results document that due to thermal expansion of the rock additional stresses are induced in the host rock, which on one hand can result in dilatant structural damage in the rock contours (near field), and on the other hand to form a region of increased compressive stresses outside the damaged area (far field). Nevertheless, the integrity of the existing salt barrier of several 100 meters was not affected.

- Tertiary basalt intrusions into the bedded Werra salt formation (e.g. Knipping & Herrmann, 1985):

Basaltic melt penetrated during the Miocene (15 - 25 million years ago) at temperatures of 1150 ° C in the salt formation forming steeply dipping basalt dykes with a thickness up to several meters. During the magma emplacement the salt was heated in the contact area to temperatures up to about 800°C; the temperatures but went relatively quickly back to below 100°C. It can be stated that in contrast to the effects of emplacement of heat-generating radioactive waste, the spatial range of the effect of these basalt intrusion is limited to a few 10 meters, due to the relatively rapid cooling of basalt body, i.e. the duration of heat was relatively short.

- Fire in Teutschenthal mine (Südkurrier, 2002):

In the former salt mine Teutschenthal comprehensive backfill measures are performed with different types of waste (e.g. filter ashes) as stabilization measures for the former mining-chambers to minimize the risk of a rock burst. In 2002 a fire occurred in chamber 216 which was attributed to self-ignition of pyrolysis coke from a recycling plant which had a high proportion of carbon and aluminum metal. The duration of the fire was more than several weeks, but after fire-out only minor disturbances of the roof stability were recognized but no generation of hydraulic pathways (pers. comm. with GTS). Thus the back-filling measures were continued.

In summary of the available knowledge it can be concluded that the additional effects of the fire are only small compared to the long-lasting effects due to excavation of the different storage rooms.

3.2.8. Assessment of the long term stability of the pillar system

The area of the StocaMine underground waste deposit was mined with room-and-pillar technology with squared pillars. The slenderness ratio $\alpha = H : W$ resulting from the mining conditions is ca. 1 : 7 (Fig. 5). Thus it can be stated that a dynamic pillar failure within the rock salt mining area due to insufficient pillar dimensioning is very unlikely due to the mechanical properties of rock salt.

As far known such an event was only documented in mining areas with very slim pillars (Berest et al., 2008). In Varangéville (France) an earthquake-like shocks occurred when a rock salt field failed in ca. 155 m depth (31.10.1873). The failed pillars had a ratio Width : Height of 1.1 and the exploitation factor was 82% (Minkley et al., 2012). The last-mentioned authors were able to reconstruct numerically the complex failure process. There, a humidity-induced base-failure within the underlying marl-layers led fundamentally to pillar capacity overload.

The extraction rate G_w follows from:

$$G_w = 1 - \frac{A_{PF}}{A_{SYS}} \tag{3-1}$$

with A_{SYS} system surface $(a_p + b_k)^2$ (650 m²)
 A_{PF} pillar plane $(a_p)^2$ (400 m²)

The system surface is that plane, which has load bearing capacity of the pillar (Fig. 5). It results from the pillar plane and half of the neighboring drift. This leads to an extraction rate of 38%. It is obvious that StocaMine was not designed to mine salt rocks. Therefore, a sufficient stability is carried out.

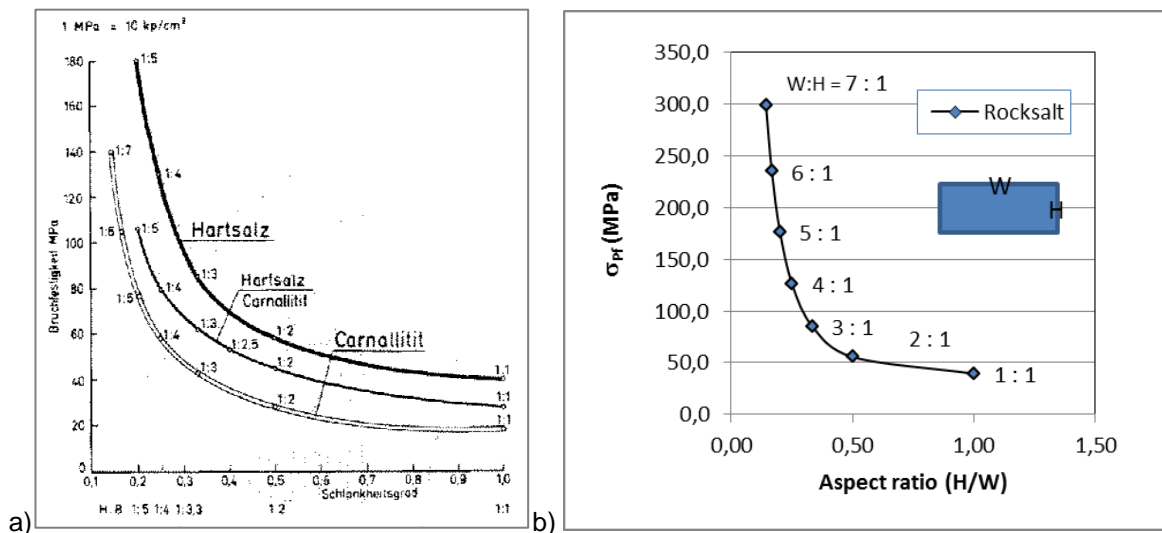


Fig. 18. Load bearing strength of quadratic salt pillars. a) Pillar strength (σ_{Pf}) of various series of loading tests on different salt species vs. pillar height-widths ratio ($H : W =$ slenderness ratio) (taken from Uhlenbecker, 1974); b) Pillar strength (σ_{Pf}) vs. aspect ratio $W : H$, after formula 4.2.

The common dimensioning method which is majorly used for mines in the Werra potash area (GER) bases on research and publications of UHLENBECKER. Uhlenbecker (e.g. 1971/74) investigated with laboratory tests the failure behavior and strength parameters of various salt types (e.g. Carnallite, hard salt etc.) as well as for different model pillar geometries. Numerous compression tests with squared pillars were performed. But, for rock salt and for pillars with rectangular dimensions only little investigations and data are available.

It is obvious that the failure strength is evidently dependent on the type of salt (e.g. carnalitite or kieseritic hard salt etc.) as well as from the aspect ratio α (Fig. 18). Although these data were originally taken from investigations with potash salt, the parameters of hard salt are used for rock salt as well. Therefore, after Uhlenbecker derived approaches can be described with:

$$\sigma_{p \text{ rocksalt}} = [(-0.325) \cdot \alpha^3 + 8.65357 \cdot \alpha^2 - 7.52143 \cdot \alpha + 38.7] \quad (3-2)$$

Further, the classic method of a stability factor is used to assess the stability of salt deposits and included repository areas (e.g. Natau (1997) regarding the underground deposit Heilbronn / GER). Here, appraisal rule for the dimensioning is the value of the dimensioning numbers. It is the ratio between pillar failure strength σ_{Pf} (in short-term tests) and pillar load bearing capacity in situ p_{Pf} and can be derived from:

$$s = \frac{\sigma_{Pf}}{p_{Pf}} \quad (3-3)$$

From known experiences, a dimensioning number $s \geq 3$ is requested to ensure long-term stability of the pillar, whereby the pillar failure strength increases with the pillar aspect ratio and is also dependent on the salt type.

The calculation of the pillar load bearing capacity follows from:

$$p_{Pf} = \rho \cdot g \cdot H \cdot \frac{A_{Sys}}{A_{Pf}} \cdot 10^{-6} \quad (3-4)$$

with p_{Pf} pillar load bearing capacity [MPa]
 ρ estimated mean density of cover rocks (2345 kg/m³)
 g gravitational acceleration (9.81 m/s)
 H depth (550 m)

Therefore it results for the StocaMine a pillar load bearing capacity of $p_{Pf} = 20.6$ MPa.

Assuming the approaches by Uhlenbecker lead to a pillar failure strength of $\sigma_{Pf} = \text{ca. } 300$ MPa. Those parameters results in a dimensioning number of $s = \text{ca. } 14.6$ (after equation 6.3). This value is much higher than requested for rock salt mining and prove for its long-term stability.

The results are in accordance to the stability assessment, performed by INERIS (2010).

In conclusion, from a geomechanical point of view, the waste disposal site with its cavities in the rock salt area is stable during its operation period and in the long-term.

3.2.9. Summary

At the StocaMine a geotechnical multi-barrier concept has been developed by MDPA, where the geological barriers (apart from the geotechnical barriers) are the decisive safety elements to ensure that no thread of the biosphere will occur in the long-term. Rock salt in the undisturbed state is attributed as impermeable, thus the concept of safe inclusion of the waste by the storage in the salt is justified as long as the geological barrier integrity is ensured during the entire period covered by the safety assessment.

Thus the analysis focused on the investigation of the actual state of the geological barrier and its long-term evolution taking into account all processes which could affect its integrity.

- **The salt barrier:** Because the outer geological barrier complex, i.e. the Upper salt zone and the cap rocks, is violated by the access shafts, which may not be tightly sealed, the Amelie and Marie-Louise mines are subject to a flooding process. Thus the efficient long-term inclusion of the waste has to be ensured by the inner barrier complex, i.e. the rock salt formation surrounding the deposit area. According to the well-known geological situation the main focus has to be given to the roof beam which consists of bedded rock salt with intercalations of marl. This rock section separates the Lower Potash Layer "CI" exploited in Amelie mine from the storage area. Its average thickness is about 25 m.
- **General knowledge about salt integrity:** It has to be stated that for salt a unique understanding of its hydro-mechanical properties exists which is essential to assess all loadings which could affect the barrier integrity under consideration of its individual lithological characteristics. This includes the general states of repository evolution, i.e. (1) the initial state – rock salts are tight; (2) transient phase, where temporary local violations of the salt integrity may occur but which are limited in range; and (3) recovery of hydraulically integrity after closure of the deposit which takes place due to the rock salt capacity for self-sealing or –healing.
- **Minimum salt barrier thickness:** Based on the geological analogue observed in the salt mine Merkers, the minimum salt barrier thickness was estimated to be around 30 m which is required to maintain the salt integrity under action of lithostatic fluid pressures. This minimum requirement is more or less fulfilled for the overlying salt barrier at the site.
- **Permeability at the site:** Measurements of fluid permeability document that the salt at the StocaMine is initially tight. Because it is well known that potential hydraulic pathways may be generated due to the occurrence of the EDZ a series of extensive permeability measurements in the contour zones around the storage chambers were performed. The results convincingly document that a zone of increased permeability (up to $> 10^{-16} \text{ m}^2$) close to the underground openings exists but in distances $> \text{ca. } 3.5 \text{ m}$ the bulk permeability is generally $\leq 10^{-18} \text{ m}^2$. This is a usual finding. Thus, it can be concluded, that the assumption of initial tightness for the salt barrier surrounding the StocaMine has been convincingly demonstrated.
- **Damage in the surrounding salt portions:** Numerical modelling using qualified material laws, supplemented by site-specific permeability and stress-measurements are a powerful tool to assess the damage state (extension of the EDZ) of the salt barriers. Investigations, performed by INERIS documented, that the damaged area (which is hydraulically of importance) extends to 3 m into the roof of the storage area, but may the effect of marl-layers in the roof may not be sufficiently considered. However, the general findings of a limited range of the EDZ of some few meters corresponds very well to observations from other sites or the results of permeability measurements performed at the StocaMine.

Remark: As a general lack no qualified analysis of barrier integrity is made explicitly related to the well-known damage and hydraulic criterions.

- **Consequences of damage caused by fire in block 15:** The impact of the fire, which occurred in 2002, is assessed to be of minor importance. As already concluded by INERIS the duration and intensity of the fire (only 10 days at maximum temperatures, ranging from 100 to 370°C) was not sufficient to induce additional damage, i.e. more than that which is already created after excavation and during action of convergence. The reach of salt disturbances in the barrier ranges up to 20 meters, but the general permeability is assessed to be low.

This finding is in agreement with results from numerical calculations of heat impact during storage of heat-generating radioactive waste ($T_{\max} = 200^{\circ}\text{C}$ over long periods), the natural analogue of basaltic intrusions in the Werra region and practical observations, made during a fire in the salt mine Teutschenthal.

- **Long term stability of the pillar system:** Because the StocaMine was installed and operated as a storage facility and not as a conventional salt mine the dimensioning of the room-and-pillar-system has significant reserves regarding stability. Thus, from a geomechanical point of view, the waste disposal site with its cavities in the rock salt area is stable during its operation period and in the long-term.

3.3. SEALING CONCEPT

3.3.1. Investigation approach

Because it is a fact that brine enters the salt structure, the dam seals have the function to delay their in- and outflow into the disposal chambers. Thus a sealing concept has been developed by ERCOSPLAN (2008, 2013) resulting in a dam concept, which has been numerically proven by ITASCA (2014).

Functionality of the sealing concept has to be analyzed with respect to the following points:

- Plausibility of the technical dam building concept as part of the safety concept
- Technical feasibility - proof of construction concept
 - Experiences, e.g. from reference buildings at the site or from other projects
 - Proof of technical operability by numerical calculations, taking into account of, e.g. damage processes which should be tested with application of strength criterions (e.g. maximal strength of building materials and onset of damage, i.e. dilatancy boundary)
 - **section 3.3.3:** Assessment in terms of the present international experiences
 - **section 3.3.4:** Proof of function of sealing dams
 - Due to the impact of salt creep progressive closure of the storage rooms will occur. Coevally temporary disturbances of the salt mass will self-seal or heal. The reliability of this assumption has to be demonstrated.
 - **section 3.4:** Recovery of hydraulic integrity

3.3.2. The ERCOSPLAN concept

If brine access into a disposal facility is unavoidable the migration pathways have to be sealed by technical measures, i.e. installing of dams. The objectives are twofold,

- to avoid or to minimize brine inflow into the disposal chambers and
- to delay their outflow into the disposal chambers.

Thus, it is intended to isolate the above stated storage area with 19 dams in single and double-drifts at 12 locations (see Fig. 14). Based on a review of available Information ERCOSPLAN (2013) developed a preliminary concept regarding the installation of dam constructions, which is depicted in Fig. 19. It bases mainly on the dam concept developed in the framework of the R&D-project in Sondershausen (Sitz, 2003).

The general hydraulic requirements on the dam concept were defined by INERIS (personal comm. with ERCOSPLAN), but because their reliability is essential for the closure concept some comments are given below:

- Each sealing element has to fulfill the following design criteria: $K / L^2 < 10^{-21}$, in which L is the length of the sealing element in meters and K is the intrinsic permeability of the sealing element in square meters. It follows, that the dam permeability (6 m length) should be in the order of $3,6 \cdot 10^{-20} \text{ m}^2$.

ERCOSPLAN remark: The requirement given before was stated by INERIS but StocaMine no longer pursues this target because subsequent investigations have led to the conclusion that it is not feasible to build dams according to this requirement.

Remark: *The statement, that this limit is not practicable for the initial construction state, is supported by technical experiences as described in the following. However, as argued in section 3.4, due to the acting rock convergence, the tightness of the seal will be improved and probably reach this requirement.*

- Preferably, bentonite should be used as the material for the sealing element as it possesses not only the required sealing properties, but also an absorbing effect on heavy metals.

Remark: *The requirement that bentonite is the preferred sealing material option is a significant limitation, which should be proven because without this requirement more efficient solutions exist which allow longer dams with better sealing capacity (see below).*

- The permeability of each dam has to be ensured during a period of 1,000 years, after full saturation of each dam until the end of flooding of the waste disposal. The saturation time will depend upon the dam properties and design.
- Full performance of the dams is ensured after their full saturation and development of few MPa of swelling pressure.

Remark: *This assumption is questionable due to the negative impact of the EDZ and the technical interface between seal and rock contour. In addition, the requirement for use of a swellable material is only valid in a non-creeping rock mass, i.e. due to the convergence of salt a swelling of the sealing element is not required. Thus alternatives exist with low-compressible sealing materials where due to the acting convergence a high confinement is efficiently developed.*

The suggested sealing dam consists of two load bearing abutment elements (length: 6 m) and an in-between situated sealing element made of bentonite bricks (length: 6 m) with a saturation wall (filter layer; made of porous Al₂O₃ blocks (corundum) for hydraulic flow to the bentonite. The realizable dam lengths would be ca. 18 m. A schematic sketch is given in Fig. 19.

The long-term sealing element is made of a pre-compacted bentonite-sand-mixture (bentonite-bricks), which requires abutments that are stable in the long-term. The requirement for the initial matrix permeability of the bentonite is at least $1 \cdot 10^{-18} \text{ m}^2$. As mentioned by ERCOSPLAN this value results in high demands on a bentonite-sand mixture and can only be structurally guaranteed by an extensive quality assurance program. If this value is reached during construction the bentonite sealing element, is immediately effective and will swell if it becomes in contact with fluids, as well as it is stable in the long-term. Homogenous saturation of the bentonite should be ensured by the filter layer.

In order to guarantee the short-term abutment function, abutments will be made of concrete mixed with saturated NaCl brine, which have the required mechanical capacity to withstand the loadings due to the convergence and the hydraulic pressure.

The EDZ was identified as the main problem, because as learned from many examples the dam construction will partly fail if fluid will migrate through the EDZ as short-circuit (as observed also during the Sondershausen test). Thus, ERCOSPLAN (2013) suggests injections of the contact zone between host rock and abutment will seal the abutment, which is an often used technique. They argue, that if the sealing function also of the abutments is realized, also the principles of redundancy and diversity are satisfied, from a technical engineering point of view. This would provide, at least, a general redundant sealing functionality, which also ensures a short-term functioning (<500 years).

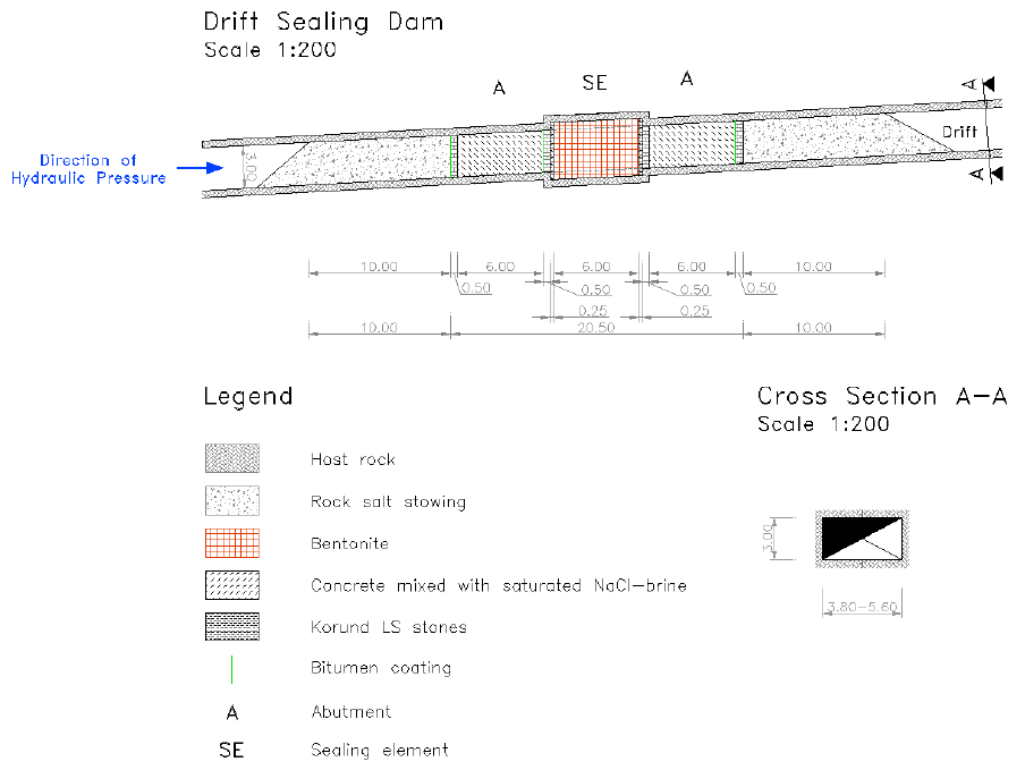


Fig. 19. Conceptual design of the drift sealing dam (taken from ERCOSPLAN, 2013)

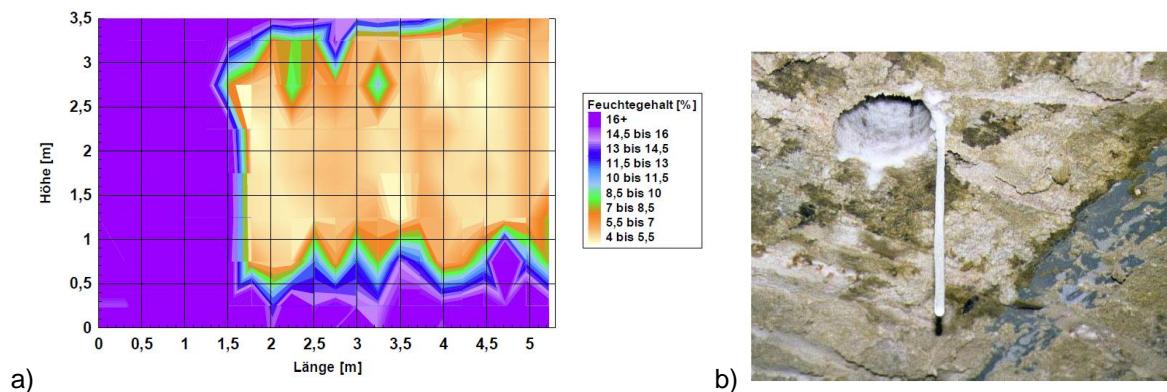


Fig. 20. Observations after dismantling the Sondershausen dam¹¹. a) Measured fluid distribution in the sealing element I (vertical cross section) b) outflow of brine from the wet rock contour through a borehole in the roof (after Sitz, 2003)

¹¹ During dismantling of the sealing elements of the Sondershausen dam (after pressurization with a fluid pressure in the order of 80 bar with volume flow rate of $Q \approx 13l/h$) a significant wetting of the rock contour was observed (Fig. 20b) and also, the saturation of the bentonite buffer was non-uniform (Fig. 20a).

As a general comment, the ERCOSPLAN-sealing concept is a possible dam concept which has been constructed and hydro-mechanically tested with a maximum fluid pressure of 8 MPa during the mock-up test Sondershausen (Sitz, 2003). Following this concept a bentonite-based drift seal between the salt mines Immenrode and Sondershausen (Aland et al., 1999) has been successfully installed.

However, it should be mentioned, that the efficiency of the seal mainly depends on its effective length and, in addition, the construction should be as simple as possible. A seal made of bentonite bricks only works if the contact between the sealing material and the rock contour is perfect, i.e. no pathways exist through the EDZ, respectively through the unavoidable technical interface between both materials because otherwise the swelling is inhibited, as learned from testing the Sondershausen dam (Fig. 20). Thus alternative concepts or improvements should be considered.

Tabl. 5 - Dam constructions of the StocaMine – geometry, mean diameter incl. dilated zones (EDZ) as well as new ALZ after removal of EDZ (drift surface cutting).

Drift ID	Dam site	Height in m	Width in m	H	W	A _{dam}	H*	W*	A _{EDZ}	Drift Type
	No.	(m)	(m)	(m)	(m)	(m ²)	(m)	(m)	(m ²)	
1-1	1	3	5,6	4,5	6,6	29,7	4,8	6,9	3,4	Parallel Drift
1-2	2	3	3,8	4,5	4,8	21,6	4,8	5,1	2,9	Double Drift
1-3	2	3	3,9	4,5	4,9	22,1	4,8	5,2	2,9	Double Drift
2-1	3	3	3,8	4,5	4,8	21,6	4,8	5,1	2,9	Double Drift
2-2	3	3	3,8	4,5	4,8	21,6	4,8	5,1	2,9	Double Drift
3-1	4	2,7	5,5	4,2	6,5	27,3	4,5	6,8	3,3	Double Drift
3-2	4	2,7	5	4,2	6,0	25,2	4,5	6,3	3,2	Double Drift
4-1	5	3	4,8	4,5	5,8	26,1	4,8	6,1	3,2	Double Drift
4-2	5	3	3,8	4,5	4,8	21,6	4,8	5,1	2,9	Double Drift
5	6	3	3,8	4,5	4,8	21,6	4,8	5,1	2,9	Single Drift
6	7	3	3,8	4,5	4,8	21,6	4,8	5,1	2,9	Single Drift
7	8	3	4,2	4,5	5,2	23,4	4,8	5,5	3,0	Single Drift
8	9	3	3,8	4,5	4,8	21,6	4,8	5,1	2,9	Single Drift
9-1	10	3	3,9	4,5	4,9	22,1	4,8	5,2	2,9	Double Drift
9-2	10	3	3,8	4,5	4,8	21,6	4,8	5,1	2,9	Double Drift
10-1	11	3	3,8	4,5	4,8	21,6	4,8	5,1	2,9	Double Drift
10-2	11	3	3,9	4,5	4,9	22,1	4,8	5,2	2,9	Double Drift
11-1	12	3	3,8	4,5	4,8	21,6	4,8	5,1	2,9	Double Drift
11-2	12	3	3,8	4,5	4,8	21,6	4,8	5,1	2,9	Double Drift
sum(m ²) =						435,45			56,5	

^{*)} Increased cross section under consideration of the additional EDZ-dimensions before (EDZ - roof (m): 0,5; EDZ - floor (m): 1 and EDZ -wall (m): 0,5) and after removal of the EDZ (new EDZ with an overall thickness of 0,15 m).

3.3.3. Assessment in terms of the present international experiences

Historically, because in several cases water inflow in salt mines occurred, early closure concepts with dams using different materials were developed. Some of them, e.g. the dam Leopoldshall¹² (Fig. 21), were working. For a historical overview see Wagner (2005).

As a result of the historical experiences, however, should be noted (DBE, 2008):

- All tight dam structures were in the rock salt
- From the beginning just a very long dam was tight
- The tightness of all shorter dams was produced subsequently by injections, where the injection pressure of the injected suspension reached the lithostatic pressure.

Meanwhile, numerous new experiences and know-how are available from drift sealing constructions dedicated to a final underground storage in saliniferous strata for nuclear waste and toxic material. It has to be pointed out, that in contrast to the general dam building concept of Sitz (2003) developed for seals in rock salt formations they preferably relate to construction and sealing concepts with monolithic dams. As an advantage such constructions could act as load-bearing elements as well as sealing elements.

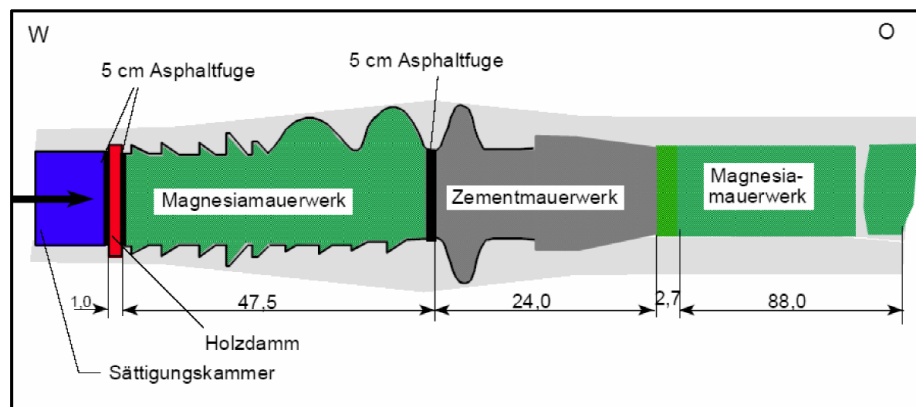


Fig. 21. The dam-building Leopoldshall (dimension in m) (after Fliß, 2003).

However, in a first step requirements have to be defined to achieve the required sealing function in the post-operational stage:

- Stability against the acting rock stresses due to convergence
- Stability against possible accidents, e.g. warranty that their function is ensured if the brine inflow occurs faster than assumed, i.e. before a sufficient confinement is reached.
- Technically impermeable to fluids
- Long-term resistance of construction materials to corrosive solutions and gases
- Simple mechanisms of action of the components; the function of each component has to proven

¹² The first in the literature mentioned horizontal underground seal was built at a depth of 300 m in the pit Leopoldshall in the Staßfurt area in 1898, including construction elements of MgO-bricks and -mortar, as well Portland cement. The total length was ca. 161.5 m. Using MgO-bricks and mortar in 1916 in the potash mine Bismarckshall (Unterbreizbach) also a dam building was erected. During operation leakage occurred which was sealed after MgO-binder injections (length: ca. 80 m).

At the special situation of the StocaMine the sealing capacity has to be ensured in the case of fluid-in- and out-flow.

Approved concepts already exist from seal concepts at the following sites, where dams were built routinely or as prototypes, i.e. the performance of each concept has been demonstrated. It has to be mentioned that sealing elements based on asphalt or bitumen are not considered because they require always abutments. Thus they can be considered as diverse element to improve a construction.

In the following, pros and cons of each construction principle will be discussed with respect to the general demands:

- **Bentonite-based drift seals**, e.g. between the salt mines Immenrode and Sondershausen (for details see Sitz, 2003 ; Aland et al., 1999)
 - Pros:**
 - + Long-term stability of bentonite in salt formations is demonstrated by analogues (e.g. Gruner et al., 2003)
 - + Swelling pressure (up to some MPa, depending on the bentonite content) ⇒ active re-compaction of the EDZ
 - + Absorption capacity for heavy elements
 - Cons:**
 - Complexe construction: difficult interface to the host rock contour ⇒ risk of hydraulical short circuits
 - development of tightness depends on the controlled saturation during flooding; uniform saturation is not ensured; localized pathways may be created due to fluid flow fingering
 - limited length, because abutments are required as support against swelling pressure
 - expensive

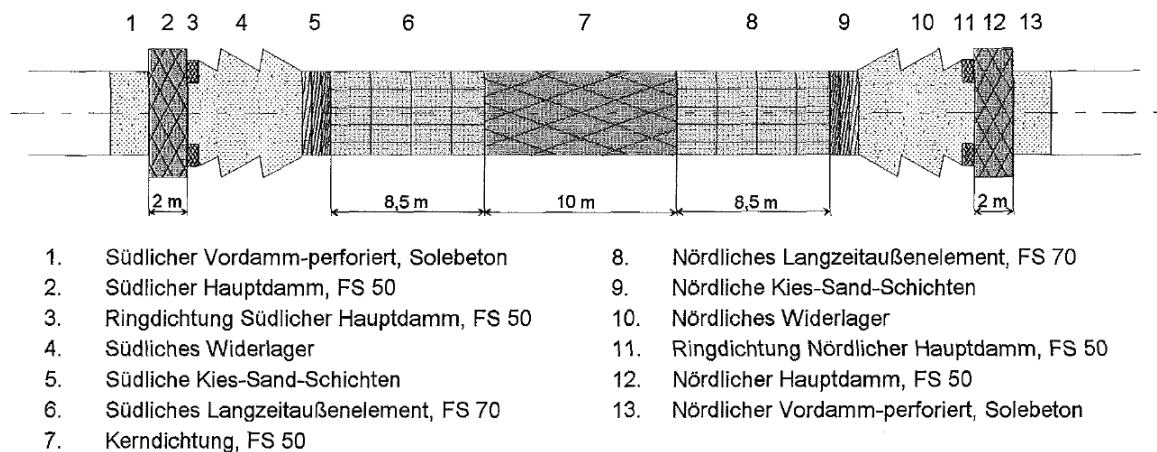


Fig. 22. Concept of the drift seal Immenrode (after Aland et al., 1999).

- **Dams on the basis of salt concrete** (crushed salt with Portland cement binder) – site concrete:
 - Drift seal test in the salt mine Hope¹³ (Fischle et al., 1987)
 - Pilot-dam Asse mine /GER (GSF, 1991, Gläß et al. 2005)
 - Repository Morsleben / GER (z.B. Eilers et al., 2003).
- Pros:** + high mechanical strength
 + low matrix permeability (delay of corrosion processes)
 + self-planishing material, i.e. homogenous site concrete
- Cons:** - no long-term stability against salt solutions ⇒ corrosion
 - thermal contraction (cracks during cooling) and autogenous shrinkage¹⁴; from the point of tightness problematic interface to the host rock contour ⇒ risk of hydraulical short circuit; specific injection measures are required at the roof
 - the complete dam has to be constructed in one cycle to minimize the risk of interfaces, acting as horizontal pathways

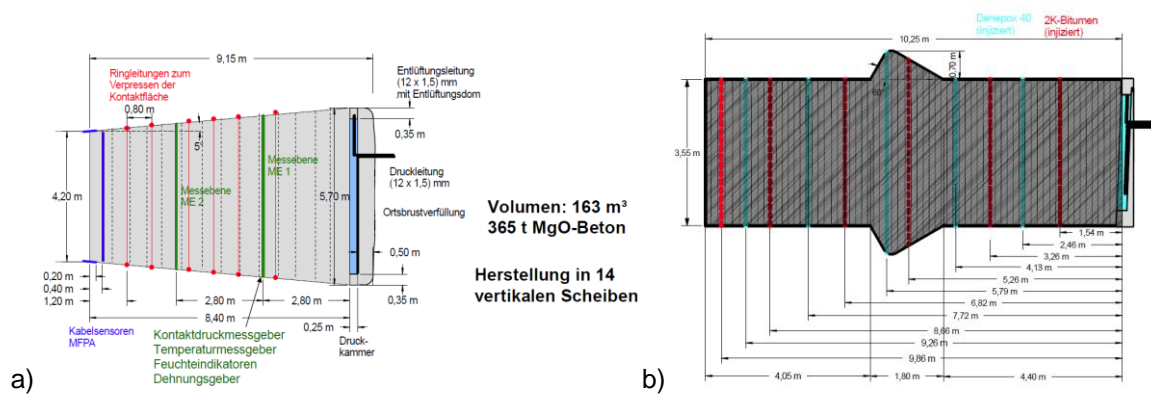


Fig. 23. Realized mock-up tests of MgO-based drift seals in R&D-project CARLA at the Teutschenthal mine. a) site concrete dam GV1. b) shotcrete dam GV2 (after GTS, 2010).

- **Dams made of Sorel concrete basis** (MgO-Binder with additives like salt or sand/grit content)
 - Construction of drift barriers in the repository Asse / GER (Heydorn et al., 2015) – site concrete of MGO-binder with crushed salt.
 - Mock-up-tests of MgO-concrete dams (silicate grain fractions as additives) in shotcrete or site concrete technology in the framework of the R&D-project CARLA in the Teutschenthal Mine / GER (GTS, 2005, 2010) – see Fig. 23.

¹³ Ahead of the planned flooding of potash and rock salt mine Hope a test dam was erected in a drift at the 500 m level. The dam consisted of two abutments and a sealing element. The building was designed to withstand a pressure of 6 MPa and consisted of two 5 m long prismatoid shaped abutments of salt concrete (portland cement, fresh water and rock salt surcharge) which are separated by a 50 cm thick sealing joint of sand asphalt. Only the initial phase of flooding was monitored because the instrumentation fail.

¹⁴ Shrinkage means the contraction or decrease in volume of the concrete over time, due to moisture loss (dehydration) and by chemical reactions or structural transformations during cure.

Remark: Comprehensive experiences from Sorel-concrete dam buildings constructed as site concrete are available. In addition, also the shotcrete technique is developed. In addition to the material properties both construction techniques have individual pros and cons:

Pros:

- + using silicate additives high mechanical strength is ensured; adding of salt delivers lower but sufficient strength properties
- + low matrix permeability
- + no matrix shrinking (the material behaves volume-constant with time)
- + Long-term stability in salt formations is demonstrated¹⁵ (e.g. Freyer et al., 2015)
- + cohesion between the building material and the rock contour
- + site concrete: self-planishing material, i.e. homogenous site concrete
- + shotcrete technology: no thermal induced shrinking / only simple and limited room-consuming equipment is necessary

Cons:

- site concrete: thermal contraction
- site concrete: the complete dam has to be constructed in one cycle to minimize the risk of interfaces, acting as horizontal pathways
- shotcrete technology : time consuming construction, i.e. the maximum thickness of each layer is in the order of 10 cm/day, but because the requirements on the technical set-up is low several parallel working places are possible

- **Dams made of standard concrete basis** (so-called Wismut-dams)
 - Construction of 16 temporary flooding dams in shotcrete technology by the WISMUT¹⁶ (for details s. Wedekind et al., 2003).

Remark: It has to be mentioned that this is not a dam realized in a salt formation, but the general concept of shotcrete dams is a significant progress for dam construction. The gained information can be used for optimization, e.g. for the construction of abutments.

¹⁵ It can be stated, that in presence of MgCl₂-bearing solutions the 3-1-8 binder phase [3 Mg(OH)₂ · MgCl₂ · 8 H₂O] represents the thermodynamically stable phase up to temperatures of 80°C. Above 80°C, the phase 3-1-8 is replaced by the 9-1-4 phase. At NaCl saturation (an obvious condition in rock salt formations) the corrosion resistance of the material increases even as the 3-1-8 phase is stable at very low Mg²⁺ solution concentrations (0.5 mol Mg²⁺ or MgCl₂ / kg H₂O).

¹⁶ The rehabilitation of the underground workings of the uranium deposits Königstein of the Wismut GmbH was carried out by means of controlled and stage-wise flooding in surface and underground monitoring to a level of 140 m above sea level through an open test drift system. To operate the downhole control system 16 so-called flooding pressure dams FDD had to be built in the 90ies of the previous century. This flooding pressure dams were built with the shotcrete technology using normal concrete B35. Care was taken to a strict limitation of temperature build-up in order to ensure the absence of cracks and leaks of these dams. This was achieved by limiting the shell width to about 10 cm and by a temperature monitoring of each shell having a plurality of sensors. The dams ensure the access to the remaining open slots and the control drift against the alreadyflooded underground openings. These dams have a length of about 5 m and a diameter of approximately 3 to 4 m, with a maximum of fluid pressure of about 12,5 bar.

The shotcrete technology has the following pros and cons:

- Pros:** + using silicate additives high mechanical strength is ensured
+ low matrix permeability (has to be proven)
+ cohesion between the building material and the rock contour
+ only simple and limited room-consuming equipment is necessary
- Cons:** - Time consuming construction, i.e. the maximum thickness of each layer is in the order of 10 cm/day, but because the requirements on the technical set-up is low several parallel working places are possible
- Autogenous shrinkage (actually not quantified, but obviously not relevant)

3.3.4. Proof of function of sealing dams in a disposal facility

Independently from the final dam construction concept of the StocaMine, a main objective is the quantification of time needed for flooding of the cavity in the area of the underground deposit. This can be estimated from the analysis of flow rates through the dam under consideration of realistic tightness assumptions.

Integral tightness parameters can be derived e.g. from the flow resistance of the dam (e.g. monolithic dam made of salt concrete) and from the lateral infiltration due to a technic-induced gap at the contact between construction material (concrete) and host rock and as well by the geomechanical-induced dilated zone in the surrounding rocks. It has to be noted that it is assumed for all sealing elements that the hydraulic tightness will enhance with time due to creep of visco-elastic properties of rock salt (as the host rock).

The integral permeability of the system consisting of the sealing structure, the contact zone and the excavation-damaged zone (EDZ) has to be below a certain limit.

As general hydraulic requirement, the following values is defined by INERIS: $K/L^2 < 10^{-21}$; it follows, that the (integral) permeability of the sealing element should be $< 3,6 \cdot 10^{-20} \text{ m}^2$ which is technically not possible for the initial state after seal construction (see below).

In literature, minimum requirements for reliable capacity of dams for insulation are given which vary due to its various demands; e.g.

- GSF (1991): planned dam construction in the former Asse mine with a complex sealing element system as a reference sealing for a potential repository for radiative waste in rock salt; consisting of several sealing and counter bearing elements - **requirement: $< 2 \cdot 10^{-16} \text{ m}^2$**

Note: This project was never finally realized due to changes in importance of scientific key aspects, but partial results were published (Gläß et al., 2005). However, results of the research project CARLA - realized under extreme weathering conditions of the host rock (Carnallite) – depict that the required value of $< 2 \cdot 10^{-16} \text{ m}^2$ was achieved even under these difficult conditions (GTS, 2010).

- Mauke et. al, 2012; Mauke & Herbert, 2015: Designed sealing elements on the basis of salt concrete dams within the repository Morsleben (GER) - **requirement: $< 10^{-18} \text{ m}^2$**

Note: These high requirements are as far as known not easily realizable due to shrinking properties of salt concrete (by thermal induced contraction and autogenous shrinkage) - even despite of the usage of special binder injections along the plug contour. Nevertheless, injection tests with brine over several years documented that the permeability reduces until the range of the requirements due to convergence (Mauke & Herbert, 2015). Similar observations in the Asse mine support these results (Heydorn et al., 2015).

For the estimation of possible flow rates the following boundary conditions were taken into account:

- Construction length: 6 m - 20 m
- Hydraulically effective profiles for 19 dams (Tabl. 5 -):
 - Dam profile + initial EDZ due to lifetime (ca. 0.5 m in contours and roofs resp. 1 m in the floor): 435.5 m²
 - New EDZ after cutting of previous EDZ: each ca. 0.15 m
(Permeability: 1·10⁻¹⁹ m²) 56.5 m²
- Integral permeability:
 - 2 · 10⁻¹⁶ m² - relative disadvantageous case of initial state; compare with project CARLA (GTS, 2010)
 - 1 · 10⁻¹⁸ m² - as known from the pilot dam Morsleben resp. Asse; technically realizable state resp. conditions after few years lifetime
 - ≤1 · 10⁻²⁰ m² - predicted final state after creep of saliniferous host
- Effect of brine pressure resp. pressure gradient Δp

The flooding of the mine is a time-dependent process. In duration from reaching of a brine level (depth 550 m) in 240 years to a complete flooding of the mine (top depth 450 m) in 350 years, the hydraulic pressure $p_{t=240a} = 0$ bar ($t = 240$ a) increases to $p_{t=305a} = 12$ bar ($t = 305$ a). Then, the brine pressure accelerates quickly to ca. 6 MPa (corresponding of brine column of 550 m height with $\rho_{\text{brine}} = \text{ca. } 1.1 \text{ g/cm}^3$).

The flow rate through the dam follows from:

$$Q = \frac{\Sigma K_j}{\eta} \cdot \frac{\Sigma A_i}{\Delta l} \Delta p \quad (3-5)$$

with Q = flow rate (m³/a), k_1 = integral permeability dam (m²), A_1 = cross section of dam (m²), k_2 = integral permeability of secondary EDZ (m²), A_2 = cross section of secondary EDZ (m²), Δl = length of dam resp. sealing element, η = dynamic viscosity (Pa·s), Δp = fluid pressure (Pa)

Variation of the given boundary conditions results in flow rates as depicted in Fig. 24. As expected the tightness in the initial state primarily dictates the brine inflow. According to the existing knowledge an initial tightness in the range of ≤ 10⁻¹⁸ m² is technically realizable even with common construction materials like Sorel or salt concrete. The resulting total flow rates are dependent on the length of the sealing element < 10 m³/a and accelerate at least in the order of 2 due to creep of the saliniferous host rocks and will result in tight/impermeable inclusion.

Bentonite sealing elements gain their impermeability not before beginning humidity penetration and a resulting swelling pressure (in the range of 1 – 2 MPa for the favored bentonite bricks (Sitz et. al., 2003)). The assumed tightness after swelling will also be in the range of ≤ 10⁻²⁰ m².

In detail, flow rates of 0.15 resp. 0.51 m³/a result from a duration $t = 240$ a to 305 a and a mean fluid pressure of ca. 3 bar (dam length: 20 resp. 6 m). After complete flooding and development of a hydrostatic pressure up to the overburden (fluid pressure $\Delta p = 6$ MPa) the flow rates will be 3 resp. 10 m³/a.

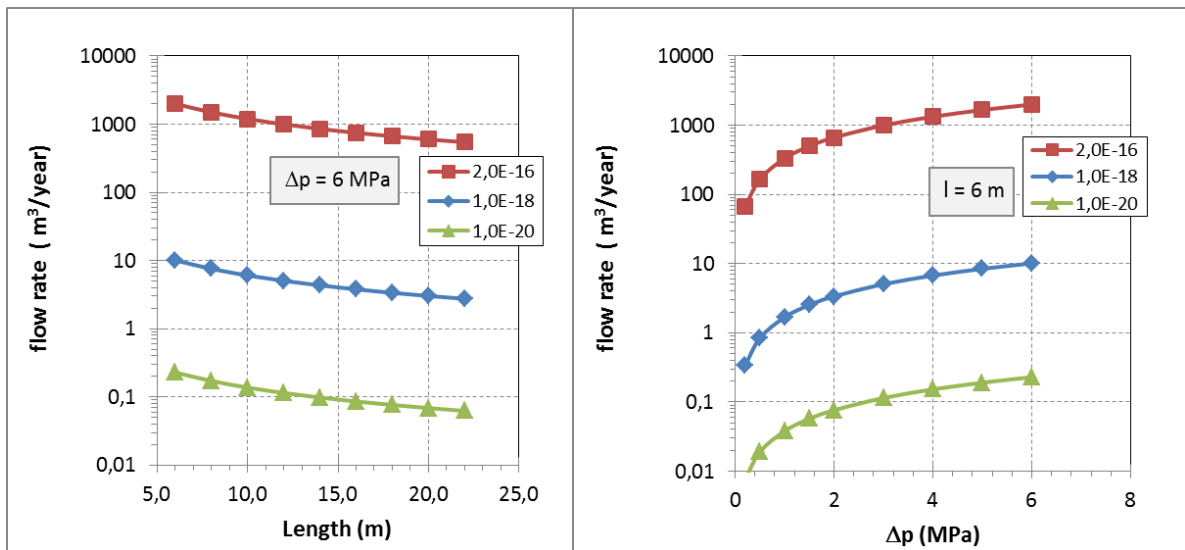


Fig. 24. Flow rates (left) vs. length of the dam (sealing element) and (right) vs. fluid pressure.

Assuming such long-lasting nearly constant flow rates for $t > 305$ a would result in convergence-dependent decreasing cavity volumes at $t = 450$ a resp. $V = 40 \text{ Tm}^3$. Due to further convergence an internal fluid pressure would occur within the sealed mining area. The flow rate would decrease the whole time. A fluid pressure in the mining area outside of the dams equal to those inside would result in a flow rate of 0.

Resulting from the further progressing – but due to the internal pressure – evidently reduced convergence rate a hydraulic pressure occurs within the sealed area which is successively higher than the brine pressure. This leads to a squeezing of brine after 1,000 years from the sealed to the non-sealed areas of the mine. A pressure difference of 5 to 10 bar leads to equality of convergence rate and flow rate and will be in the range as already given for $t > 500$ years.

That means convergence-dependent squeezing and its quantity are strongly dependent on the tightness and impermeability of installed dams. If the integral permeability is – as estimated – $< 10^{-18} \text{ m}^2$ no significant squeezing of brine will occur within the next 1,000 years. This results from low-pressure inflow in the initial state and the effect of storage of brine volume in the repositories cavities.

3.3.5. Back-filling measures in the storage area

ERCOSPLAN (2013) suggested also a backfilling for the remaining underground openings of the storage area which, apart from the construction of long-term stable drift sealing dams in the access main drifts to the waste disposal area, focuses on the following objectives:

- minimization of remaining voids
- stabilization of roof convergence
- delay of water access to the waste

The remaining cavity volume is approximately:

- Drift system cavity volume: $54,700 \text{ m}^3$
- Remaining cavity volume of the storage blocks: $94,300 \text{ m}^3$

The suggested backfill materials and sources are:

- Rock salt debris: Easy to be mined but a new extraction area has to be excavated.
- Salt concrete: The salt concrete is obtained from a mix of cement, fly ashes, crushed salt and saturated NaCl brine. The crushed salt replaces sand and gravel as additive and the brine replaces the water. The filling mortar is obtained from a mix of sand, hard rock gravel (granite), cement and NaCl brine. This composition creates a uniform stress distribution, used for corrections of the blocks irregularities.
- Filling mortar (mixed with brine).

ERCOSPLAN argues,

- that since there are no demands on the inner barrier of the multi-barrier-system with regard to the permeability as well as the long-term stability of the construction materials, because the task of isolating the waste disposal area is entirely taken over by the geotechnical barriers “drift sealing dams”, the so-called inner barrier mainly serves the purpose of reducing the reactive void.
- Thus filling mortar (mixed with brine) or salt concrete should be investigated as preferred backfill material options, which both could be pumped, whether from a surface backfill-mixing plant (in the case of filling mortar) via tubes down to emplacement areas, or has to be prepared (in the case of salt concrete) close to the underground openings. In terms of cost-effectiveness, the filling mortar is assumed as the best alternative.
- A filling ratio of 95% of cavities, corresponding to around 140,000 m³ should be realized by pumping liquid material into the underground cavities.

It has to be mentioned that long-lasting experiences exist in German salt mine using different types of “filling mortar” for backfilling measures, e.g. in Werra region (Unterebreizbach) and the Teutschenthal salt mine, but most of experiences are not published.

However, although the backfill measures are not précised the following remarks should be made:

- Filling mortar, or in more detail hydraulic minefill represents a popular mining backfill method applied in several salt mines because significant material volumes can be pumped into the mine, e.g. at the Teutschenthal mine ca. 150,000 m³ per year.
 - As a general challenge the specific properties of the backfill have to be defined. Usually, hydraulic backfill consists of a granular mineral fraction with small amounts of pozzolanic binder such as cement, fly ash, gypsum or slag, as additives, to improve the mechanical minefill stability. Hydraulic fills and paste fills are the most common types of backfills used but their hydraulic and the resulting properties may significantly differ.
 - It has to be taken in mind, that depending on the composition of the filling mortar significant amounts of water or brine (the preferred option to avoid dissolution effects) are necessary to prepare a hydraulic pumpable filling mortar, e.g. in the Teutschenthal case the minefill consists of around 50 vol.-% mixing water, which is only partially bonded by the reactive components of the binder. Thus, during emplacement of the material an direct outflow of ca. 10% water is observed, which has to be managed (e.g. pumped to the plant and used again for mixing). However, numerous loading tests (simulating in situ-stress conditions) demonstrated that most of the water can be pressed out from filter mortar during the action of convergence. Thus in the respective geo-mechanical safety concepts for closure of the Teutschenthal mine it is assumed that the complete water content may be squeezed out, which has to be stored in an internal reservoir in the isolation-rock-zone.
- ⇒ With respect to the safety concept the content free water should be minimized in the emplacement area to avoid solution effects mobilizing heavy metals. Thus hydraulic backfill measures are not the preferred option.

⇒ However, if a granular backfill is used (e.g. gravel or pneumatically injected filter ashes) all aspects of roof stability are given and also additional storage capacity exists to buffer a water inflow through the dams, which would result in a delayed and minimized contaminated fluid outflow.

3.3.6. Summary

The outcome of the above mentioned knowledge, gained from conventional mining and hazardous waste storage projects, in comparison with the geo-technical barrier concept developed for the StocaMine can be summarized as follows:

- As a general statement, based on the existing experiences from other sealing projects, **the construction of long-term drift seals in rock salt formations with sufficient tightness is generally possible** but always the local situation have to be considered.
- The initial integral permeability of dam buildings should be in the order of $<10^{-18} \text{ m}^2$, which is possible from a technical point of view. Under such conditions, the flow rates through the dam will be $<10 \text{ m}^3/\text{year}$.
- The effective hydraulic length of the dam should be as long as possible (up to 20 m) due to the following reasons:
 - (1) Possible negative effects, e.g. lateral flow through the EDZ, respectively creation of additional, pervasive pathways due to the inflow of under-saturated solutions, will be of importance only in the front section of the dam. In addition, despite end effects with local failure due to mechanical overload a tight dam section will be preserved.
 - (2) The resulting pressure gradient at the inflowing solution front will be lower, depending on the flow distance.
- The fact, that historically some dams were only tight after injection measures (with injection pressures in the order of the lithostatic pressure) indicates, that by such a procedure only the conditions of an artificially confined dam are created, i.e. if a dam building will be loaded due to convergence this process results in a rebuild of the rock stresses. For the confined dam it can be assumed its function is ensured.
 - **This underlies the importance of confirmation of the convergence induced sealing- and healing processes (see section 3.4).**
- The ERCOSPLAN-sealing concept is a possible dam concept, but the following has to be considered:
 - The requirement that bentonite is the preferred sealing material option is a significant limitation, which should be proven because without this requirement more efficient solutions exist which allow longer dams with improved sealing capacity (see below).
 - The abutments should be constructed as combined sealing and load-bearing elements, following also the principle of redundancy and diversity. The preferred option seems to be construction of abutments based on the shotcrete technology, following the concept of the Wismut-dams because the negative impact of high temperatures during hardening is avoided.
 - Because high stresses at the free end faces of the dam buildings are unavoidable due to the acting convergence they must be supported by additional back-filling measures, e.g. to back up crushed salt or gravel.

- In addition, injection measures are recommended but their efficiency should be specified and tested (e.g. nature of the injection material and injection procedure).
- Alternatively a longer dam concept consisting of only one monolithic material (e.g. Sorel-based shotcrete technology) should be proven, whereby different material options exists:
 - The unique advantage of Sorel-based building materials is that they show no autogenous shrinkage, i.e. the material is volume constant in the long-term. In addition, also the geochemical long-term stability in NaCl-dominated solutions.
- Backfill measures in the center part of the repository area are recommended to minimize negative effects of convergence and to support the roof stability. But the planned measures have to be specified in more detail to avoid “new” negative impacts. Material options with filling mortars or mine fill consist significant amounts of only physically bound water, which will be squeezed out during action of convergence, directly in the repository.
 - **The realization of “dry” backfill is an imperative from the safety concept.**

Alternatives as backfill materials are e.g. crushed salt (actually not available at the site), gravel or fine grained materials (e.g. filter ashes, which may pneumatically deposited in the open underground volumes).

- The possibility of installing a permanent fluid reservoir (e.g. using gravel or dry filter ashes for the backfill measures) in the actual existing and still open underground openings of the StocaMine should be proven because this seems to be an effective option to reduce the outflow of contaminated brine from the repository area.

3.4. RECOVERY OF HYDRAULIC INTEGRITY WITHIN THE STORAGE REPOSITORY

With the concept of safe disposal of hazardous waste in a rock salt formation it is usually assumed that the excavated underground openings will be closed and the resulting disturbed zones in the adjacent contour zones (EDZ) will be sealed or even heal, as a consequence of convergence and salt creep. As assumed, this process requires a period of some hundred or thousand years (depending on the convergence rate) until the salt rock is completely healed. The demonstration of this process is a central question of the safety assessment for a waste repository because it prevents negative impacts due to the existence of secondary pathways around the sealing plug.

Experiences from laboratory and field tests, supported by numerical calculations, and observations from natural analogues can be used to demonstrate that these properties are given under repository conditions.

3.4.1. Lab results

In the lab the evolution of the temporal compaction and the permanent healing of rock salt can be investigated only with long-term tests using pre-damaged samples, i.e. after triaxial strength testing (e.g. Bérest et al., 2001; Schulze, 2007). The relevant parameters to be measured are whether permeability and/or porosity. Exemplarily results of time dependent measurements performed on two dilated rock salt samples are depicted in Fig. 25.

The re-compaction is performed at $T = 25 \text{ °C}$ by the application of an isostatic pressure which is increased stepwise up to $p_{\text{iso}} = 10 \text{ MPa}$ (whole testing time: ~35 d). The initial permeability is in the order of $10^{-15} - 10^{-16} \text{ m}^2$ (corresponding to the initial state observed at StocaMine, see section

3.2.5). Isostatic loading of the dilated specimens results in a spontaneous but rather small decrease of permeability, respectively porosity, (not shown here). During constant loading sections, the porosity and the permeability are further decreasing, where a short transient behaviour with a more rapid decrease in the first stage of a section is detected until a more or less stationary decrease is obtained.

In a first approach the results of our long-term compaction experiments with durations of several months demonstrate that permeability of dry salt at a given hydrostatic pressure decreases exponentially with time:

$$k = k_0 \cdot e^{(-a \cdot t)}$$

with k_0 = initial permeability; a = compaction coefficient (given in Fig. 26a) and t = time (d)

As shown in Fig. 26a the compaction coefficient a varies by a factor of 10 depending on pressure, whereas temperature seems to be of minor importance. **Extrapolation of the efficiency of such compaction processes suggests that at isostatic conditions dilated-rock salt can be sealed mechanically in short time scales (Fig. 26b).** But it has to be mentioned that in reality the efficiency of compaction also depends on the micro-crack structure, e.g. if crack planes are translated or if mylonitization has happened, thus impeding crack closure.

Nevertheless, as demonstrated in Fig. 27 it can be stated, that re-compaction of salt with crack-closure is more efficient, than the reverse case, creation of a pervasive network. This can be easily understood, because already local interruptions of existing pathways are sufficient for a significant permeability decrease.

However, also healing of fractures is a fact as nicely documented in direct tensional tests on formerly fractured salt samples after triaxial confinement (Fig. 28) where new fracture were created instead of activating old fracture planes.

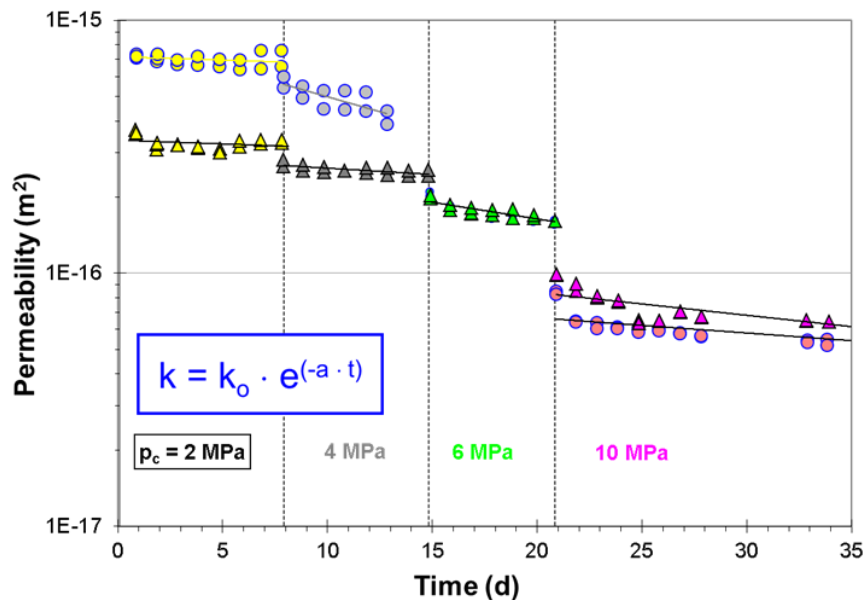


Fig. 25. Evolution of permeability in dependence on time during stepped isostatic loading with a time dependent transient compaction and decrease of the permeability. Experimental results of two experiments (arrows and circles) are depicted, which represents similar pre-damage conditions (Popp et al., 2012).

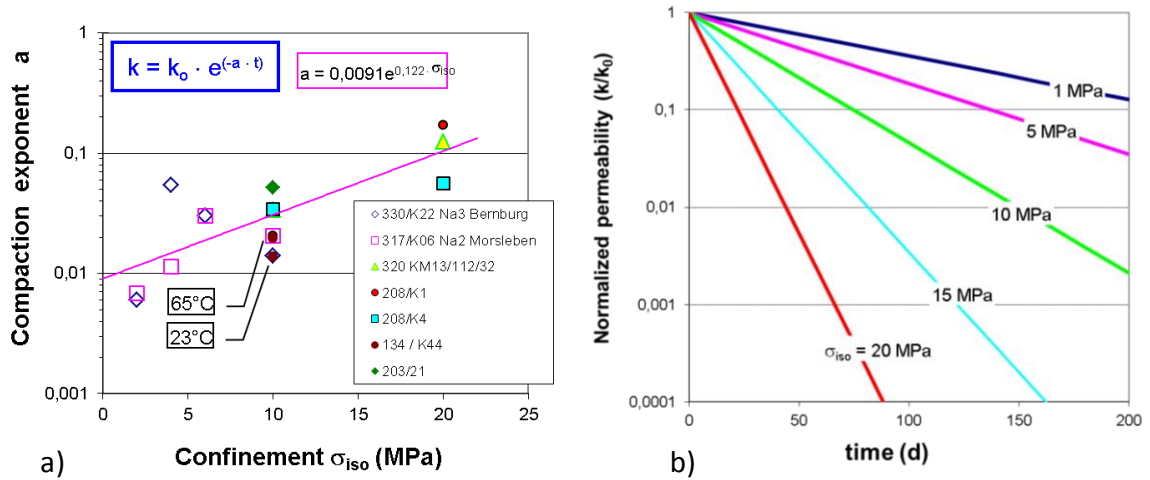


Fig. 26. Fig. Pressure induced permeability decrease with time. a) Evaluation of isostatic long-term compaction tests with continuous permeability monitoring (compare Figure 8) using a simple exponential approach. b) Development of the normalized permeability with time at various pressure stages according to the respective compaction coefficients a as determined before (Popp et al., 2012).

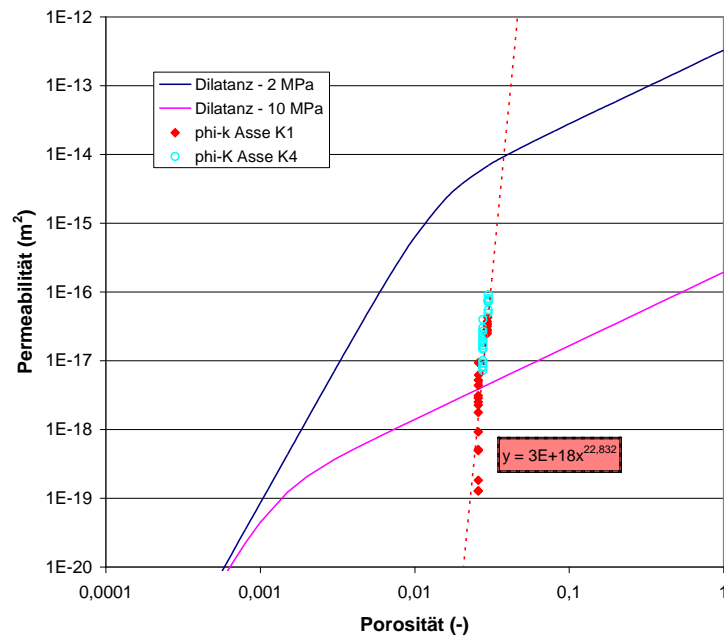


Fig. 27. Permeability-porosity relationship for dilated rock salt at $\sigma_{min} = 2$ and 10 MPa (taken from Popp, 2002) and the reverse case case during compaction of pre-dilated salt (Asse-rock salt: Proben 208 / K1 und K4) (after Popp et al. 2007).

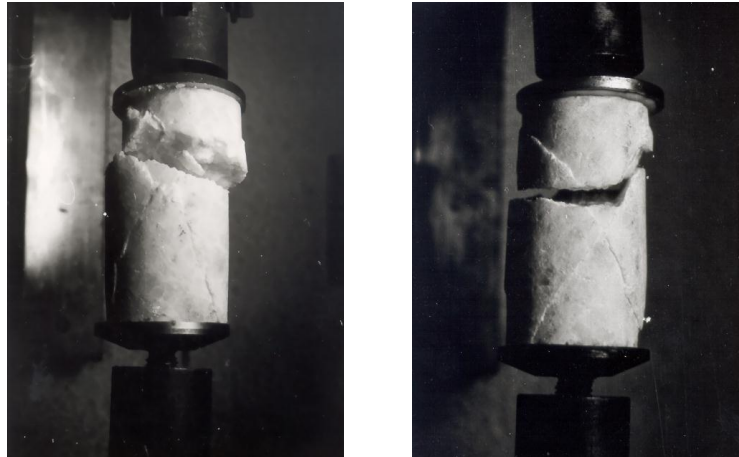


Fig. 28. Development of new fracture planes during direct tensional strength tests after healing of already fractured salt samples (after MINKLEY et al., 2005).

3.4.2. Field observations

In the post-closure phase, after the end of excavation and backfilling the shear stress in the rock salt is continuously decreasing by creep, as documented by rock convergence, until the isostatic state of stress is reached (Fig. 29). Therefore, the state of stresses in the EDZ will consequently move from the dilatant into the non-dilatant domain. At least, this causes re-compaction and the related decrease of the permeability in the EDZ.

Reestablishment of hydraulic integrity of the EDZ at in situ conditions, at least partial, has been recently confirmed by in situ investigations at a unique test site existing on the 700-m level of the Asse salt mine (Wieczorek & Schwarzianek, 2004). There, a cast steel liner of about 20 m length had been installed in a drift and backfilled with concrete as early as in 1914. Permeability measurements demonstrate that under the floor of the open drift, a typical EDZ with 1.5 m extent and permeability up to above 10^{-16} m^2 had evolved. Around the lined drift, however, the permeability had diminished to values between 10^{-20} m^2 and 10^{-19} m^2 .

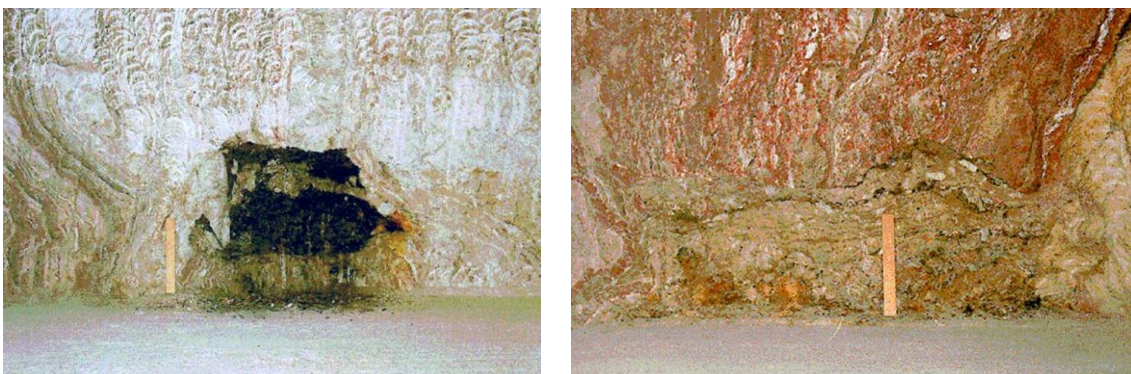


Fig. 29. Closure of underground openings; observations at the Asse salt mine from partly back-filled drift (residuals of potash hot-leaching) – scale bar ca. 30 cm.

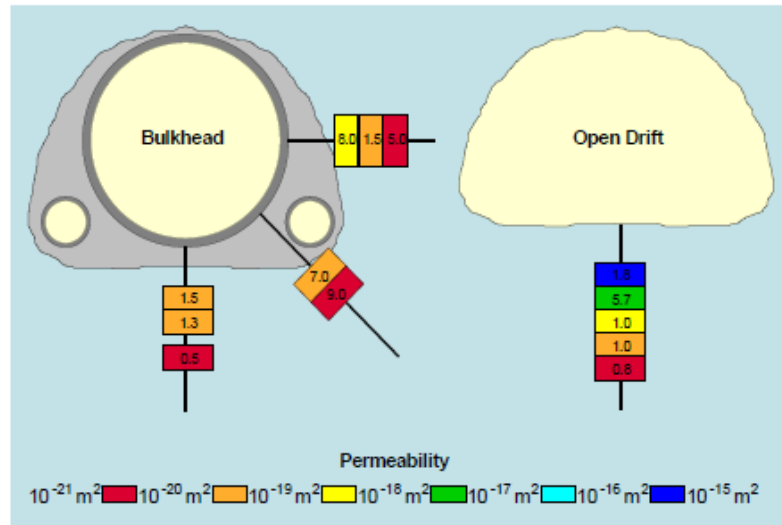


Fig. 30. Profiles of permeability around the bulkhead (left) and the neighbored open drift (right) (after Wieczorek & Schwarziemek, 2004).

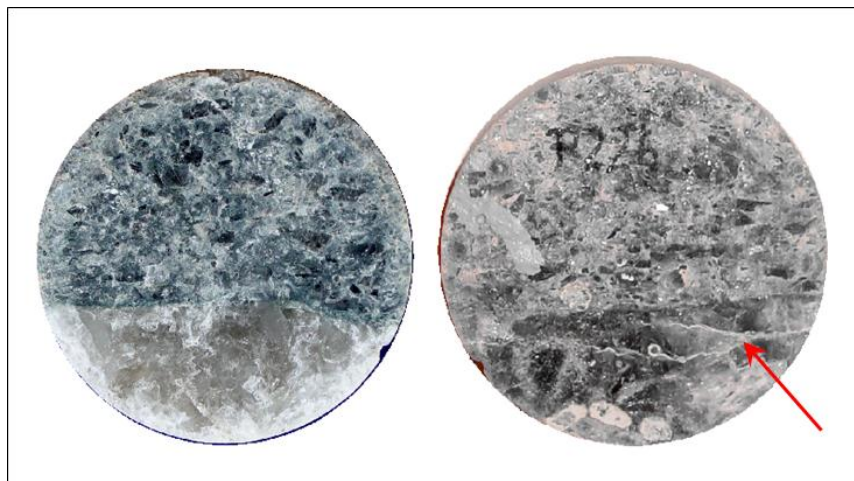


Fig. 31. Cross sections of core material ($\varnothing = 100$ mm) from the contact zone between salt concrete and salt. (right) The arrow indicates sealed salt contour fractures.

The recovery of permeability is referred to stress build-up in the rock contour, which was recently confirmed by performing hydro-frac measurements at the site. However, because a steel liner does not represent a real drift-seal, made of a sealing material, a more realistic example demonstrating healing of the contact-zone is observed for the so-called pilot dam of the Asse. There an abutment was constructed as site salt-concrete at the beginning of the 90ies in depth of ca. 950 m (GSF, 1991). Despite this element was constructed as a “load-bearing” abutment, it offers the change of investigating its properties in relation to (1) healing efficiency of the EDZ, and (2) for assessment of salt concrete dams as potential multi-function elements.

Approximately 15 year after plug construction a complex measuring program was performed, including (for details see Gläß et al. 2005):

- Permeability measurements,
- Hydrofrac investigations,
- Ultrasound examinations of the contact zone

- Laboratory testing (shear and tensile strength of the interface between salt and concrete, etc.)

Although this pilot-dam was only planned as an abutment without any special requirements for hydraulic tightness, the permeability measurements showed as result:

- Concrete mass: $k = 6 \cdot 10^{-19}$ to $4,4 \cdot 10^{-24}$ tm^2 ,
- EDZ: $k = 6,5 \cdot 10^{-21}$ to $2 \cdot 10^{-24}$ tm^2 ,
- Contact zone between salt and the dam material: $k < 10^{-18}$ m^2 .

Referring to the contact zone, it has to be mentioned, that in one case in the roof (representing a position with minor concrete quality, due to manually stopping of the roof joint) was observed. However, tensional and shear tests demonstrated a high cohesion between the salt concrete and the salt, i.e. the tensional strength is in the order of intact salt:

- Direct tensional strength: $\sigma_T = 1,2 \pm 0,3$ MPa

Thus, it can be concluded that the recovery of hydro-mechanical integrity of the salt contour zone and building material itself has been convincible demonstrated, but the impact of the depth respectively the resulting minimal stress as a function of time is the main factor.

3.4.3. Evaluation of the site conditions - Numerical simulations

Despite the general assumption of the self-capacity of dilated salt for time- and load-depending sealing or even healing can be attributed as a fact the relevancy of this process has to be proven for the StocaMine site.

ITASCA (2013b) presents a comprehensive numerical analysis about the evolution of salt permeability with time at long term. The aim of this study was to estimate the evolution of the salt permeability around the bentonite sealing dams in the Wittelsheim repository site.

Models of single and double tunnels located at sealing dam positions were created using FLAC3D. As initial state for their calculation the salt constituting the drifts where dams should be constructed were introduced at 10 years of creep, counted from the end of the excavation. The evolution of stress in the salt around the sealing dams was then considered to allow for the estimation of the permeability evolution with time of the near field salt.

Based on a porous media model ITASCA introduced an empirical description which relates the change of permeability to stress changes due to elastic deformation of pores:

$$k = k_0 \frac{e^{-x C_p \Delta \sigma}}{1 - \phi_0 - x C_p \Delta \sigma} \quad (3-6)$$

With k_0 and ϕ_0 are respectively the initial permeability and porosity of the intact rock; $-x$ is a factor that accounts for the tortuosity (representing the non-linear character to the fluid trajectories in the porous media) and also for the fact that changes in the porosity can be associated to the creation of new pores or to the increase in the opening of existing pores.

C_p is the compressibility of pores that relates the variation of the pores structure to the mean stress

In a simplified way it can be written

$$k \propto \phi^n \quad \text{with } n = 1 \text{ to } 5, \text{ according to Stormont \& Daemen (1992)} \quad (3-7)$$

Tabl. 6 - Calibrated parameters of Stormont's law for the Wittelsheim rock salt.

Parameters	Symbol and unit	Value
Pore compressibility	Cp (MPa ⁻¹)	0.45
Kozeny-Carmen term	x (-)	4.5
Initial porosity	\varnothing_0	0.1%
Initial permeability	k_0 (m ²)	10 ⁻²¹

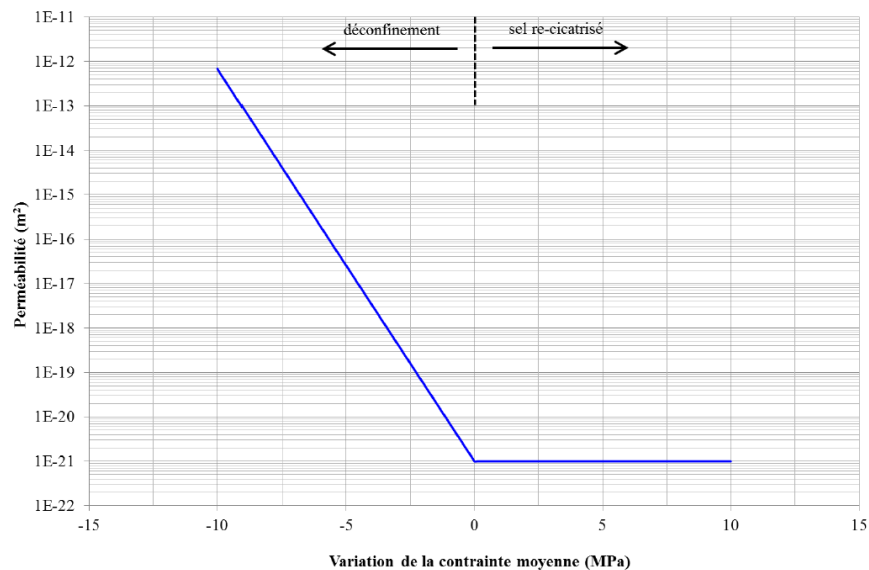


Fig. 32. Permeability vs. mean stress variation law for the rock salt (ITASCA, 2013b).

Using the measured permeability data of IBEWA the parameters of Stormont's formulation (i.e., the compressibility of the pores, Cp and the term of Kozeny-Carman, x, were calibrated, as depicted in Tabl. 6 - . As outcome, a permeability/stress relationship is obtained (depicted in Fig. 32) which represents a tool for evaluating the evolution of permeability as a function of stress. As a reasonable limitation a minimal value of permeability for the healed rock salt was considered, equal to the initial permeability of the intact rock salt (10⁻²¹ m²). The permeability cannot decrease below this value even for a stress state higher than that of the initial intact rock.

Remark: It has to be mentioned, that the poro-elastic approach, used by ITASCA is a significant simplification because not the process of real damage is simulated which depends on plastic deformation of salt under the acting stress field. As a consequence, of this only phenomenological description, a change of stress state in salt would results instantaneously in quasi-crack-closure or -opening, respectively in permeability changes. Thus, the permeability changes in the surrounding salt barriers are over-estimated, if only the stress gradient is considered. This is not plausible¹⁷.

¹⁷ An example for a more realistic description is given by the example depicted in Fig. 16, where first dilatancy (new crack-porosity) is calculated and then via a qualified porosity-permeability relation the resulting permeability is estimated. It comes out, that the dilated contour zone, which corresponds to a hydraulic permeable zone is limited to some few meters because at a contours depths of 1 or 2 m the increased minimal stress limits the permeability, as confirmed by the permeability and hydrofrac measurements.

However, the calculations give a first overview about the temporal evolution of the permeability state at the site.

The calculation of the permeability evolution around the dam locations is done in two steps, covering generally a time period of 5000 years:

- (1) As initial state ITASCA simulated (1) an excavation phase by progressive stress relaxation of the tunnel section and (2) a creep simulation over a period of 10 years. It follows a significant unloading of the near-field of the underground-openings which is related, using the above mentioned permeability stress-relationship, with permeability changes.

The obtained permeability values at the contour are in the order of $>10^{-18} \text{ m}^2$ to 10^{-15} m^2 and higher, depending on the contour depth and the stress field geometry. This corresponds to the measured values of IBEWA (see section 3.2.5).

- (2) In the second step, after installation of the drift, a recovery of normal stresses in the contour occurs due to the interaction of convergence and the more or less stiff dam inclusion. The stress recovery is time dependent on to the acting creep but the numerical results document an efficient decrease of permeability with time.

Fig. 33 shows the permeability evolution at various contour depths with time over a period of 5000 years. It becomes clear, that the development of normal stress and the corresponding decrease in permeability with time happens very quickly in the first 100 years. During this phase the dam elements are compressed and the surrounding rock salt is re-confined, reaching minimum permeability values of 10^{-21} m^2 .

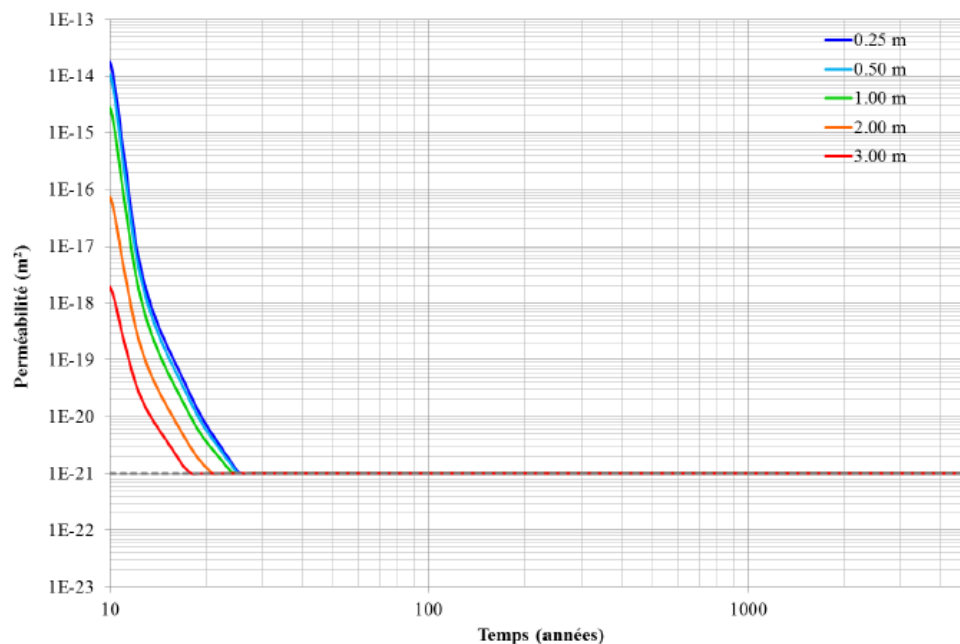


Fig. 33. Permeability evolution over 5,000 years along a vertical profile in the roof of a sealed drift (taken from ITASCA, 2013b).

3.4.4. Conclusions

As outcome of the studies, presented before, it can be stated,

it is a fact that dilated salt rock has the capability to seal (and probably heal¹⁸) existing damages if the stress state changes back to the initial state after installing dams and after closure of the repository.

This is essential for a safe inclusion of waste, because it is well known that during construction of underground openings a damage zone (EDZ) is unavoidable created which may act as hydraulic short-circuits. This has been demonstrated at different scales in lab and field tests:

Observations from in situ, i.e. technical analogues, demonstrate the recovery of hydraulic integrity inside the dilated salt mass and the EDZ. Well documented references are:

- The bulk-head at the Asse mine
- The pilot-dam at the Asse mine
- The Merkers site, recovery of hydraulic integrity after the rockburst 1989 (see section 3.2.4)

New laboratory tests allowed to study the time and stress dependence of crack closure and healing of formerly dilated rocksalt in terms of permeability and porosity under well-controlled conditions.

It has to be stated that no unique permeability/porosity relationship exist, which is valid both for dilatant deformation and the reverse case, triaxial compaction. However, the reverse process of crack closure during re- compaction is more effective, i.e. a permeability decrease occurs already at low reductions of porosity, than the initial process of crack percolation in the dilatant case (e.g. Popp et al., 2007).

In addition, healing of salt fractures under the action of normal stresses and water is a fact, despite actually qualified material laws are not available.

Using a simplified permeability-stress approach, based on poro-elasticity, ITASCA (2013b) performed a comprehensive study illustrating the most relevant stages during excavation and closure of underground cavities at StocaMine:

- The excavation of the drift and the initial creep over a period of 10 years induce an increase in the permeability up to 10^{-14} m² close to the tunnel walls. With increasing contour depth the permeability is generally smaller, in the order of 10^{-18} to 10^{-19} m² at a distance of 3 m. Moreover, it was also observed that main permeability variations take place very quickly after the excavation of the tunnel, in the beginning of the creep simulation.
- Installing the sealing dam induces a drastic reduction of the convergence rate in the rock salt around the bentonite and concrete parts of the dam. The associated re-confinement of the surrounding rock salt causes a fast decrease in the permeability during the following first decades. The permeability is reduced down to its initial value of 10^{-21} m². Therefore, a sudden flooding of the repository by the brine appears unrealistic, if dams are installed.
- In the long-term, far-field stress changes will occur due to the closure of overlying mined areas. However, this will results only in further stress build-up, ending at depth related lithostatic stresses at isostatic conditions. Thus, the permeability of salt around the dams is not affected by this change and remains in the order of 10^{-21} m² even at the long term.

¹⁸ Healing means, from a physical point of view, the recovery of cohesion between crack planes, which is mainly supported by fluid-assisted creep and recrystallisation phenomena, as described e.g. by Urai & Spiers, 2007. However, a well-based description which can be used for quantifying this effect is actually not available.

Thus, the performance of the dam buildings in the StocaMine is already given after a period of less than 100 years. This has a significant impact on the water in-flow scenario into the storage area.

3.5. GROUNDWATER INFLOW AND OUTFLOW SCENARIO INSIDE THE WASTE REPOSITORY

LITERATURE

- ABVO (1996): Allgemeine Bergverordnung über Untertagebetriebe, Tagebaue und Salinen im Oberbergamtsbezirk Clausthal-Zellerfeld
- Aland, H.-J.; Handke, N.; Leuschner, J.; Bodenstern, J.; Maelzer, K.; Sitz, P.; Gruner, M.; Springer, H. (1999): Langzeitfunktionstüchtiger Streckenverschluß aus kompaktiertem Bentonit im Bergwerk Sondershausen. Glückauf 135 (1999) 3, S. 134 - 139 + Kali und Steinsalz 12 (1999) 9, S. 24 - 29 + Geotechnik 22 (1999) 1, S. 56 - 62
- Beauheim, R. L., & Roberts, R. M. (2002): Hydrology and hydraulic properties of a bedded evaporite formation. J. Hydrology 591, 66-88.
- Berest, P., Brouard, B., Feuga, B., Karimi-Jafari, M. (2008): The 1873 collapse of the Saint-Maximilien panel at the Varangéville salt mine. Int. Journal of Rock Mechanics & Mining Sciences 45 (2008) 1025-1043.
- Berest, P., Brouard, B. U& de Greef, V. (2001). The influence of permeability and stress on spherical hollow salt samples. Salt permeability testing RFP 98-1-part 2.
- BGR (1977): Langzeitsicherheit radioaktiver Abfälle - Katalog geeigneter geologischer Formationen in der Bundesrepublik Deutschland. Bundesanstalt für Geo-wissenschaften und Rohstoffe, Hannover.
- BGR (1995): Endlagerung stark wärmeentwickelnder radioaktiver Abfälle in tiefen geo-logischen Formationen Deutschlands. Untersuchung und Bewertung von Salzformationen. Hannover: BGR-Archiv-Nr. 111 089 (im Auftrag des BMU).
- BGR (2006): Untersuchung und Bewertung von Regionen mit potenziell geeigneten Wirtsgesteinsformationen. Hannover (im Auftrag des BMWi).
- Comité de pilotage StocaMine (COFIL) (2011): Rapport d'expertise. Juillet 2011. <http://www.StocaMine.com/media/1061/Conclusions%20COFIL.pdf>.
- Cosenza, P. (1996): Sur les couplages entre comportement mécanique et processus de transfert de masse dans le sel gemme. Thèse de l'Université Paris 6.
- Cosenza, Ph., Ghoreychia, M., Bazargan-Sabeta, B. & de Marsilyc, G. (1999): In situ rock salt permeability measurement for long term safety assessment of storage. Intern. J. Rock Mechanics and Mining Sciences. Vol. 36 (4), 509–526.
- Cristescu, N. & Hunsche, U. (1991): A constitutive equation for salt, 7th Int. Cong. Rock Mech., Aachen, Sept. 16-20, Balkema.
- Davies, P.B. (1991): Evaluation of the role of threshold pressure in controlling flow of waste-generated gas into bedded salt at the Waste Isolation Pilot Plant WIPP. Sandia National Laboratory Report SAND 90 3246.
- DBE / DBE Technology GmbH (2008): Überprüfung und Bewertung des Instrumentariums für eine sicherheitliche Bewertung von Endlagern für HAW: AP5: Nachweiskonzept zur Integrität der einschlusswirksamen technischen Barrieren.- Peine, April 2008.
- Eilers, G., Mauke, R., Gläß, F., Preuss, J., Fischle, W., Linn, M., Schmidt, H., Müller-Hoeppe, N., & Schimpf, C. (2003): Sealing of the Morsleben Repository, Germany, Proc. WM'03 Conf., Tucson AZ, USA, 2003.

- ERCOSPLAN (2013): Conceptual design for dam constructions and partial backfill for the isolation of the StocaMine underground waste disposal site. Follow-up report N° EGB 07-042N01.
- Fleiß, Th. (2003): Entwicklung eines Algorithmus zum Entwurf und zur Abschätzung der mehr-axialen Beanspruchungen von Mauerwerksverbänden unter Berücksichtigung der Langzeitstabilität, sowie Bestimmung der Verbandsparameter. - Dissertation, TU-Freiberg.
- Fischle, W.; Schwiager, K. (1987): Untersuchungen an einem Abschlussbauwerk im Kalisalzbergwerk Hope. Kali und Steinsalz 9 (1987), Heft 11.
- Freyer, D., Gruner, M. & Popp, T. (2015): Zusammenhang von Chemismus und mechanischen Eigenschaften des MgO-Baustoffs / Relationship between geochemical and geomechanical properties of magnesia building material. FKZ 02E10880, Project duration: 01.12.2010 – 30.09.2014, Final Report, 150p.
- Gläß, F., Mauke, R., Eilers, G., Preuss, J., Schmidt, H., Lerch, C. & Müller-Hoeppe, N. (2005): Investigation of a salt concrete seal in the Asse salt mine. WM'05. Conference, 27.02. – 03.03. 2005, Tucson, AZ.
- GRS (2008): Endlagerung wärmeentwickelnder radioaktiver Abfälle in Deutschland. Gesellschaft für Anlagen und Reaktorsicherheit GRS mbH, Öko Institut e. V., Sept. 2008.
- Gruner, M.; Elert, K.-H.; Schwandt, A.; Sitz, P. (2003): Salzton - natürliches Analogon für Bentonitdichtelemente im Salinar. Kali und Steinsalz (2003) Nr. 2, S. 12 - 17.
- GSF - Stockmann et. al. (1991): „Dammbau im Salzgebirge - Testplan—“; GSF-Bericht 35/91, 1991.
- GTS (2005): Grube Teutschenthal Sicherungs GmbH „Entwicklung eines Grundkonzeptes für langzeitstabile Abschlussbauwerke (Streckendämme) im leichtlöslichen Salzgestein (Carnallit) in UTD und UTV (02C0942)“ März 2005.
- GTS (2010): Grube Teutschenthal Sicherungs GmbH (Knoll P., FINDER M. und Kudla W.) „Entwicklung eines Grundkonzeptes für langzeitstabile Streckendämme im leichtlöslichen Salzgestein (Carnallit) (02C1204), Teil 2: Erprobung von Funktionselementen in situ.“ Dezember 2010.
- TB6 (Teilbericht 6): „Modellberechnungen für das Komplettbauwerk“, IfG vom 31.08.2010, 55 Seiten, 17 Abbildungen, 1 Tabelle sowie 116 Seiten Anlagen.
- TB7 (Teilbericht 7) Priestel U., Glaubach U. und Kudla W. „Errichtung und Test von Funktionselementen (Modulen)“, TU Bergakademie Freiberg, 3.12.2010.
- Heydorn, M., Teichmann L., Meyer T., Schneefuß J. (2015): „Schachanlage Asse II - Anwendungsversuch Pilotströmungsbarriere PSB A1.“ Fachgespräch Verschlussysteme aus Magnesiabaustoff, Freiberg 28.-29. April 2015 Materialienband unter http://www.ptka.kit.edu/downloads/ptka-wte-e/FG_Verschluss_2015_Vortraege_Web-Version.pdf.
- Hunsche, U. (1993): Failure behaviour of rock salt around underground cavities, 7th symp. on Rock Salt, Kakihana H. Ed., Elsevier B., Amsterdam.
- Hunsche, U., and Schulze, O. (1996). Effect of humidity and confining pressure on creep of rock salt. In: Ghoreychi, M., Berest, P., Hardy Jr., H. R., and Langer, M. (eds.), "The Mechanical Behavior of Salt III: Proceedings of the 3rd Conference", held at Palaiseau, France, 1993. Trans Tech Publications, Clausthal Zellerfeld.
- Hunsche, U. & O. Schultze (2002): Humidity induced creep and its relation to the dilatancy boundary. In Proc. 5th Conf. Mech. Beh. of Salt, 73–87. Rotterdam: Balkema.

- Hunsche, U., Schulze, O., Walter, F. & Plischke, I. (2003): Projekt Gorleben. Thermomechanisches Verhalten von Salzgestein. 9G2138110000, BGR, Hannover.
- Hunsche, U. & Schulze, O. (2003): The dilatancy concept – a basis for the modelling of coupled T-M-H processes in rock salt. In: Davies, C., and Bernier, F. (eds.; 2005), "Impact of the excavation disturbed or damaged zone (EDZ) on the performance of radioactive waste geological repositories – Proceedings of a European Commission Cluster Conference and Workshop", held at Luxembourg; 3 5 November 2003. European Commission Report EUR 21028.
- IBEWA (2013a): StocaMine, France – Determination of in situ permeability in the StocaMine – Preliminary results. Document IBeWa « KB_k-T2-1+2_IBeWa_170113.pdf ».
- IBEWA (2013b): StocaMine, France – Determination of in situ permeability in the StocaMine – Preliminary results. Document IBeWa « ZB_k-T2-4_IBeWa_250313.pdf ».
- INERIS (2010): Etude géomécanique du stockage de StocaMine. Rapport d'étude N° DRS-10-108130-14273A.
- ITASCA (2013a): Evaluation des flux potentiels de saumure contaminée à partir du stockage de Wittelsheim. Rapport d'étude N° 13R-001/A3.
- ITASCA (2013b): Wittelsheim waste repository. Rock salt permeability evolution. Report No. 13R-016/A3E.
- Kamlot P., Weise, D., Gärtner G. & Teichmann L. (2012): Drift sealing elements in the Asse II mine as a component of the emergency concept— assessment of the hydro-mechanical functionality. In: Berest, P., Ghoreychi, M., Hadj-Hassen, F. & Tijani, M.: Mechanical Behavior of Salt VII. Taylor & Francis group, London N, ISBN 978-0-415-62122-9, 479-489.
- Kazan, Y. N. (1994): Comportement Thermo-Elasto-Viscoplastique des ouvrages souterrains dans le sel gemme. Dissertation for the ENSMP.
- Knipping, B. & Herrmann, A.G. (1985): Mineralreaktionen und Stofftransporte an einem Kontakt Basalt-Carnallit im Kalisalzhorizont Thüringen der Werra-Serie des Zechsteins. - Kali und Steinsalz, Vol. 9, S. 111-124.
- Kock, I., Eickemeier, R., Frieling, G., Heusermann, S., Knauth, M., Minkley, W., Navarro, M., Nipp, H.-K., Vogel, P., (2012): Integritätsanalyse der geologischen Barriere. Bericht zum Arbeitspaket 9.1, Vorläufige Sicherheitsanalyse für den Standort Gorleben, GRS-286, Gesellschaft für Anlagen- und Reaktorsicherheit (GRS) mbH; Köln.
- Laouafa, F. (2010): Critical analysis of the geomechanical studies of StocaMine storage, study report INERIS-DRS-10-108130 - 04240 2 April.
- Mauke, R.; Stahlmann, J.; Mohlfeld, M. (2012): In-situ verification of a drift seal system in rock salt – operating experience and preliminary results: Proceedings of the 7th Conference on the Mechanical Behaviour of Salt, April 2012, Paris. 401 - 411.
- Mauke, R. & Herbert, H.-J. (2015): Large scale in-situ experiments on sealing constructions in underground disposal facilities for radioactive wastes – Examples of recent BfS- and GRS-activities. Progress in Nuclear Energy. 05/2015; DOI: 10.1016/j.pnucene.2015.04.010.
- MDPA, (2008): Mémoire 5: Mining subsidence and stabilisation of the land, p. 556-631.
- Minkley, W. (2004): "Back Analysis Rock Burst Völker-shausen 1989," in H. Konietzky, (Ed.): Numerical Model-ing of Discrete Materials in Geotechnical Engineering, Civil Engineering & Earth Sciences. 1st Inter-national UDEC/3DEC Symposium, Bochum, Germany, September 2004, Leiden: Balkema, 105-112,.

- Minkley, W. (2004): Gebirgsmechanische Beschreibung von Entfestigung und Sprödbrucherscheinungen im Carnallitit. - Schriftenreihe des Institutes für Gebirgsmechanik - Band 1, Shaker Verlag, Aachen.
- Minkley, W., Mühlbauer, J., Naumann, D. & Wiedemann, M. (2005): Prognose der dynamischen Langzeitstabilität von Grubengebäuden im Salinar unter Berücksichtigung von Diskontinuitäts- und Schichtflächen, Förderkennzeichen 02 C 0892, Abschlußbericht, Institut für Gebirgsmechanik GmbH, Leipzig 30.07.2005.
- Minkley, M.; Popp, T. (2010): Sicherheitsabstände zur vorläufigen Dimensionierung eines untertägigen Endlagers für wärmeentwickelnde Abfälle im Salzgebirge. VSG-Memo (IfG). 29.10.2010.
- Minkley, W.; Berest, P.; Schleinig, J. P.; Farkas, F.; Böttge, V. (2012): Dynamic back calculation of the collapse of the Saint-Maximilien mining field during mining on rock salt in Varangéville (1873). p. 241-252, Taylor and Francis, The Mechanical Behavior of Salt: 7th Conference (SaltMech7): Paris, France.
- Minkley, W., Popp, T., Salzer, K., Gruner, M., Böttge, V. (2013): Hydro-mechanical properties of the Red Salt Clay (T4) – Relevancy of the minimum stress criterion for barrier integrity. Physics and Chemistry of the Earth, Parts A/B/C. Available online 3 June 2013 <http://www.sciencedirect.com/science/article/pii/S1474706513000545>.
- Natau, O. (1997): Geotechnische Nachweise zur Standsicherheit von Untertagedeponien im Salzgestein. Felsbau 16 (1997), S. 466-472.
- Peach, C. J. (1991): Influence of deformation on the fluid transport properties of salt rocks. Geol. Ultraiectina. 77, 233 pp.
- Pelzel, J., Hemmann, M. & Seifert, G. (1972): Ursachen und Entwicklung der Senkungserscheinungen und Erdfälle bei der Flutung der Grube Friedenshall bei Bernburg. Ber. Deutsch. Ges. geol. Wiss, A, Geol. Paläont., 17 (2), 191-219.
- Plischke, I. (2007): Determination of mechanical homogenous areas in the rock salt mass using creep properties for a Classification scheme. Proceedings of the 6th Conference on the Mechanical Behavior of Salt "SALTMech6", Hannover. Germany, 22-25 May 2007.
- Popp, T. 2002. Transporteigenschaften von Steinsalz – Modellierung der Permeabilitäts-Porositäts-Beziehung. Meyniana 54, Seite 113-129, Kiel.
- Popp, T., Kern, H., and Schulze, O. (2001). Evolution of dilatancy and permeability in rock salt during hydrostatic compaction and triaxial deformation. J. Geophys. Res. 106(B3), 4061-4078.
- Popp, T., Wiedemann, M., Kansy, A. & Pusch, G. (2007): Gas transport in dry rock salt – implications from laboratory investigations and field studies. In: Wallner, M., Lux, K., Minkley, W., and Hardy Jr., H. R. (eds.), "The Mechanical Behavior of Salt – Understanding of THMC Processes. Proceedings of the 6th Conference (SaltMech6)", held at Hannover, Germany; 22-25 May 2007.
- Popp, T., Salzer, K., Weise, D. & Wiedemann, M. (2010): Hydraulische Barrierenintegrität von carnallitischen Salzgebirge, Kali und Steinsalz, Heft 2/2010, 16 – 23.
- Popp, T., Minkley, W., Salzer, K. & Schulze, O. (2012): Gas transport properties of rock salt—synoptic view. In: Berest, P., Ghoreychi, M., Hadj-Hassen, F. & Tijani, M.: Mechanical Behavior of Salt VII. Taylor & Francis group, London N, ISBN 978-0-415-62122-9, 143-153.

- Popp, T., Minkley, W., Wiedemann, M., Salzer, K. & Dörner, D. (2015). Gas pressure effects on salt – the large scale in-situ test Merkers. *Mechanical Behaviour of Salt VIII*, Ed.: L. Roberts, CRC Press 2015, pp. 127–135.
- Pouya, A. (1991): Comportement rhéologique du sel gemme. Application à l'étude des excavations souterraines. ENPC dissertation.
- Rothfuchs, T., Wieczorek, K., Hunsche, U., Hansen, F., & Brewitz, W. 2005. EDZ in rock salt. Section 4.2 in. Davies, C., and Bernier, F. (eds.; 2005), *“Impact of the excavation disturbed or damaged zone (EDZ) on the performance of radioactive waste geological repositories – Proceedings of a European Commission Cluster Conference and Workshop”*, held at Luxembourg; 3 5 November 2003. European Commission Report EUR 21028.
- Siemann, M. G. (2007): Herkunft und Migration mineralgebundener Gase der Zechstein 2 Schichten in Zielitz. *Kali und Steinsalz*, Heft 3/2007, 26 – 41.
- Sitz (2003): Entwicklung eines Grundkonzeptes für langzeitstabile Streckenverschlussbauwerke für UTD im Salinar, Bau und Test eines Versuchsverschlussbauwerkes unter realen Bedingungen.- BMBF - Förderkennzeichen 02C05472.
- Schreiner, W. & Kamlot, P. (1991a): Berechnungsmethodik zur Prognose der zeitlichen Übertragung der beim Salzbergbau untertägig induzierten Senkungsvorgänge durch das Deckgebirge bis zur Tagesoberfläche. *Neue Bergbautechnik*, 21. Jg., Heft 5 • Mai 1991, 184-188.
- Schreiner, W. & Kamlot, P. (1991b): Berechnungsmethodik zur Prognose des untertägigen Senkungsgeschehens bei Anwendung des Kammerbaus mit nachgiebigen Pfeilern im Salzbergbau *Neue Bergbautechnik*, 21. Jg., Heft 8, August 1991, 305-310.
- Schulze, O. (2007): Investigation on damage and healing in salt. In. M. Wallner, K.H. Lux, W. Minkley & H. R. Hardy. *The Mechanical Behaviour of Salt – Understanding of THMC Processes in Salt. 6th Conference (SaltMech6)*, Hannover, Germany, 22–25 May 2007. Publ.. Taylor and Francis, ISBN. 9780415443982, 17 – 26.
- Salzer; K., Schreiner, W., & Günther, R. M. (2002): Creep law to describe the transient, stationary and accelerating phases. In: Cristescu, N. D., Hardy Jr., H. R. Simionescu, R. O. (eds.), *“The Mechanical Behavior of Salt V; Proceedings of the 5th Conference (MECASALT V)”*, held at Bucharest, Romania; 9 11 August 1999.
- Stormont, J. C. & Daemen, J. J. K. (1992): Laboratory study of gas permeability changes in rock salt during deformation. In: *International journal of rock mechanics and mining sciences & geomechanics abstracts*. Pergamon. p. 325-342.
- Südkurier (2002): Rätsel um Pyrolyse-Koks-Brand. Südkurier 03.09.2002. <http://www.suedkurier.de/region/hochrhein/rheinfelden/Raetsel-um-Pyrolyse-Koks-Brand:art372615,34001>.
- Thorel, L. (1994): Plasticité et endommagement des roches ductiles – Application au sel gemme. *École Nationale des Ponts et Chaussées dissertation*.
- Thorel. L. Ghoreychi, M. & Cosenza, P. (1996): Rocksalt damage & failure under dry and wet conditions, 4th Conf. on the Mech. Behavior of Salt. Penn-State Univ (USA), June 17-18, 189-202.
- Tincelin, E. & Wilke, L., (1991). Gemeinsame gutachterliche Stellungnahme für die Flutung und Aufgabe des Salzbergwerks Plömnitz. unveröff..
- Uhlenbecker, F. W. (1974): Neuere Forschungsergebnisse in der Gebirgsmechanik aus dem Salzbergbau. In: *Kali und Steinsalz* 6 (1974), H. 9, S. 308 – 314.

- Uhlenbecker, F. W. (1978): Neuere Forschungsergebnisse in der Gebirgsmechanik im Hinblick auf den Abbau von carnallitischen Kaliflözen. Fünftes Internationales Salzsposium in Hamburg 1 (1978), S. 413 – 422.
- Urai, J.L., Spiers., C.J., Zwart, H.J. & Lister, G.S. (1986): "Water weakening effects in rock salt during long term creep," *Nature* 324, pp. 554-557.
- Urai, J., and Spiers, C. (2007): The effect of grain boundary water on deformation mechanisms and rheology of rock salt during long term deformation. In: Wallner, M., Lux, K., Minkley, W., and Hardy Jr., H. R. (eds.), "The Mechanical Behavior of Salt – Understanding of THMC Processes: Proceedings of the 6th Conference (SaltMech6)", held at Hannover, Germany; 22 25 May 2007.
- Vouille, G. (1990): Safety study of a project to store toxic waste in the Amélie Mine. Mechanical aspects of the problem. École des Mines de Paris.
- Wagner, K. (2005): Beitrag zur Bewertung der Sicherheit untertägiger Verschlussbauwerke im Salinargebirge, Dissertation, TU Bergakademie Freiberg.
- Warren, J. K. (2006): *Evaporites. sediments, resources and hydrocarbons*. Springer.
- Wedekind, C., Schreyer, J. & Groß, U. (2003): Standsicherheits- und Gebrauchsfähigkeitsanalyse – Ergebnisse der Überwachung der Flutungsdruckdämme bei der Flutung der Grube Königstein. Vortrag zum 32. Geomechanik Kolloquium am 14.11.2003 in Leipzig.
- Wieczorek, K. & Schwarzianeck, P. (2004): Untersuchung zur Auflockerungszone im Salinar (ALOHA2), Gesellschaft für Anlagen- und Reaktorsicherheit (GRS) mbH, GRS Bericht GRS 198.
- Wolf, J. & Noseck, U. (2015): Natural Analogues for containment providing barriers for a HLW repository in salt. *Swiss Journal of Geosciences*. April 2015. DOI 10.1007/s00015-015-0184-1.